Review Article

Syed Sohail Akhtar*, Rashid Ali Laghari, Amer D. Alotaibi, Abba A. Abubakar, Samir Mekid, and Khaled S. Al-Athel

A critical review on functionally graded ceramic materials for cutting tools: Current trends and future prospects

https://doi.org/10.1515/rams-2023-0141
received May 28, 2023; accepted October 13, 2023

Abstract: This review is an attempt to explore the challenges that need to be addressed to fully utilize the potential of ceramic-based functionally graded cutting tools (FGCTs). The various aspects covered in the review include the most recent experimental and numerical work related to FGCTs, the current research trends and the need for these tools, the identification of potential material combinations, synthesis techniques and their limitations, and finally a presentation of the most recent work. To find general tribological performance, various wear mechanisms involved in the cutting process are explored. Some recent experimental and numerical works related to the self-lubricating phase in functionally graded structure and the need for self-lubricating ceramic tools, identifying potential high-temperature solid lubricants, and their limitations are also discussed. More recent and dominating fabrication methods are also discussed in detail along with a brief review of some promising methods. The implementation of numerical modeling and computational frameworks validated through experiments is found to lead to the design and development of cost-effective and efficient FGCTs. Finally, some research gaps are identified and future directions for innovative FGCT materials are proposed.

Keywords: functionally-graded, ceramic composites, cutting tools, sintering, machining process

*** Corresponding author: Syed Sohail Akhtar,** Mechanical Engineering Department, King Fahd University of Petroleum and Minerals, Dhahran 31261, Saudi Arabia; Interdisciplinary Research Center for Intelligent Manufacturing and Robotics, King Fahd University of Petroleum and Minerals, Dhahran, 31261, Saudi Arabia, e-mail: ssakhtar@kfupm.edu.sa
Rashid Ali Laghari: Interdisciplinary Research Center for Intelligent Manufacturing and Robotics, King Fahd University of Petroleum and Minerals, Dhahran, 31261, Saudi Arabia
Amer D. Alotaibi: Materials Science and Engineering Department, King Fahd University of Petroleum and Minerals, Dhahran 31261, Saudi Arabia
Abba A. Abubakar, Khaled S. Al-Athel: Mechanical Engineering Department, King Fahd University of Petroleum and Minerals, Dhahran 31261, Saudi Arabia; Interdisciplinary Research Center for Advanced Materials, King Fahd University of Petroleum and Minerals, Dhahran, 31261, Saudi Arabia
Samir Mekid: Mechanical Engineering Department, King Fahd University of Petroleum and Minerals, Dhahran 31261, Saudi Arabia; Interdisciplinary Research Center for Intelligent Manufacturing and Robotics, King Fahd University of Petroleum and Minerals, Dhahran, 31261, Saudi Arabia

1 Introduction

Functionally graded materials (FGMs) are materials with a graded composition to achieve desirable properties. This graded composition is designed to meet specific performance needs in a specific application [1–3]. This transition can be either continuous or gradual, but unlike traditional composites, there are no defined surfaces that could cause delamination or separation [4–6]. FGMs were developed in Japan in the 1980s to lower the thermal stresses of conventional laminated composites in aerospace applications, and they were first employed in the space shuttle [7,8]. Since then, much progress has been made in the design, production, and testing of FGMs. The requirements of FGMs arise due to their ability to the structural integrity of the material during service under severe conditions; such types of great examples of FGMs are found in the human body such as the teeth, skin, and bones. These various parts have a variation in mechanical properties, such as hardness and ductility [9–12]. FGMs are utilized to address challenges that cannot be resolved by conventional bulk materials such as ceramics or superalloys. Since 1980, there has been a substantial increase in the number of yearly publications on FGMs as shown in Figure 1, extracted from the SCOPUS database.

The fabrication process is one of the challenges encountered in the development of functionally graded

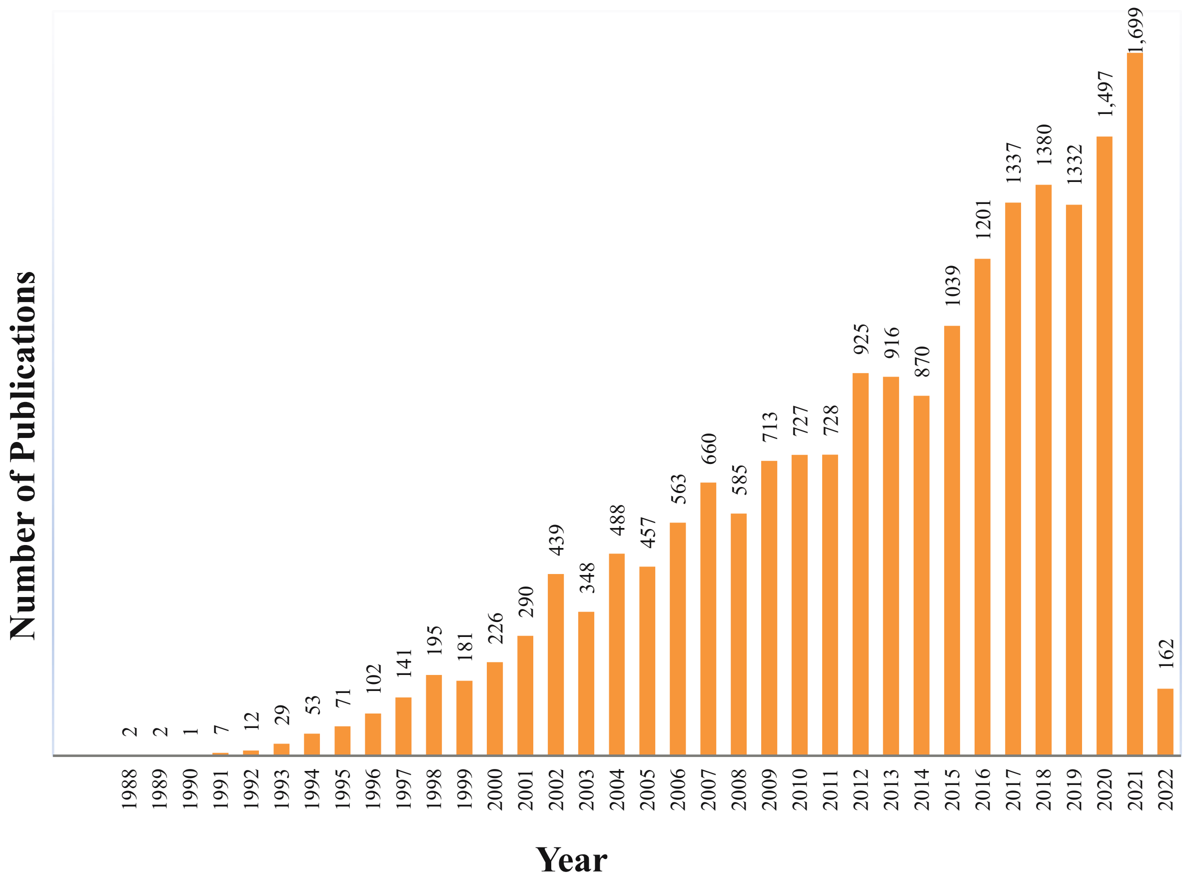

Figure 1: Number of publications per year on the FGMs as retrieved from the Scopus.

cutting tools (FGCTs). To obtain the intended performance, the material's graded composition must be accurately controlled. However, recent developments in manufacturing technology have enabled the fabrication of FGCTs with outstanding precision. For example, FGCTs can be produced using the manufacturing method known as additive manufacturing (AM). AM makes it feasible to precisely regulate the material's composition and structure, enabling the production of FGTs with the required qualities. The capacity to locally alter alloy composition and properties to develop bulk, complex geometry FGMs using AM is one of the abilities that are still under investigation [13]. The main benefit of the AM particularly the laser-directed energy deposition method appears to be its unrivaled multimaterial aptitude and its capability for *in situ* change of the starting material's composition, especially in light of the industry and researchers' growing interest in multimaterial structures [14]. By matching the coefficients of thermal expansion between dissimilar materials, graded deposition has been under consideration. Furthermore, it has been shown that components aiming for unique mechanical properties can be manufactured from new alloy designs or composite materials.

FGMs are designed to solve very specific problems, as seen in the Japanese space shuttle where traditional composites under high thermal stress are delaminating [8,15]. The use of difficult-to-machine alloys imposes additional stress on the industry overall to find alternatives to low-performing cutting tools such as high speed steel , carbides, and other traditional cutting tools during machining operations [16–19]. The extensive use of super alloys like titanium or nickel alloys has brought about specific challenges in the machining industry [20]. Although, in the literature, there is a significant number of research articles and technical reports on FGMs since the 1980s, it is also noted that there has been a slow adaptation of the research activities related to FGCTs in the machining applications. FGMs have the potential to significantly improve the machinability characteristics of different hard-to-cut materials in terms of enhancing surface integrity, chatter formation, cutting force, motor power, and current saving [21–24]. In addition, researchers have extensively examined the machinability characteristics of various difficult-to-cut materials through the use of functionally graded (FG) self-lubricating ceramic cutting tools in the literature. They have found that the performance of these cutting tools is excellent and can greatly improve the machining process [25–27]. According to Figure 2 derived from SCOPUS, on average, only 1.8% of the research conducted on FGMs has been focused on machining applications since 1995. As FGCT demand grows, it is anticipated that they will be used in a broader range of applications in the future. The research of FGCTs has the potential to revolutionize cutting tool technology. This could lead to the development of new materials and manufacturing procedures in the future, allowing for the production of even better cutting tools. Overall, FGCT research is significant because it can lead to increased cutting tool performance, versatility, and potential. This has the possibility of having a considerable impact on manufacturing operations as well as the development of new synthesis technologies.

The cutting tool is the most vital component in the machining process, which performs the material removal process to give proper size, shape, and dimension to the workpiece. Tool life is the amount of time a tool may be used to cut reliably before it needs to be repaired or discarded. In other terms, tool life is the number of minutes between two consecutive cutting tool changes. Since a lot of time is lost every time a tool needs to be changed and reset, tool life is crucial in the machining process. The machine tool, tool material and shape, work material, coolant, and lubricant conditions, as well as other cutting conditions, all affect tool life. The problem of tool wear and tool life has recently gotten more complicated due to the development of numerous new tool materials specifically designed to process numerous new workpiece materials [28]. In addition to cutting time and cutting path length, other factors that affect tool wear include the geometry of the tool (rake, flank, inclination angles, radius of the cutting edge, and so on), cutting regimes (cutting speed, feed, depth of cut), characteristics of the work material (toughness, hardness, structure, and so on), the presence and characteristics of the cutting fluid, and numerous other machining system parameters [29,30]. The geometry of a cutting tool directly affects its life. The geometry of the tool defines the magnitude and direction of the cutting force, the sliding velocity at the tool–chip interface, the distribution of thermal energy released during machining, and the temperature distribution in the cutting wedge [31]. The cutting force occurs on the rake face of the cutting tool, which is constant with the chip flow. The interface between the two is known as the tool–chip interface [32–34]. The rake face of the cutting tool is subjected to significant tensile stresses, and traditional ceramics cutting tools are in fact unable to carry out cutting operations effectively under such high tensile stresses. During the machining process, the

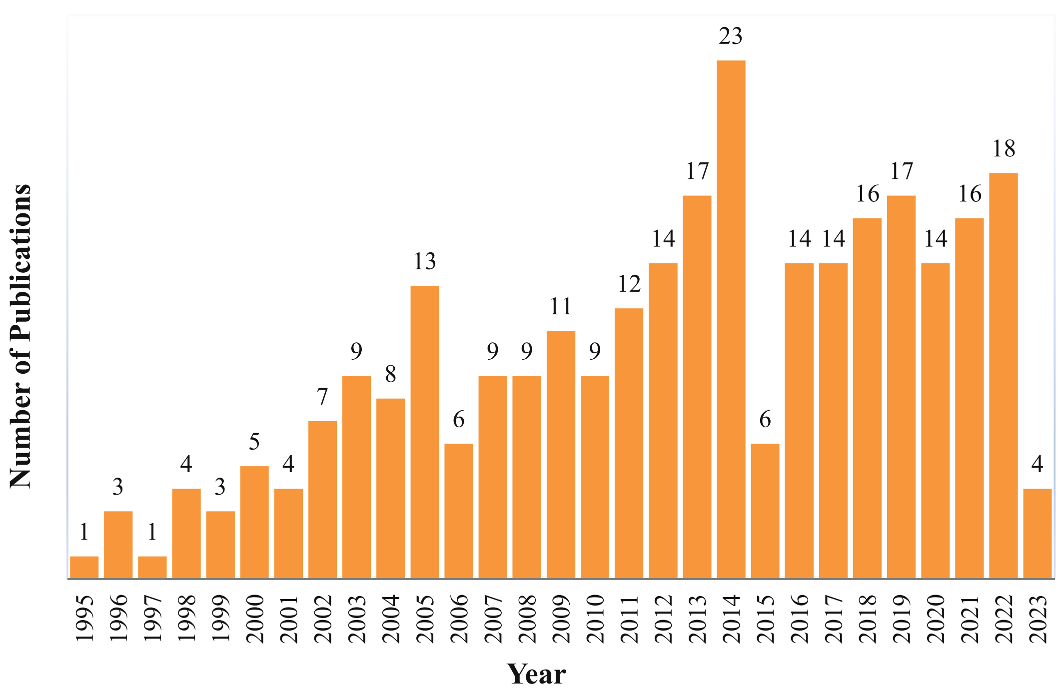

Figure 2: Number of publications per year on the FG ceramics used as tools in either cutting or milling, as retrieved from the Scopus.

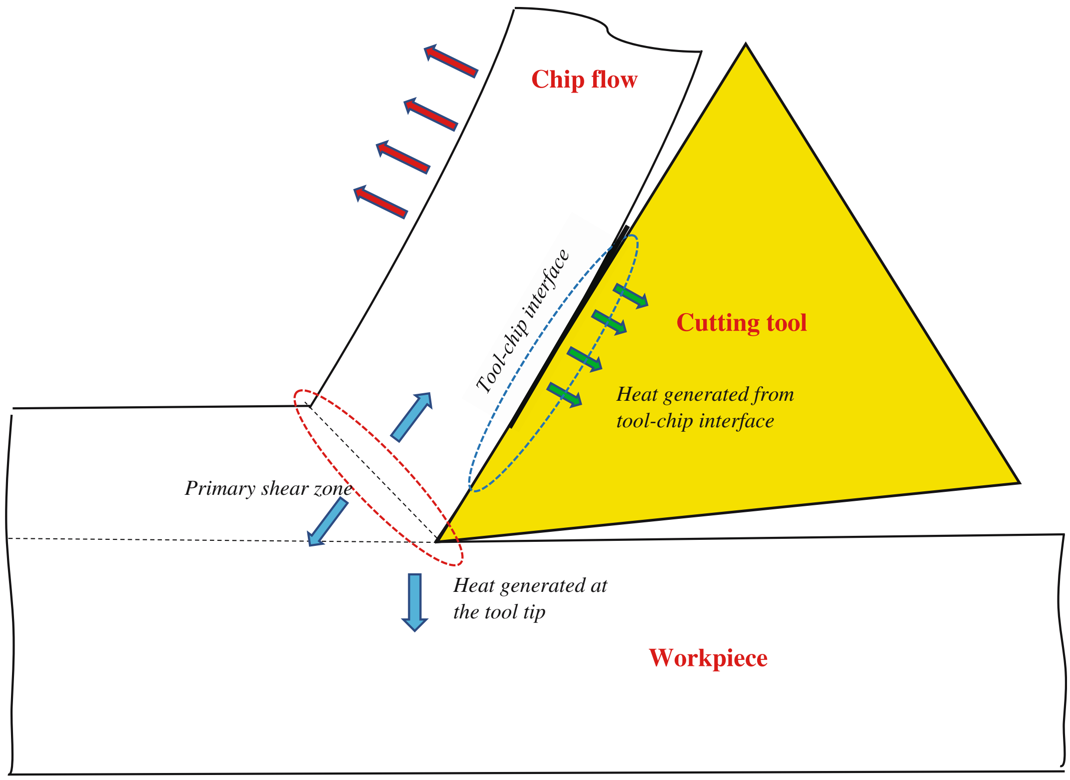

Figure 3: The heat generated by the shear forces during cutting process.

shorter tool life, due to sudden fracture or wear and tear of the cutting tool, causes interruptions during the manufacturing process, which results in higher delay times and lower productivity [35]. During tool–chip interactions in the machining process, the material is deformed, which results in forces and temperature changes on the cutting tool across various cutting zones [36]. Figure 3 depicts the shear forces phenomena, which produce a significant amount of heat during the cutting process, which requires cooling by various lubricants as depicted in Figure 4 [36]. Researchers have extensively studied green cutting technologies to prevent the severe adverse impacts of metal cutting fluids. They also have studied novel tools, solid lubrication, and dry cutting in particular. Cooling agents

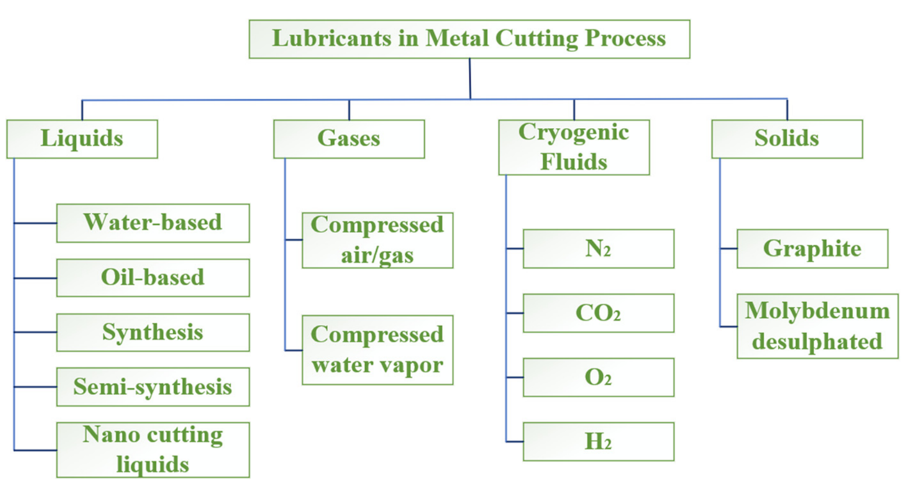

Figure 4: Most widely used lubricants in the cutting industry.

are not necessary while cutting dry. Because appropriate cooling and lubrication are typically missing, dry cutting can quickly result in a decline in surface quality when treating difficult-to-machine materials. Although solid lubrication has a high load-bearing capacity, continual cutting operations' unidirectional motion causes the solid lubricant to be continuously taken away by the chips. A useful method of cutting emissions and carbon in production is minimum quantity lubrication (MQL) technology, which decreases the amount of lubricating media while considering green manufacturing [37]. However, the degradation of the surface due to the insufficient heat transfer capacity is a major issue that has recently been reported to be resolved with the use of nanofluids. Duan *et al.* [38] have recently reported the use of nanofluids so-called nanofluid MQL during the milling of aluminum alloys and found these lubricants to be an excellent option due to high thermal conductivity and tribological properties.

Following a review of the literature on the cutting of challenging materials, we discovered ongoing issues with tool wear brought on by friction damage and deterioration of workpiece surface integrity, suggesting difficulties in adhering to engineering practice standards. Researchers recently completed a thorough analysis of environmentally friendly machining technology, which included metal-cutting fluid replacement technology. FG self-lubricating ceramic cutting tools can be an excellent alternative for efficient heat dissipation and tribological performance in machining operations to improve tool life and increase manufacturing process productivity.

The selection of materials is another issue in the development of FGCTs. The graded composition's materials must be compatible with each other and have the desired properties. Many researchers are currently involved in extensive research to identify and develop new materials for FGCTs. Different types of cutting tool materials are used in various machining processes such as turning, milling, and drilling to perform the machinability of different versatile components [39–41]. For a cutting insert to be developed and used in the manufacturing process for cutting hard-to-cut materials [42], it must exhibit the required suitable mechanical and thermal properties, which could be developed from the FGCTs for performing the cutting operation for respective materials [43]. These properties are highly influenced by the material being cut since cutting, for example, aluminum has different requirements than cutting nickel alloys. Cutting tools must be able to withstand both high mechanical loads and high temperatures. The temperature at the chip/tool interface can reach over 700°C in some cases. The friction between the tool and the removed chip, as well as the friction between the tool and the newly machined surface, is also very high [44]. The following list includes some of the necessary characteristics for any traditional or FGCTs to carry out efficient cutting operations [45–48].

- High hardness.
- High stiffness.
- High fatigue resistance to withstand several cutting processes.
- High fracture toughness.
- High thermal conductivity.
- Thermal shock resistance.
- Wear resistance.

FGCTs address difficulties inherent in ceramic cutting tools such as brittleness, low thermal shock resistance, and low flexural strength. The presence of secondary phases, fracture deflection caused by different expansion coefficients of each layer, the use of nano- and micro-sized inclusions, and the graded structure can all be used to improve these properties [49,50]. By applying self-lubricants just to the surface of the ceramic inserts rather than compromising the entire tool, the functional grading of these inserts can also be advantageous. In the current literature, these composites primarily use three matrices. As a result, this review categorizes the numerous FG ceramics according to their matrix, which includes alumina (Al_2O_3), silicon nitride (Si_3N_4), and SiAlON [51–53]. Figure 5 presents the possible materials development stages in the synthesis of FGCTs.

Figure 6 shows classifications of FGM manufacturing methods [11], while Figure 7 presents various fields of applications of FG ceramic materials with some examples. Because these composites are particularly used in the

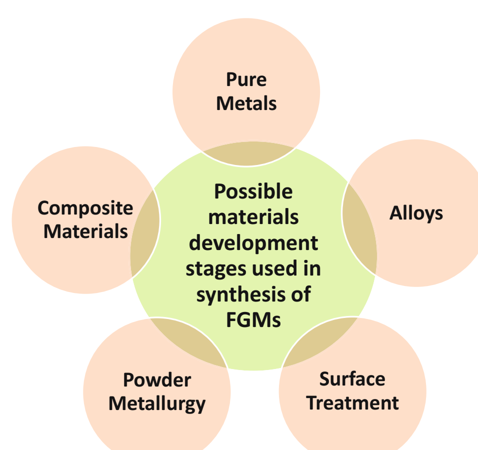

Figure 5: Possible materials development stages used in synthesis of FGCTs.

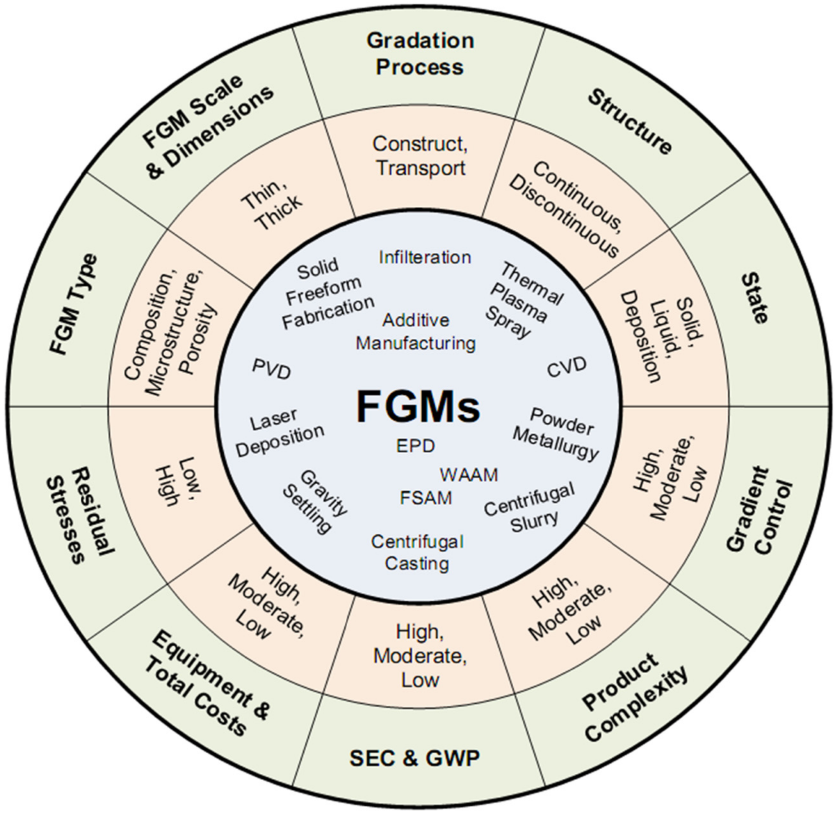

Figure 6: Classifications of FGMs manufacturing methods [11].

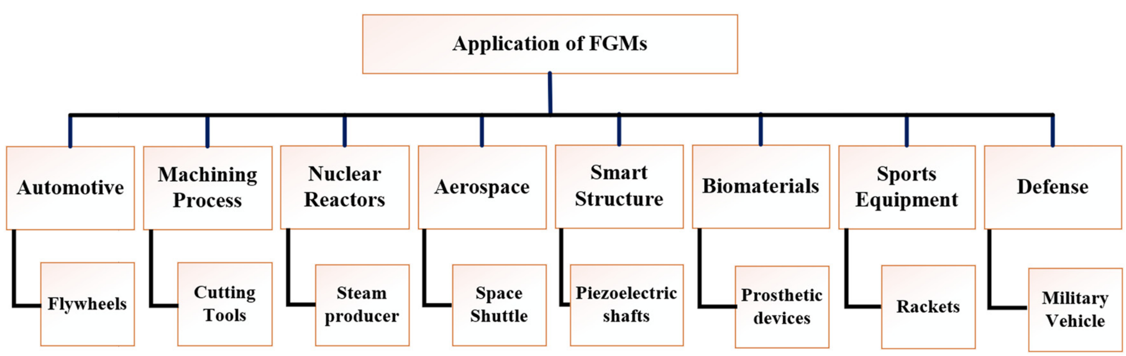

Figure 7: FG ceramic materials: fields of application and examples.

synthesis of cutting inserts in various machining operations, an extensive section of this review has been devoted to exploring the various tribological characteristics and wear mechanisms, as well as current self-lubricated FG ceramics. The synthesis techniques such as spark plasma and microwave sintering (MS) processes will be covered in a separate section in this review, which have been the most significant synthesis processes for the development of FG composites particularly cutting tool inserts.

2 The need for FGCT inserts

FGCTs have the potential to increase cutting tool performance in a range of applications. However, further research is required to generate economically viable FGCTs. The market size of the cutting tool companies in the United States is in high demand and spend around USD 117.41 billion by 2028 on the metal-cutting processes [54]. The most significant factors that have an impact on the metal-cutting industries are the downtimes and energy and raw material waste brought on by cutting tool replacements that necessitate interrupting the machining operation. The development of FGCTs for a specific application of the cutting process can address the critical issue of the tool life of the cutting tools during the machining process [50] especially in machining difficult-to-cut composites and alloys, such as MMCs [55–57], Inconel 718, which leads to a reduction in production capacity [32].

To increase the performance of cutting tools in a variety of applications, self-lubricating FGCT inserts are required. Traditional cutting tools are often built of a single material that must balance the competing demands of wear resistance, toughness, and machinability. However, this can lead to performance drawbacks. A cutting tool that is extremely wear resistant, for example, may be brittle and prone to chipping. This limitation is overcome by self-lubricating FGCT inserts, which have a graded material composition that contains a solid lubricant. The solid lubricant is typically distributed throughout the material matrix and aids in the reduction of friction and wear at the cutting edge. As a result, the self-lubrication cutting tool will play an important role in the machining process with the introduction of FG techniques for the machining operation of hard-to-cut materials [58]. Using lubricant throughout the cutting process extends tool life reduces cutting tool wear and tear and reduces cutting force [59,60]. The use of lubrication methods in the development of FG cutting tool inserts, particularly those with self-lubricating abilities, is essential to the long-term viability of the machining process and the reduction of environmental hazards [61,62]. The MQLs used in traditional non-self-lubricated inserts include no hazards or hazardous chemicals, and they have frequently disposed of while carrying the cutting particles, which are also harmful to individuals [36]. Along with the environmental and health concerns associated with traditional lubricants, processing, and disposal of those lubricants, which include particles, costs between 7 and 17% of the entire machining cost. One of the most significant drawbacks of solid lubricants is their potential to reduce the mechanical qualities of cutting insert materials [63], which ultimately reduces the tool life. This is the primary goal of grading cutting inserts that contain solid lubricants: to achieve an optimal balance of mechanical properties and self-lubrication [64].

Composite materials, as well as nickel and titanium alloys, which are considered difficult-to-machine materials, have been widely used in structural parts in the oil and gas industry as well as automobile engine parts due to their outstanding properties and high-temperature resistance. They are used in compressor disks, turbine disks, bearings and blades, and other aircraft engine components that must be lightweight, strong, corrosion resistant, and temperature resistant [65–67]. A superalloy of nickel, chrome, and iron called Inconel 718 accounts up about 50% of a jet engine's weight [68]. They maintain their mechanical properties, hardness, and corrosion resistance even at high temperatures [69,70]. Because nickel alloys are more difficult to machine compared to other materials, there is higher tool wear during the machining process, which leads to reduced tool life, increasing tool prices, and decreasing productivity. However, there is an immense need for nickel alloys in a variety of applications in the oil and gas, aerospace, nuclear, and marine industries [71]. Due to their excellent properties such as superior corrosion and oxidation resistance, creep properties, toughness, and strength at elevated temperatures compared to other classes of alloys, nickel alloys have the capability to maintain mechanical properties at temperatures as high as 650°C. Compared to other alloys, nickel alloys have lower thermal conductivity and thermal diffusivity [65]. As a result, machining these difficult-to-cut materials can be challenging due to their superior structural and thermal properties. Although this alloy has a tensile strength of approximately 1,393 MPa at room temperature, it is only 8–20% as machinable as the rest of the steel [65]. FGCTs are required for these high-performance exhibiting materials to provide dimensional accuracy during the machining process [50,72]. Furthermore, while evaluating FGMs cutting inserts for various materials, the material removal process performance of cutting insert material must be compared with a conventional cutting tool on a number of difficult-to-cut composites and alloys for their outstanding performance.

The most difficult aspect of machining nickel alloys is determining how the alloy impacts tool wear. The tool is more susceptible to mechanical wear, adhesion wear, diffusion wear, and oxidation because of the alloy's high strength at high temperatures. These effects become even worse at high temperatures during the cutting process [41,65]. High-performance FG coatings (FGM coatings) are also applied to cutting tools to prevent higher diffusion and oxidation at elevated temperatures. These coatings enable the smooth machining of such materials thanks to the development and use of FGM-coated cutting tools [73].

As reported earlier, FGCTs are superior to traditional cutting tools in a variety of ways. Hence, it is expected that these tools will be used in a larger range of applications in the future as consumer demand for them grows. This might result in large increases in output, profits, and product quality. Moreover, the increasing demand for high-performance cutting tools capable of machining difficult-to-cut materials is driving the demand for innovative FGCT materials. Researchers are always attempting to develop materials with desirable properties for a wide range of applications. The following section focuses on some of the most important tool materials, with a particular emphasis on ceramics used in the developing new FGCTs.

3 Current cutting tool materials

There are many different materials that are used to make cutting tools, each with its own advantages and disadvantages. The material of the cutting tool is determined by several aspects, including the material being machined, the cutting conditions, and the required surface finish. New cutting tool materials are constantly being developed. As new materials develop, it is possible that they will be employed to make even more efficient and effective cutting tools.

Metals, ceramics, cemented carbide, polycrystalline diamond (PCD), and cubic boron nitride materials are employed to produce the most frequently utilized cutting tools and inserts [74–76]. Cutting inserts are used in a variety of machining operations such as turning, milling, and drilling. Depending on the technique, the cutting inserts are either coated or uncoated. Coated cutting inserts are commonly used for some tool materials, such as cemented carbides, which are coated to resist the high friction forces created during the cutting operation [36,77,78]. This is accomplished through the use of several coating processes such as chemical vapor deposition and physical vapor deposition [79]. According to Astakhov [32], cutting tools are utilized at the rated cutting operation 48% of the time, and only 57% of tools are used for the entire intended predicted tool life period, while the current cutting tool material is properly selected 30% of the time. Carbide cutting tools have been utilized at low cutting speeds in the range of 10–50 m·min^{-1} to cut metal matrix composites, nickel alloys, and other super alloys such as titanium. Coated carbides, such as coated WC-Co tools, have been employed for higher-speed operations up to 200 m·min^{-1} [80].

An important characteristic in selecting the cutting tool material for performing the cutting operation, especially for high-speed machining is the high hardness property to limit wear and tear at elevated temperatures. Figure 8 shows the hardness values of various cutting tools at different temperatures. High-speed machining has been carried out by traditional cutting tools of cBN, ceramics, and coated carbides. Ceramics cutting tools have been used

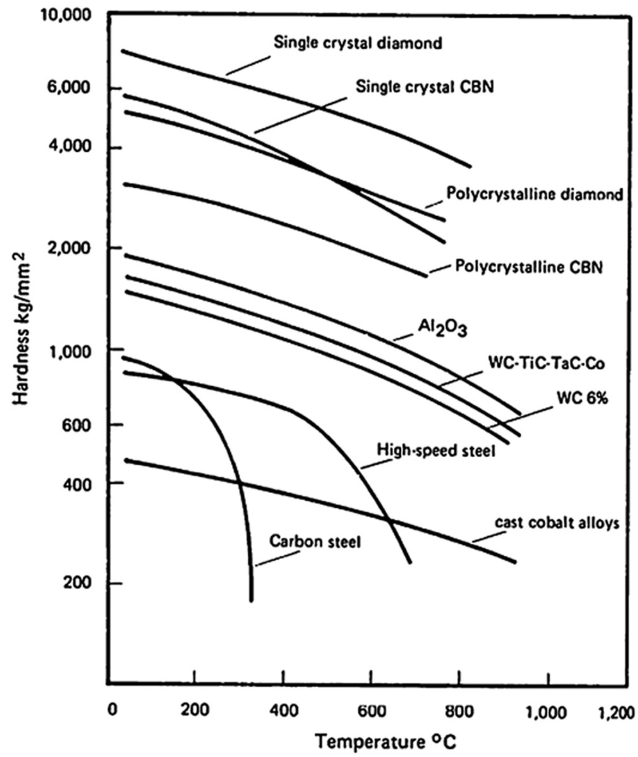

Figure 8: Hot hardness values of various used tool materials [81].

to machine nickel alloys, while they were not possible to machine titanium alloys due to their reactivity with titanium alloys [81,82]. High-speed machining is defined as a milling operation that has a rotational speed of up to 100,000 rpm when taking the diameter of the workpiece and the milling tool are taken into consideration [83,84].

One of the most important developments that enabled high-speed machining of metal and alloys is because of the fact of high hardness and durability of cutting tools, which is possible due to the use of powder metallurgy in the making of cutting tools. cBN has been used extensively in hard machining applications. Prior to the use of powder metallurgy for the development of cutting tools, the high-speed cutting process was only kept for hard carbide tools. Today, different types of cutting tool materials are used for the high-speed cutting process, such as PCD, which alloys cutting of high silicon aluminum alloys at a speed up to 11,000 m·min^{-1} [32].

Ceramic cutting tools are considered for high-speed cutting applications, especially for Al_2O_3 and silicon carbide (SiC) that are the most widely used ceramics as cutting tool inserts [74]. The major advantage of ceramic cutting tool inserts is that they are generally softened at high elevated temperatures of 2,200°C in contrast to traditional cutting tools such as carbide cutting tools that soften at 870°C. The ceramic cutting tool inserts are very stable mechanically as well as chemically at high temperatures especially up to 1,000°C [74]. While comparing the ceramic cutting tool inserts with the carbide cutting tool inserts, it is seen that the ceramic cutting tool inserts do not suffer from secondary binder phases and have higher melting temperatures, which makes them more appropriate for high-speed machining [81]. Ceramic cutting tools have an advantage over their counterparts in the high-speed machining space due to their high-temperature resilience during the cutting process, higher cutting speeds lead to higher cutting temperatures, and thus, the workpiece material is softened [83,85,86]. Ceramic cutting tool inserts have a lower strength than tungsten carbide cutting tools and other metals, and they also have a lower resilience to thermal shock [74]. A similar phenomenon is depicted in Figure 9 in comparison to tungsten carbide and cermets [45]. The rake face on a cutting insert is subjected to tensile stresses and that leads to cracking for the ceramic-based inserts due to their brittleness [87].

While ceramics have advantages in machining, their brittleness, low toughness, and low thermal shock make them less suitable for intermittent milling, where tool durability and reliability under varied conditions are essential. It has been reported in the literature that ceramic tools have poor toughness, which means they can absorb little energy and resist crack propagation. Intermittent milling frequently results in changes in cutting forces and vibrations, which can cause cracks in the tool material and early tool failure. However, because turning is a continuous process that allows for rigid tool installation and reduces the need for high fracture toughness, ceramics are better suited for such operations [88,89].

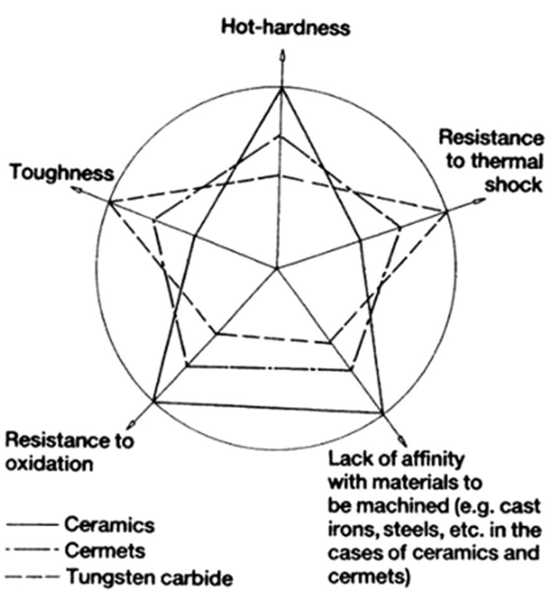

Figure 9: Mechanical properties of ceramics, cermets, and tungsten carbide [45].

As the need for ceramic FG cutting inserts grows, they are expected to be used in a broader range of applications in the future. Ceramic cutting tool inserts are used for hard-to-machine materials including composites and such alloys [45]. There are requirements for the development and fabrication of ceramic inserts, as shown in Figure 10 [45].

Ceramics used as cutting tools can be categorized into four major categories [45].

(1). Al_2O_3 based
(2). Si_3N_4 based
(3). SiAlON based
(4). Cermet tools (70% ceramics and 30% titanium carbide).

3.1 Al_2O_3-based FG ceramics

Al_2O_3-based materials have excellent high-temperature properties, but due to their brittleness and low fracture toughness, they are used in combination with other materials such as titanium carbide at 30–40% composition [45]. Through the fabrication process, a small amount of ductile metal is introduced to increase the Al_2O_3's fracture toughness [90]. Similarly, flexural strength and fracture toughness can be enhanced by incorporating the secondary phases in Al_2O_3 [91]. While developing the Al_2O_3-based FG ceramics, the most frequently used secondary phases for enhancing mechanical properties of Al_2O_3 are SiC [92,93], WC [94], TiB_2 [95–97], and TiC [98]. Furthermore, it is also found in the literature that the zirconia has also been shown to increase the toughness and strength of the composite [9].

Al_2O_3-based FGMs with SiC and titanium carbide (TiC) have shown an increase in thermal shock resistance compared to pure Al_2O_3 for the former with no decrease in the flexural strength compared to SiC for the latter have shown an increase in toughness, which is essential in the development of these ceramics cutting tool inserts [74]. One major drawback of the Al_2O_3-based cutting tool inserts is their brittleness. Due to the widespread usage of whiskers as reinforcements in Al_2O_3-based cutting tool inserts that are distributed throughout the matrix, the toughness of the tools can be enhanced [74].

Various studies are conducted by different researchers on the fabrication process of Al_2O_3-based FG composite along with different percentages of materials such as Fe_2O_3 [99], SiC [100], Mo, TiC, Ni [101], TiC along with ZrO [102] to improve the properties of Al_2O_3 composite. A detailed study of the process was presented by Xu and Todd [99] who have fabricated an Al_2O_3-based FG composite with 10 wt% of Fe_2O_3, which was cold isostatically

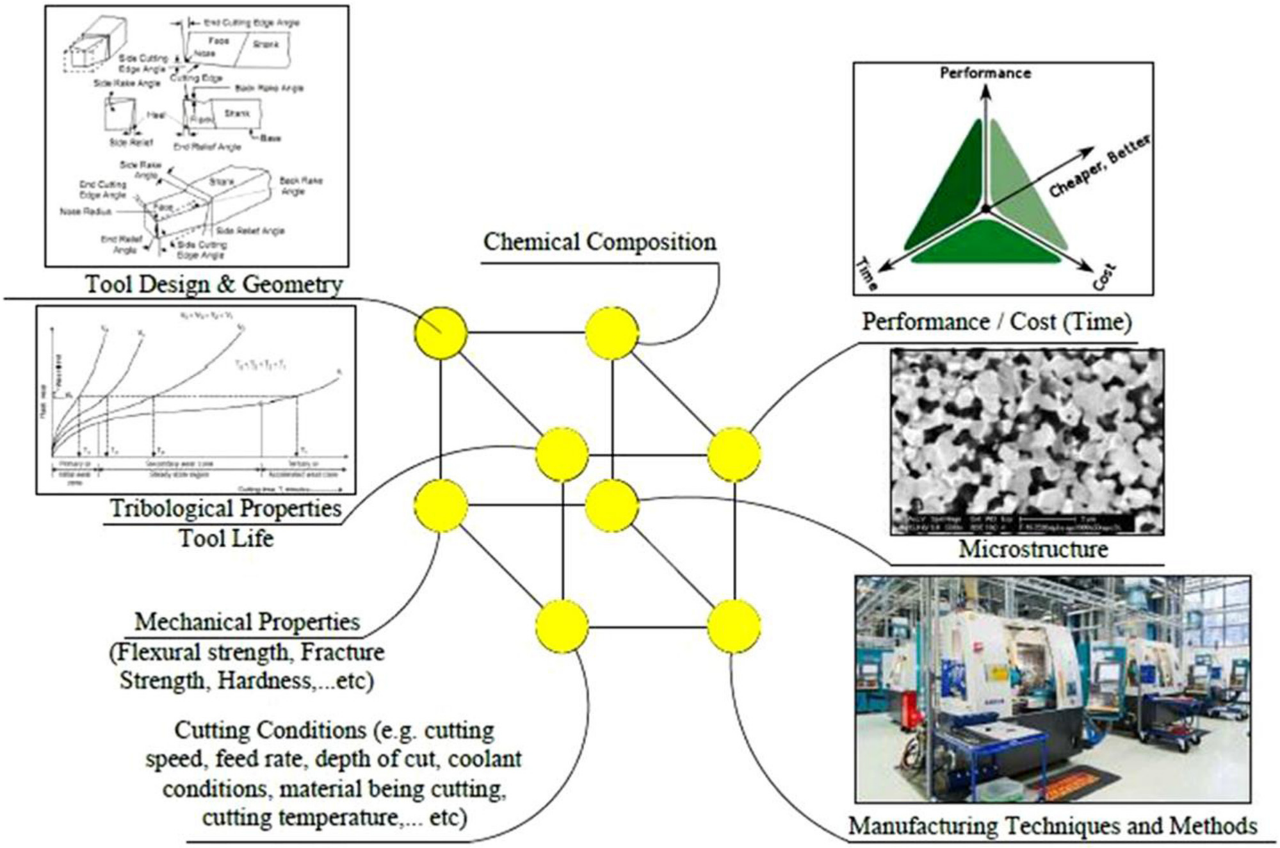

Figure 10: Requirements for ceramic cutting tools [45].

pressed at 150 MPa and sintered pressure in the air at 1,450°C for 5 h. Heat treatment was done following the pressure-less sintering that began by annealing the solid solution at 1,350°C for 20 h under 4 vol% of H_2/N_2 atmosphere. The density achieved was 98% of the theoretical density. The purpose of this heat treatment is to promote the evaporation of iron from the surface, which is intended by design to create a thermal expansion mismatch creating a surface residual compressive stress of 500 MPa and a gradation in the composition. This evaporative process is also responsible for the relatively high porosity measured at the surface, which also resulted in a lower hardness when compared to pure Al_2O_3 of 11.9 GPa. Wear testing was done using the ball-on-disc method using a chrome steel ball. There was a five times improvement in the wear resistance when compared to pure Al_2O_3, and the surface of the wear track appeared to be smoother and showed less pull out of the particles. Furthermore, the study performed by Dancer *et al.* [100] has been designed on the fabrication of Al_2O_3 composite with an outer layer that contains 10 vol% of SiC. This study performs the hot-pressing method at a temperature of 1,650°C for 30 min with a uniaxial pressure of 25 MPa. The purpose of this configuration is to introduce biaxial residual compressive stresses at the surface layer to improve wear resistance. This compressive stress reduces the wear rate by the decrease in the amount of surface pullout. The compressive stresses were measured in CR^{3+}, which indicated a biaxial stress of 126 MPa that increased the wear resistance of the fabricated sample with respect to pure Al_2O_3 by a factor of 8. Application of hot pressing is found frequently for the fabrication process of developing the FG Al_2O_3, in which different layers of materials are added to form the laminated FG composites. For example, application of hot pressing is found frequently for the fabrication process of developing the functionally graded Al_2O_3, in which different layers of materials are added to form the laminated functionally graded composites such study was performed by Qi *et al.* [103]. They prepared laminated Al_2O_3-/Mo-Al_2O_3 composite by hot pressing. The outcomes demonstrate the superior mechanical and self-lubricating and fracture toughness of layered composites. Similarly, the implementation of hot pressing was used by Gong *et al.* [101] in their study of a multidimensional FG ceramic tool developed using hot pressing having five layers as shown in Figure 11. The FG ceramic contains Al_2O_3, TiC, Ni, and Mo. The nickel

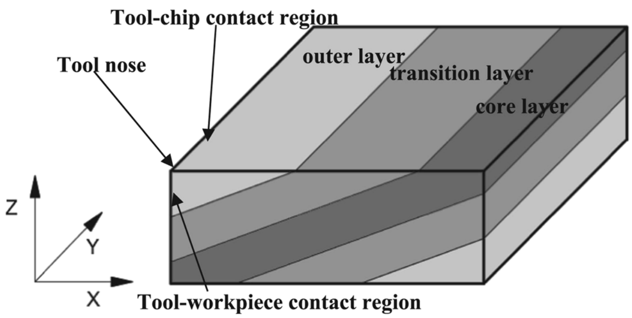

Figure 11: The design of the multidimensional graded ceramic tool [101].

and molybdenum are added to the outer layer to increase the hardness and the toughness of the tool from the outer layer to the core. The multidimensional functional grading was done to overcome fatigue fracture in the alternating machining operations of the steel where there were some small cracks commenced in the extreme stress zone on the rake face of the cutting tool, which further prolongs at the high shear stress planes. When the crack propagates from the brittle area to the ductile area, the fracture toughness and resistance to cracking are increased. In this multidimensional functional grading, the crack deflection occurs while passing over the interface of the grading process. Crack deflection is also influenced by the sintering temperature and holding time. The sample was prepared at 1,700°C for 15 min and at an inclination angle of 30° while having a thickness ratio of 0.4. This configuration shows the optimum properties for developed FGCT inserts. Furthermore, Dong *et al.* [102] also hot-pressed Al_2O_3 and TiC along with ZrO at 1,650°C for 30 min, and were able to improve the toughness over the Al_2O_3–TiC ceramic.

The study performed by Xing *et al.* [104] developed an FG Al_2O_3/TiC cutting tool that focused on the purpose of having high heat conductivity on the surface while interacting during the cutting process. Results show that the high heat conductivity at the surface with the least thermal expansion coefficient can be achieved by increasing the amount of surface compressive residual stresses, which occur during the fabrication phase and that was done by hot pressing at 1,700°C for 20 min.

3.2 Si_3N_4-based FG ceramics

The development of Si_3N_4-based ceramics for cutting tools started since the 1980 [45]. Si_3N_4 as cutting tools are made into two forms: (1) α-Si_3N_4, which is made by nitriding silicon at temperatures up to 1,300°C with an amount of aluminum and yttria Y_2O_3, and (2) β-Si_3N_4 is made by hot pressing 4–12% of yttria and 96–98% of Si_3N_4 at a temperature and pressure of up to 1,775°C and 20 MPa, respectively, with some traces of oxygen. These compounds exhibit excellent oxidation resistance and hardness at elevated temperatures [81].

Si_3N_4-based FG ceramics cutting tools are utilized as the best candidate for the metal cutting process, especially as it is an excellent choice for machining materials with high fracture toughness, high hardness, and thermal shock resistance such as cast iron [105]. The machining performance and excellent wear mechanisms of Sialon-Si_3N_4 based FG nanocomposite ceramic cutting tools were experimentally evaluated *via* the turning process of difficult-to-cut Inconel 718 alloy while comparing with the traditional cutting tools. The result elevated the excellent performance in surface finish and tool life for FG Sialon-Si_3N_4-based cutting tool particularly for higher resistance to fracture [106]. Kovalčíková *et al.* [107] have introduced hexagonal boron nitride hBN of nano and micro sizes in the concentration of 1–5 wt% into Si_3N_4, which was hot pressed at 1,700°C for 3 h. The addition of (hBN) increases the fracture toughness of the ceramic composite, compared to monolithic Si_3N_4 due to crack deflection, crack branching, and pull-out of the hBN platelets. The addition of 1 wt% of micro-sized hBN resulted in a 78% lower specific wear rate compared to monolithic Si_3N_4. As the composition of nano hBN increases to 5 wt%, the specific wear rate becomes comparable to that of monolithic Si_3N_4 as the content of boron nitride increases, and as the coefficient of friction also increases, the similar finding is also found in the research work of Carrapichano *et al.* [108] who have reported a sharp increase in the coefficient of friction when the BN volume fraction increases above 10%. Furthermore, the study depicts that the addition of hBN does not influence the coefficient of friction extensively in developed sample components; it is also shown from the results that the improved wear resistance of the ceramic is attributed to the increased toughness of FG Si_3N_4/BN. The study presented by Tian *et al.* [109] has prepared an FG ceramic tool with five layers based on Si_3N_4. The developed FGCT had five symmetrical layers, which have the composition by volume, where SWT20 is the top layer, SWT20G is the second layer, and SWT20G3 is the middle layer, and the thickness ratio between the layers is 0.2 where the middle layer is the thickest. The (W,TiC)C and cobalt were added to the mixtures for the purpose of enhancing its mechanical properties, especially toughness, which is also the reason for utilizing nanoscale Si_3N_4 particles. The powders with the right volume fractions were laminated in a graphite die and hot pressed at 1,700°C for 45 min in a vacuum and a load of 30 MPa. The disks were then cut into standard triangular shapes, and their edges were chamfered to eliminate machining flaws.

In another work by Tian *et al.* [110,111], they used the hot pressing method to develop Si_3N_4/(W, Ti)C/Co graded composite ceramic tool material. The cross-sectional and fractured surface morphology of the graded material is shown in Figure 12. The surface layers were made of composites that did not contain Co, while the inner sections were made of composites that did contain Co. Following that, the cutting performance of the graded ceramic cutting tool in turning the iron-based high-temperature alloy GH2132 was compared to a standard reference tool. The purpose of adding Co in the second and middle layers is that the final FG ceramic tool would have a high thermal expansion coefficient, which increases from the top surface to the center during cooling from the sintering temperatures and will impose compressive stresses on the outer layers. Figure 12(a) depicts the cross section of the graded ceramic tool. Because a symmetric structure is used, both of an insert's two opposite sides were used as the rake face. The microstructure of the fractured surface of the tool is shown in Figure 12(b), where both rod-like β-Si_3N_4 and needle-like α-Si_3N_4 are marked. Grain in the shape of a rod is important for the strength improvement of the graded tool, while the grain in the shape of the needle is important for the compactness of the tool along with increasing the strength of the grain boundaries in which they work as pins "pinning effect."

Well-designed FGCTs are found crucial for the application of particular machining processes for difficult-to-cut materials such as Inconel 718, Ni, and Ti, or materials that need machining on particular parameters for which the graded cutting tools are designed [112,113]. There are several studies showing the application of graded cutting tools such as the study by Zheng *et al.* [114] who presented an experimental study on the fabrication process of a FG ceramic tool for the ultra-high-speed dry cutting of Inconel 718. Ultra-high-speed machining in the range of 500–1,600 $m \cdot min^{-1}$ is beneficial for the machining of Inconel 718 since the specific shear energy decreases as the cutting speed increases. The authors developed a five-layered ceramic insert in a circular shape, where the outer layers are made of both nano and micro Si_3N_4 and 10% of the volume of $TiC_{0.7}N_{0.3}$ powders, the first symmetrical layer has a thickness of 0.402 mm, the second symmetrical layers contains Si_3N_4 and 15% of volume of $TiC_{0.7}N_{0.3}$ and has a thickness of 1.338 mm, and the center layer contains 20% of volume of $TiC_{0.7}N_{0.3}$ and has a thickness of 4.460 mm. The powders are hot pressed in a vacuum furnace at a temperature of 1,700°C and a pressure of 35 MPa for 60 min to promote densification of Si_3N_4, and α-Al_2O_3 and Y_2O_3 powders were added as additives in 8% of volume fraction.

3.3 SiAlON-based FGCT insert materials

SiAlON is a modification to β-Si_3N_4 in which oxygen and aluminum are added to the mixture during sintering in which silica (SiO_2), Al_2O_3, Si_3N_4, and either yttria or magnesium oxide are added as additives and sintered, which results in a ceramic material that outperforms Al_2O_3-based ceramics in wear resistance [81].

SiAlON is an abbreviation for ceramic material that contains silicon, aluminum, oxygen, and nitrogen. It was developed to have a simpler fabrication process than monolithic Si_3N_4 since it is difficult to sinter due to its low diffusion at high temperatures [45]. SiAlON has been developed in the early 1970s and has been developing ever since with improving properties through a FG technique for particular applications in various fields such as cutting tool inserts for the machining process of metal and alloys [115,116].

The difference between Si_3N_4 and SiAlON ceramics is that the former has higher strength, toughness, and

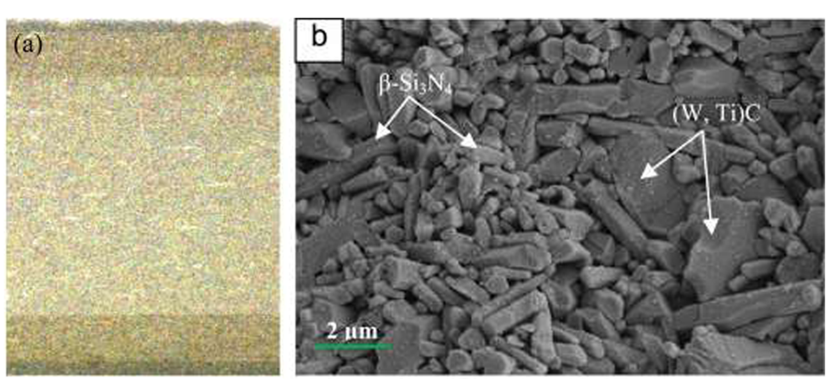

Figure 12: (a) The cross-section of Si_3N_4/(W, Ti)C/Co graded ceramic tool and (b) SEM image representing the fracture surface of the graded cutting tool [110,111].

thermal shock resistance, while the latter has higher chemical stability and wear resistance [115]. The FG SiAlON tool can be used to machine cast iron and nickel alloys, which are considered difficult to machine, but they cannot be used for machining steels due to severe diffusion wear [117]. SiAlON has an excellent ability to withstand the higher temperature and harsh environments due to their enhanced properties such as thermal, mechanical, and chemical, but they have poor tribological performance, especially at elevated temperatures means, and they are better suited to be equipped with solid lubricants [118,119]. Most work on SiAlON is performed at room temperature conditions [120,121]. Lee *et al.* [122] performed the amalgamation of Si_3N_4–Al_2O_3 using the different layers of sample through FG techniques to develop the FGM for increasing the residual stress and withstand at the elevated temperatures and avoid the failure cracks. The study presented the FGMs-developed Si_3N_4–Al_2O_3 performance improvement in thermal and residual applications. Furthermore, the study by Bulić *et al.* [113] suggested that the gradient structures in SiAlON's possess an excellent ability to for the performing the cutting operations smoothly and improve the cutting tool life at a higher level. Šajgalík [123] synthesized a three-layered composite using hot pressing composing of Si_3N_4/(β-SiAlON + TiN) and were able to achieve much higher bending strength and fracture toughness when compared to monolithic β-SiAlON + TiN of almost one order of magnitude.

α-SiAlON has a equiaxed grain and is known to have a high hardness of 2,000 HV but low fracture toughness K_{IC} = 4–5 MPa·m$^{0.5}$, while the β phase has a needle like grains, which attributes to its relatively higher fracture toughness of K_{IC} = 7–8 MPa·m$^{0.5}$, but it also has a lower hardness of 1,600 HV1 [113]. There is a trend in the recent literature in using the functional grading approach to combine both strengthening properties of the two phases of SiAlON. It makes sense for cutting operations to have more resistance to the fracture phase in the core, while the surface has a higher hardness, which leads to enhanced wear properties. Bulić *et al.* [113] have developed a FG SiAlON, where the outer shell is composed of α phase and the core is composed of β phase using a proprietary chemical method and cold pressing at 100 MPa into a green compact and pressureless sintering in N_2 atmosphere for 1 h at 1,600°C. Finally, the sample was hot pressed with a pressure of 30 MPa at 1,780°C for 2 h. The Vickers hardness (VH) measured at the surface is around 20 GPa, and it decreases as it gets to the center, i.e., 16 GPa, which is aligned with the compositional changes as intended. Lin *et al.* [124] have synthesized a Ca-α-SiAlON/Ti_3SiC_2 composite using hot pressing that is composed of three layers, and the ceramic powder Ti_3SiC_2 was reactively synthesized at 1,450°C with a hold of 30 min from a powder of 3Ti:SiC:C. The layering was done with the following sequence Ca-α-SiAlON/Ti_3SiC_2/Ca-α-SiAlON. The synthesis was done by rolling and hot pressing at 1,600°C for 60 min with a uniaxial pressure of 20 MPa. Shear fracturing was done, and the fractured surface was analyzed for the layered composite. It is shown that the outer layer is 250 micron (μm) in thickness and the inner layer of Ti_3SiC_2 is 500 μm. Crack deflection was one of the advantages that FG ceramics provide.

Mandal and Acikbas [125] have fabricated a FG SiAlON composite by tape casting and lamination to achieve a stack of 25 layers composed primarily out of five different ratios of α to β (85a:15b, 70a:30b, 55a:45b, 40a:60b, and 25a:75b). The lamination was prepared by a 66methyl ethyl ketone/34 ethanol (vol%) mixture. Two samples were prepared one that was sintered with a uniaxial pressure of 15 MPa and another with a pressure of 7 MPa followed by cold isostatic pressing at 300 MPa. The sintering was done at 1,800°C for 1 h in a boron nitride crucible. In the case of the CIP sample, hardness decreased from HV_2 = 17.5–14.5 GPa as the content of the α-SiAlON decreased from the top to bottom. SEM and XRD analysis indicated a gradual change in composition as a result of tape casting, which renders the samples prepared FG.

The synthesis conditions play an important role in the overall properties and machining process through ceramic cutting tool inserts as determined by Calis Acikbas *et al.* [126], where they have fabricated various 25α:75 β-SiAlON samples by controlling the dopants (Y:Sm:Ca) ratios with the following ratios (9:0.5:0.5 and 3:6:1) and controlling the cooling rates at either 50 or 5°C·min^{-1}. Heat treatment was also conducted with different soaking times at 1,600°C for 2, 4, and 6 h. Machining tests were done on high alloyed cast iron and compared to commercial Si_3N_4 cutting tools. Heat-treated and slow-cooled samples showcased improved wear resistance due to the presence of a crystalized secondary phase, which was prevalent in resisting the notch wear caused by chemical attack.

For cutting operation, there is a need to have β phase, which has relatively high fracture toughness, as the bulk to act as the "the backbone" of the insert while the harder superior α phase should be concentrated on the surface of the insert. A similar configuration was achieved by Çaliş *et al.* [127], where authors have synthesized a two-layer laminar α and β FG SiAlON by hot pressing at 1,700°C for 1 h. The purpose of this configuration is to combine the advantages of both phases of SiAlON, which are the increased hardness of the α phase and the relatively higher fracture toughness of the β phase due to the elongated grains. The hardness was measured to be gradually decreasing from HV_2 = 19 GPa at the α region to 15 at the β region.

Sarkar *et al.* [128] have fabricated a WC composite bonded with 20–40 wt% of β-SiAlON in an spark plasma sintering (SPS) at 1,750°C for 25 min and a uniaxial pressure of 40 MPa, and mechanical testing indicated the VH HV_{10} to be 18 GPa and fracture toughness K_{1C} = 6.8 MPa·m$^{0.5}$. All the prepared samples have almost achieved their theoretical density, and SEM investigations revealed the formation of principally equiaxed μm-sized WC grains surrounded by the sub-μm and μm-sized SiAlON phases, using a ball disk wear test using a β-Si_3N_4 ball against the WC/30 wt% β-SiAlON composite, which indicated 46–55 times higher wear rates of the counter body against a pure WC.

The type and composition of doping during sintering play a key role in the tribological properties of the synthesized SiAlON ceramic as indicated by Abo-Naf *et al.* [129]. Using the ball on the disc method, the Yb- α-SiAlON ceramic showed the highest coefficient of friction compared to the Nd-doped β and α/β-SiAlON at the same testing conditions. The Nd-doped SiAlON with an α to β ration of 88:12 showed the best wear resistance from all the prepared samples and by SEM investigation, and it was shown that wearing starts with abrasion followed by a formation of plastically deformed tribo-layer and this formed layer reduces the coefficient of friction.

As discussed, tribological performance of cutting tool is an important aspect of their performance and lifespan. Tribology is the study of interacting surfaces in relative motion, with an emphasis on friction, lubrication, and wear. A number of factors influence the tribological performance of cutting tools. The tribological performance of cutting tools is a complex issue, and it is important to consider all of the factors involved to optimize the performance and lifespan of the cutting tools, which is the focus of the next section with respect to the FGCTs.

4 Tribological performance

A great deal of research interest has been shown by several researchers to develop the tribological properties of cutting tools in recent years due to higher efficiency and quality demands in manufacturing [32,130–132]. A number of factors govern the tribological performance of cutting tools, including:

- The material of the cutting tool
- The material of the workpiece
- The cutting conditions
- The use of coolant or lubricant

There is a substantial amount of energy wasted during the metal cutting process for the material removal process, and only 30–50% of the energy is consumed for doing useful work to achieve the desired size and the shape for a particular product during the conventional machining process [32,133,134]. The wasted energy is consumed by the tool chip and workpiece interfaces, which are governed by the tribological system. Due to the nonoptimized tribological system, additional power is consumed during machining, which leads to higher temperatures at the interfaces and subsequently higher wear rates for cutting tools and therefore reduces the tool life. Complex components like turbine blades or biomedical parts that require several machining operations carried out with various levels of energy efficiency should receive specific attention. They are obviously thought to substantially increase energy consumption. However, this strategy enables the development of an energy balance throughout the total life cycle of the product [135].

One of the biggest energy wastes in the cutting process is the plastic deformation of the removed layer into a chip, although it is a greatly important phenomenon to the cutting process, and it consumed the greatest amount of wasted energy. For optimization of the cutting process, there is a need to put focus on the plastic deformation zone for improving the machining energy efficiency. As wasted energy reduction is critical to lowering energy consumption, it could be accomplished using FGMs that focus on the required properties for improved performance [32,113]. It can improve by increasing tool life and reducing the tool wear particularly due to thermal load, and it is possible by enhancing the tribology performance of the cutting tool in the deformation zone during the machining process. Tool wear is very important because it determines the accuracy of the machined parts, the tolerances that can be achieved, the surface roughness, and the cost of machining [136]. The cutting tools are worn by two general mechanisms [65], mechanical (abrasion), which is thermodynamically denoted as wear, and chemically (diffusion) thermo-chemical process. These general mechanisms contain the following modes [137–139].

- Adhesion
- Abrasion
- Diffusion
- Oxidation
- Fatigue

Tool wear is not a material property but rather a system response. It strongly depends on many factors, such as the cutting process and its parameters of speed and rate, the workpiece material, the cutting tool insert material, lubrication, or cryogenic process [36,140,141]. All these system parameters influence the wear

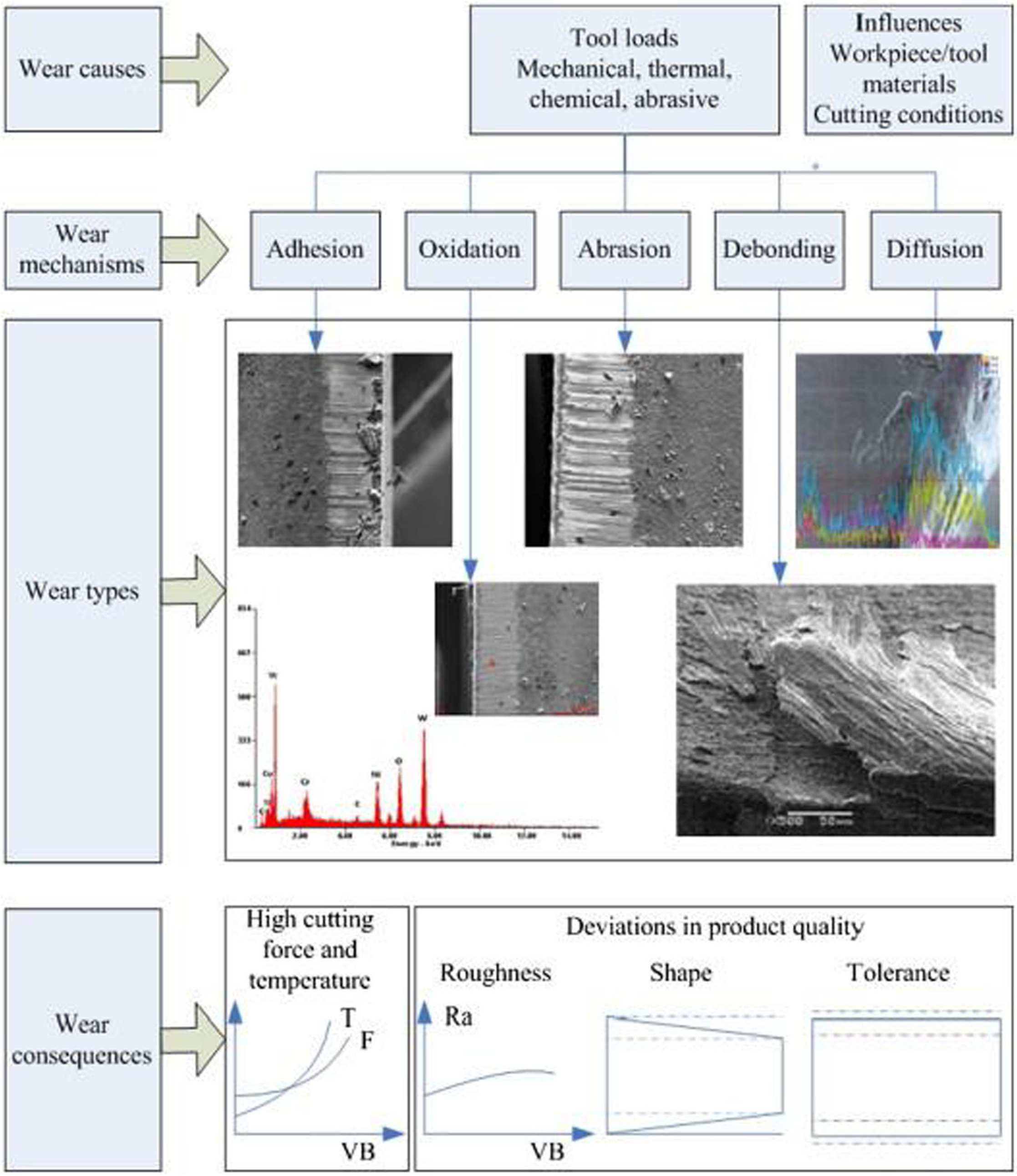

Figure 13: Causes, types, and mechanisms of tool wear in the machining of nickel-based superalloys [65].

mechanisms mentioned earlier. Coatings on the tools are traditionally considered, which permits longer tool life and higher cutting performance, and is made to address such problems of tool wear and failure related with cutting tools. The coating is anticipated to act as a thermal barrier and minimize the coefficients of friction, adhesion, abrasion, and diffusion [136]. Figure 13 shows a basic summary of various types and wear mechanisms in the machining of nickel-based superalloys [65].

According to previous studies [142,143], advancements in ceramics cutting tool materials for enhanced properties such as thermal and residual stress, toughness, and tribological properties employing functionally grading techniques have a lot of potential. The wear mechanisms that affect cutting tools for difficult-to-cut materials such as Inconel 718 superalloy are similar to those that affect cutting tools for general-purpose materials. However, the high cutting forces and temperatures generated when machining difficult-to-cut materials can accelerate these wear mechanisms [144,145]. Abrasion and adhesion are reported as being the two most common wear mechanisms for materials made of nickel alloys [146], and they occur at both high and relatively low temperatures. Furthermore, they are quite dependent on the lubrication conditions, the material of the tool, the workpiece, and contacting load. Both low and high temperatures cause these two wear mechanisms to become active, and as the temperature increases, other damage mechanisms including diffusion and chemical wear are effective [72,145,147,148].

The following subsections discuss common wear types particularly adhesion and abrasion with a coverage of other miscellaneous wear mechanisms. The discussion is mostly focused on the relationship of these wear mechanisms and their impact on high-performance ceramic inserts while cutting difficult-to-machine alloys like Inconel 718 [149].

4.1 Adhesion wear

Adhesion, also known as the cold-welding process, is the recombination of workpiece and tool atoms as a result of plastic deformation caused by an adhesive force generated by relative motion. Adhesion occurs between the flank face and the workpiece; as the temperature in the cutting zone rises, so does the adhesion force at tool and workpiece contact [150]. Because of their lower fracture toughness and flexural strength, and the formation of cracks during the machining process, ceramic tools behave differently than typical hard carbide tools; additional adhesion leads those cracks to propagate. The new wear resistance of ceramics has been investigated extensively to increase the wear resistance properties and performance of the FGMs [151].

Çelik *et al.* [83] developed two SiAlON-based milling tools, one with a standard composition and the other with a SiAlON composite including TiN. The tools were prepared by mixing high-purity powders with organic additives for powder consolidation and isostatically pressing them into standard rods at a pressure of 2,000 bar, followed by a 1-h heat treatment at 600°C to remove the binders. The specimens were sintered in a gas pressure sintering furnace at 1,950°C and 100 bar N_2 pressure for 1 h of holding time. It has been found out by carrying a diffusion pair test that diffusion between the Inconel and the SiAlON sample started after a flat period in the temperature range of 900–1,600°C when the SPS pistons started to move closer to each other, which indicated flow between the samples. They found that SiAlON can be used with high-speed machining of Inconel 718 without any severe degradation due to abrasion or fracture, and the most dominant wear mode was adhesion and diffusion due to the high machining temperature of >1,000°C. But overall it is a lower wear when compared to a SiAlON and steel pair that undergoes severe diffusion [117]. The diffusion process leads to the formation of a scale of Al and Ti oxides [83]. The diffusion pair test conducted in the SPS is a great way of simulating the expected adhesion wear of the tool. Comparisons can also be made based on the thickness of the diffusion zone if more than one sample is prepared with varying compositions. Bertolete *et al.* [152] used the SPS process to synthesize two different classes with six-layered FGCTs with the WC (as cemented carbide) and Al_2O_3 (as ceramic) as major materials. Figure 14(a) and (b) shows the SEM images of the two FG structures, namely, Al_2O_3–ZrO_2 + WC-Co and Al_2O_3–TiC + WC-Co, respectively. They found improvement in thermal and structural properties together with improved wear resistance using FGM samples as compared to homogeneous ceramic ones. SEM images of FGCTs are displayed in Figure 14(c)–(f). Figure 14(c) and (e), respectively, show the rake faces of FG AlZr and FG AlTiC. On the main cutting edge, a small spalling is confirmed for FGM AlZr, and a large one, notch wear formation, for FGM AlTiC. In addition, as shown in the EDS image, the adhesion of martensitic stainless steel (the material of the workpiece) on the tool rake face is also seen. Due to the short machining time, no cutting tool exhibits significant abrasion wear signs when the tool flank (clearance face) is analyzed, as shown in Figure 14(d) and (f).

Tsuda [153] reported the development of a titanium-based ceramic surface layer, a tough cemented carbonitride core containing Bl type and WC phases, and an intermediate layer with graded composition. The material's abrasion resistance and fracture toughness were found to be significantly greater when used as cutting tools than those of a conventional cermet of uniform composition. When compared to coated tools, ceramic surface coating has extended longevity because of its graded composition's high adhesive strength. Ming *et al.* [154] found that while cutting the FGH96 super alloy using SiAlON, the cutting edges are covered with an adhering layer formed as a result of chemical wear since the temperature during cutting reaches 1,200°C, and this was found after milling for 480 mm at speeds ranging from 225 to 315 $m \cdot min^{-1}$ at dry conditions. EDX analysis indicated that the composition on the flank face of the tool is mainly composed of Ti, Ni, Cr, and Co, which is basically the composition of the FGH96 super alloy.

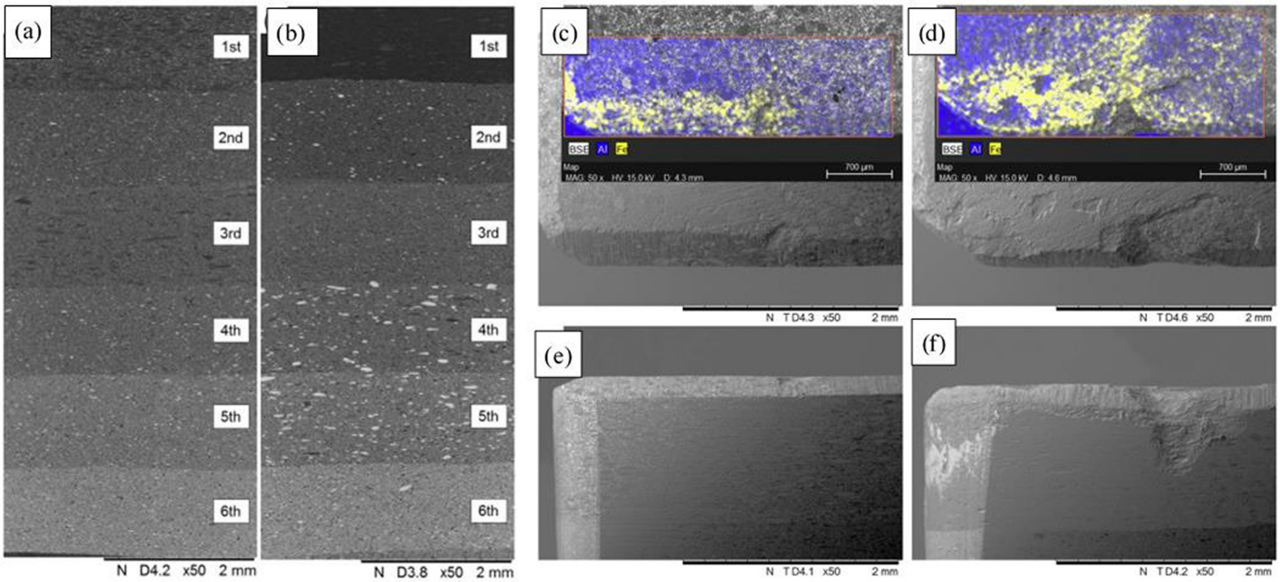

Figure 14: SEM images of FGM tools. (a) FGM structure of Al_2O_3–ZrO_2 + WC-Co; (b) FGM structure Al_2O_3–TiC + WC-Co; (c) rake face of FGM AlZr with EDS highlighting workpiece material adhesion; (d) tool flank of FGM AlZr with small spalling on the main cutting edge; (e) rake face of FGM AlTiC with EDS highlighting adhesion and large spalling; and (f) tool flank of FGM AlTiC with the presence of notch wear [152].

Zheng *et al.* [114] developed functionally graded layered Si_3N_4 and $TiC_{0.7}N_{0.3}$ cutting tools with varying compositions and tested them while cutting the Inconel 718 workpiece. The performance of these layered tools was compared with tools including bulk Si_3N_4, $TiC_{0.7}N_{0.3}$, and commercially available KY4300 insert. The cutting speed ranged between 500 and 1,600 m·min^{-1}. For such high cutting speed levels, the chips showed a tendency of ductile to brittle transition, which was evident from the sparsening of the chip and the change in color caused by the high shear strain rate as a result of high cutting speed. The development of the five-layered ceramic cutting tool insert was executed in a circular shape, where the outer layers are made of both nano and micro Si_3N_4 and 10% of volume of $TiC_{0.7}N_{0.3}$ powders. The first symmetrical layer of the ceramic cutting tool insert has a thickness of 0.402 mm, the second symmetrical layer contains Si_3N_4 and 15% of the volume of $TiC_{0.7}N_{0.3}$ with a thickness of 1.338 mm, and the center layer possesses 20% volume of $TiC_{0.7}N_{0.3}$ and a thickness of 4.460 mm. The powders are hot pressed in a vacuum furnace at a temperature of 1,700°C and a pressure of 35 MPa for 60 min, to promote densification of Si_3N_4, and Al_2O_3 and yttria powders are added as additives as 8% of vol fraction. The thermal expansion coefficient of Si_3N_4 is 3.2×10^{-6}/K and that of $TiC_{0.7}N_{0.3}$ t is 8.6×10^{-6}/K, which means that the outer layers have compressive residual stresses due to the fabrication process. Due to the high temperature generated during the machining of alloys, which softens the workpiece, the cutting forces drop as the cutting speed increases. It has been found that the ideal cutting speed for the least force is 900 m·min^{-1} by measuring the cutting forces using a piezoelectric component dynamometer at various speeds. However, the mechanical properties of the cutting tool also decreased, which result in an increase in the measured cutting forces. When cutting nickel alloys using ceramic cutting tool inserts, the appropriate speed between the softening of the workpiece and the tool materials must be carefully adjusted for a smooth machining operation to improve the tool's life and machinability

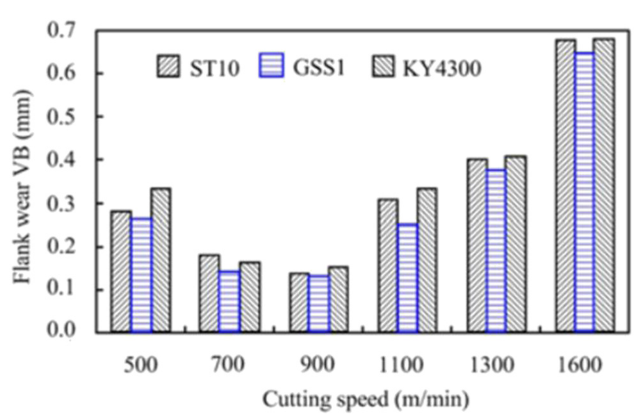

Figure 15: Effect of cutting speed on the flank wear where f_z = 0.07 mm·z^{-1}, depth of cut is 1.5 mm, and volume of metal removal is 2.85 cm^3 [114].

features. Figure 15 shows the extent of flank wear on the three cutting tools, GSS1, which is the graded tool, and ST10 and KY4300, which are the homogenous tool and the ceramic/ SiC_w tool, respectively. It is clear from this figure that the graded tool had the least amount of flank wear rate at all the cutting speeds, which is due to the low cutting forces generated during the machining process, and it is also depicted from this figure that the optimum cutting speed is around to be 900 m·min^{-1}.

Zheng *et al.* [114] reported a relatively higher wear performance of the graded cutting tools in comparison to the other cutting tools, which was attributed to the lower cutting forces along with better properties such as higher fracture toughness and flexural strength. The graded tool has shown some amount of flaking, rake chipping, and notch wear, especially at high cutting speeds as shown in Figure 16. Adhesion is a major contributor to the failure mode since at ultra-high cutting speeds, the temperature at the cutting edge is believed to be more than 1,200°C, which was represented by molten chips adhered to the cutting tool. The compressive stresses subjected to the graded cutting tool outer layers were added by design in the modeling and computation phase which is intended to counteract the tensile stresses that are subjected on the cutting tool rake face, which increases the notch resistance of the cutting tool.

Zheng *et al.* [155] have developed an FG Si_3N_4/SiAlON ceramic composed of five layers and conducted ultra-high-speed machining at 1,100 m·min^{-1} and studied the morphology of the machined face of Inconel 718 and its roughness. The topography is shown in Figure 17, which shows adhesive wear damage on the machined surface due to the high-temperature effect on the workpiece at high cutting speeds, which increases adhesion between the alloy and the cutting tool. Also, chipping and flaking damages were found.

Tian *et al.* [109] have prepared graded ceramic cutting tools with five layers based on Si_3N_4 with the addition of

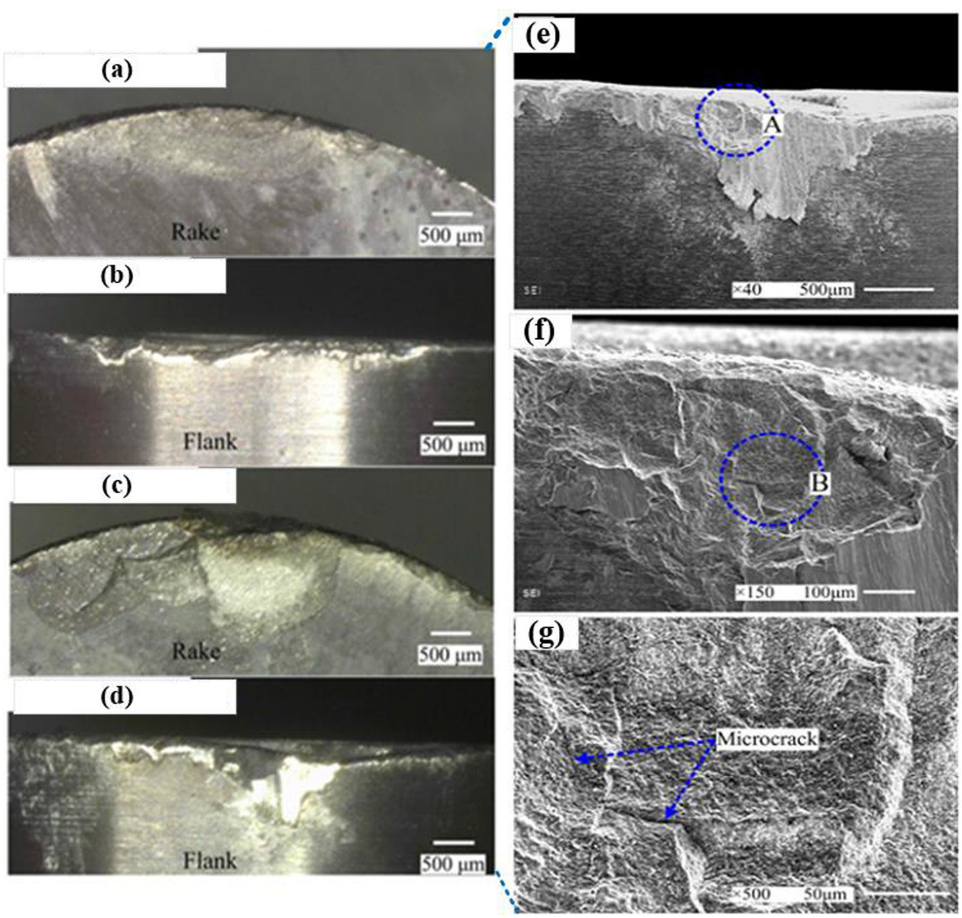

Figure 16: Failure characteristics of the graded tool GSS1, where f_z = 0.07 mm·z^{-1}, depth of cut is 1.5 mm, and volume of metal removal is 2.85 cm: (a) and (b) flank and rake wear at v = 1,300 m·min^{-1}, respectively, (c) and (d) rake and flank wear at v = 1,600 m·min^{-1}, respectively, (e) the flank face wear phenomena, (f) enlarged view at A, and (g) the enlarged view at B [114].

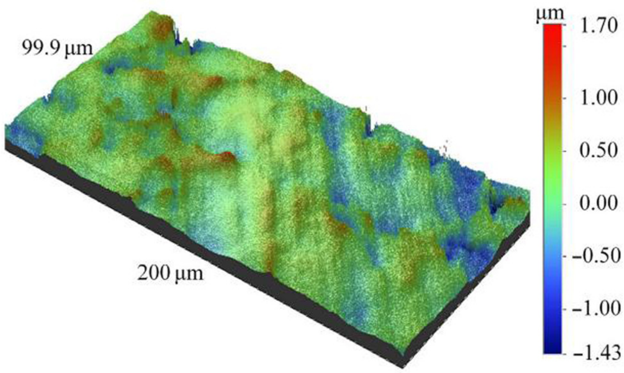

Figure 17: Machined surface topography at V_c = 1,100 m·min^{-1}, f_z = 0.07 mm·z^{-1}, a_p = 0.5 mm, and a_e = 19 mm [155].

cobalt and (W, Ti)C and carried out intermittent turning tests under dry conditions on the age-strengthened superalloy GH2132, which is similar to A286. This alloy contains 24–27 wt% nickel and 13.5–16 wt% of chrome along with Ti, Mo, V, B, and Al. The intermitted cutting results indicated that at the same impact number of times and at the same cutting speeds, the homogeneous tool shows higher flank wear values in comparison to the graded tool. The graded ceramic cutting tools were found to fail by fracture at the cutting tool tip, with chipping and flaking on the damaged surface, as well as adhesion wear in the form of the material removal process and peel-off.

4.2 Abrasive wear

Abrasive wear occurs when the cutting tool and the workpiece are in relative motion and their hard asperities or inclusions are trapped at the interface as demonstrated in Figure 20 [156]. They are characterized by their sharp lines and grooves that are present on the flank face of the cutting tool [65,156]. Work hardening occurs during the metal cutting process, most nickel alloys contain hard carbide phases, and these carbides act as an abrasive medium to the cutting tools. Due to the work hardening, the chips that are produced from the cutting operation are also tough and hard, which degrades the tool by seizure and catering [71].

Kitagawa *et al.* [157] investigated the high-speed machining of Inconel 718 and Ti–6A1–6V–2Sn using ceramic cutting tools. Two kinds of ceramic cutting tool materials have been used for machining processes such as Si_3N_4 and TiC + Al_2O_3. It is found from experimental investigation that the Inconel 718 exhibits wear severity by notch wear, which is a clear indication of the abrasion wear mechanism on the flank face of the cutting tool. The titanium carbide and Al_2O_3 cutting tools demonstrated superiority in wear resistance at high temperatures at 1,200°C and high cutting speeds reaching 600 m·min^{-1}. The notch wear was attributed to the plastic flow and the work hardening of the chips and the workpiece. It was also found that the two ceramic cutting tools showed different wear morphologies due to abrasion, and Si_3N_4 craters developed and the TiC + Al_2O_3 showed notch wear at the same cutting speeds during the machining process.

Jianxin *et al.* [158] have conducted cutting tests on Inconel 718 using Al_2O_3 + TiB_2 + SiC_w with variation in the volume fraction to produce five different cutting tool samples. The study demonstrated that the addition of higher content of the SiC whiskers increases the fracture toughness of the specimen along with its hardness at a volume fraction of up to 30%. They observed different failure modes of cutting tools during the material removal process, which includes the flank and rake wear mechanism as well as the total breakage of the cutting tool while machining Inconel 718. The most predominant wear mode was on the flank face of the cutting tool by abrasion wear, which was present in the form of grooves and ridges. Figure 18 shows the wear profile of one of the samples used, which contains 20 vol% of SiC_w at a cutting speed of 80 m·min^{-1}. Both the flank and rake faces were damaged during the material removal process. The grooves on the flank face are shown in Figure 18 [158].

Zheng *et al.* [106] studied SiAlON–Si_3N_4 FGCT in cutting operation and reported the damage morphology of the tool during cutting Inconel718. They found from experimental results that the performance of the cutting tool is less sensitive to different wear mechanisms and types. They found abrasion and adhesion as the major wear mechanisms.

4.3 Miscellaneous wear mechanisms

High temperatures are generated at the chip–tool and tool–workpiece contacts during dry, high-speed machining. The dissolution and diffusion of tool material into the workpiece material, a specific type of chemical wear, becomes the primary mode of tool wear at these temperatures. The chemical incompatibility of the materials such as steels at high temperatures makes commercially available uncoated hard metals, cermets, and Si3N4-based inserts unsuitable for high-speed and dry machining. Diffusion happens when the two materials come into contact and the temperature is high enough for the atoms to migrate [159]. When atoms diffuse inside a cutting tool, it leads to brittle and crack. It is challenging to gain knowledge about the chemical tool–-workpiece interaction since the chips eliminate any "evidence" of chemical interaction. Adhesive layers on the flank face of tool inserts may be occasionally employed for the

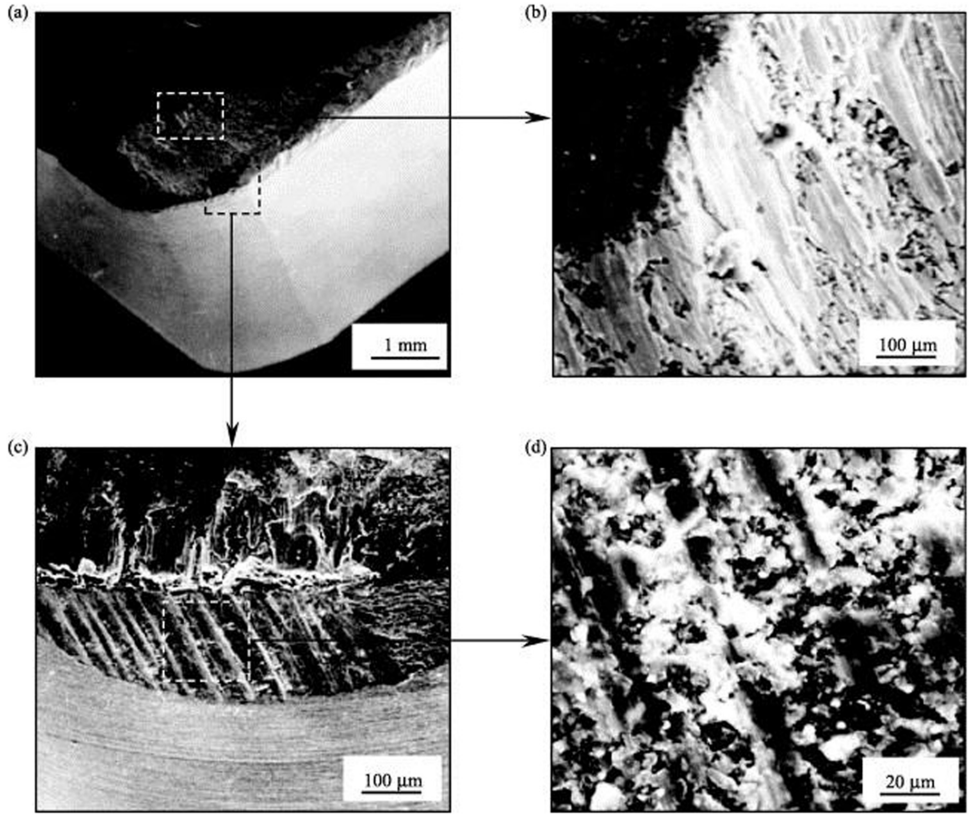

Figure 18: (a) SEM image of the wear profiles on the rake and flank faces of $Al_2O_3/TiB_2/20$ vol% SiCw tool when machining Inconel 718 nickel alloy, (b) SEM micrograph of the rake face at higher magnification, (c) A close-up view of wear surface on the flank face of the tool, and (d) A higher magnification view of flank face showing ridges and mechanical plowing grooves indicative of typical abrasive wear [158].

study. Bertolete *et al.* [152] reported that when the workpiece and tool have a chemical affinity and the cutting temperature is relatively high, crater wear can be observed. In the case of machine steel, certain ceramics, like Al_2O_3 whiskers and Si3N4, have a diffusion mechanism. Although it can also be seen on the flank, the wear in this instance is seen as a smooth crater on the rake face.

Since nickel alloys have high strength at high temperatures, the high temperature of the cutting process leads to chemical degradation of the cutting insert along with the diffusion of material at the tool–chip interface [71]. Due to the poor thermal properties especially the diffusivity of nickel alloys, it increases the temperature at the tool tip introducing a thermal gradient and generating large thermal stress on the tool and the workpiece.

A new form of wear mechanism the so-called cobalt leaching has been reported in recent tribological investigations in cemented carbide tools that use cobalt as a binding agent, where it wets the tungsten carbide grains during the sintering process [32]. Using binders is important in the sintering process to limit porosity and achieve high toughness and strength. There are many reasons for this kind of damage; one of those is the chemical corrosion process with a corrosive media as it is contacted with cobalt. This leaching dissolute cobalt leaves tungsten carbides in exposed skeletons with little to no structural integrity. Binding agents have used extensivity in the sintering of various ceramic tools, and their effect on the mechanical and tribological properties is thoroughly investigated [160]. This is an important wear mechanism to highlight since Co is used extensively in FG ceramics to impose additional residual compressive stresses at the surface.

5 FG tools for dry cutting

The conventional machining process involves direct contact of tool–workpiece during the cutting process for performing the material removal process, and it is a fact that the 20% of total energy during the cutting process is spent to overcome the frictional forces of the cutting process produced by the cutting tools inserts at the flank and rake faces [36]. Traditionally this was overcome by improving the lubricating medium added to the cutting process. Recently, advances have been made to improve the self-lubrication properties of the cutting tool inserts themselves. One of the main challenges in incorporating solid lubricants in homogeneous ceramic cutting tool inserts is the fact that the surface continuity of the ceramic cutting tool insert is destroyed by the constant flowing of the layered structural solid lubricant phase, which ultimately reduces the mechanical properties [161] and wear resistance [162]. For this particular reason, functional grading has been investigated recently to incorporate solid lubricants into the inserts without sacrificing any of the mechanical properties. Various additives can be utilized as solid lubricants, and for each, there are advantages and limitations. There are basically four major types of solid lubricants that are used in cutting inserts [119].

1- Soft metals
2- Lamellar solids with layered structures
3- Mixed and single oxides
4- Alkaline earth metal fluorides

Zhang *et al.* [161] have developed a FG $ZrO_2(3y)$ – $Al_2O_3/ZrO_2(3y)$ laminated composite utilization commercially available powders of Al_2O_3, ZrO_2, Y_2O_3, CuO, and TiO_2. The FG composite was first milled in a ball milling machine, stacked in a graded fashion in a hot-pressing machine and hot pressed at 1,350–1,400°C for 100–120 min at 25 MPa of pressure in an Argon atmosphere. The configuration of FG material is shown in Figure 19(a), while Figure 19(b) shows an SEM image of the corresponding configuration. Self-lubricating elements are added to the mixture during the hot-pressing phase, which enables the enhanced tribological properties of this composite. The self-lubricating elements used in combination are graphite + CaF_2 + $BaSO_4$ and graphite + CaF_2 to produce two different self-lubricated composites, As the numbers of the laminated layers are increasing in this Al_2O_3/Al_2O_3 – $ZrO_2(3Y)$ composite so do the mechanical properties until it reaches 41 layers shown in Figure 19(c). The FG self-lubricated ceramic showed excellent tribological performance

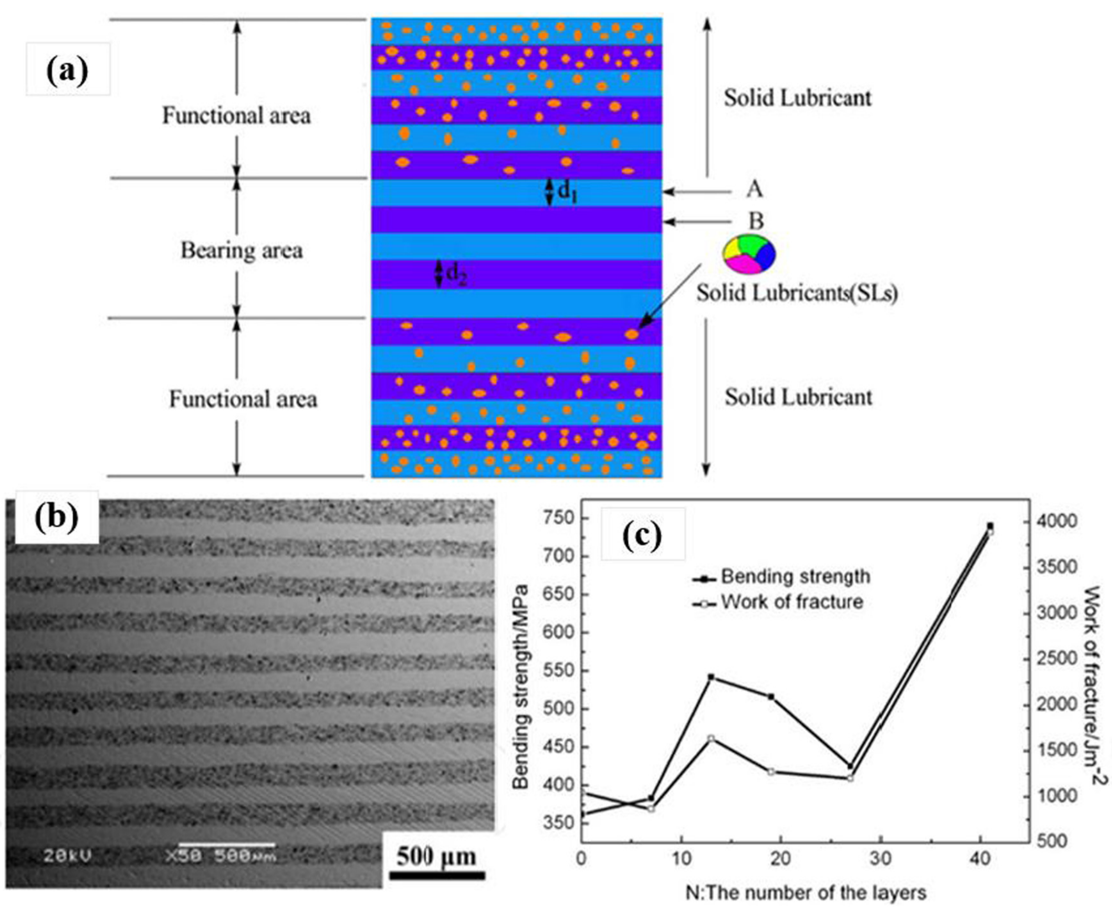

Figure 19: (a) The overall configuration of the laminated structure along with the self-lubricating additives, (b) SEM image of the laminated composites, and (c) effect of layering and number of layers on the bending strength and fracture resistance [161].

in comparison to monolithic Al_2O_3 and zirconia from temperature ranges from 25 to 800°C where the coefficient of friction was measured as less than 0.55, which is half of that shown by the monolithic ceramics. This is due to the presence of graphene, CaF_2, and $BaSO_4$ that have excellent lubricating properties over a wide temperature range. The selection of the lubricating elements depends strongly on the desired cutting temperature, i.e., from room temperature to 300°C for grapheme, from 250 to 1,000°C for CaF_2, and $BaSO_4$ has a very wide temperature range.

CaF_2 can also be incorporated with MoS_2 in a ZrO_2 matrix to achieve excellent wear properties as shown by Kong *et al.* [163]. MoS_2, a solid lubricant, is better suited to be used at low temperatures since it tends to oxide at higher temperatures [164]. Shell core structures can also be used while incorporating the solid lubricants in the graded ceramic as was done by Chen *et al.* [165], where the Al_2O_3/TiC graded composite with CaF_2@Al_2O_3-coated lubricant showed the best mechanical properties during the experimental analysis of the fabricated graded composite.

Tang *et al.* [166] have prepared a graded and self-lubricating insert composed of WC, TiC, Ni_3Al, and CaF_2 and conducted cutting operation on a CNC lathe at cutting speeds ranging from 100 to 250 $m{\cdot}min^{-1}$ on AISI 1045 steel with a hardness of 190 HB. Their study also focused on the measurement of the cutting force using a three-way piezoelectric dynamometer and a charge amplifier. They have found that the coefficient of friction between the cutting tool and the chip of both the graded cutting tools which contains CaF_2 as a lubricant and the homogeneous cutting tool material $WC-TiC-Ni_3Al$, Which is less for the graded self-lubricated cutting tool not only that but it decreases as the cutting speed is increased unlike the homogenous cutting tool, where it increases with increasing cutting speeds. The addition of CaF_2 reduces the coefficient of friction by 12.9–42.6% and reduces the cutting forces subjected to the cutting tool.

Sun *et al.* [167] have developed multilayer graphene-reinforced FG tungsten carbide nano-composite where it was sintered into two steps utilizing hot pressing to avoid possible damage to the structure of the graphene multilayers, since it is damaged if the sintering temperature is kept at a prolonged period, and to obtain highly dense and compact sized grains. Utilizing lower sintering temperatures leads to an increase in hardness while utilizing graphene in an Al_2O_3 matrix [168]. Al_2O_3 is added in this graded ceramic in small percentages from 3 to 6 wt% depending on the sample, and it serves a great purpose in lowering the sintering temperature of WC and suppresses the formation of W_2C. Further adding of TiC can advance the hardness of WC based composite. Besides, combined addition of VC and Cr_3C_2 with a Cr_3C_2/($Cr_3C_2Cr_3C_2$ + VC) ratio of 0.6 to WC–TiC–Al_2O_3 composite become enable to executed higher effectiveness ability for grain

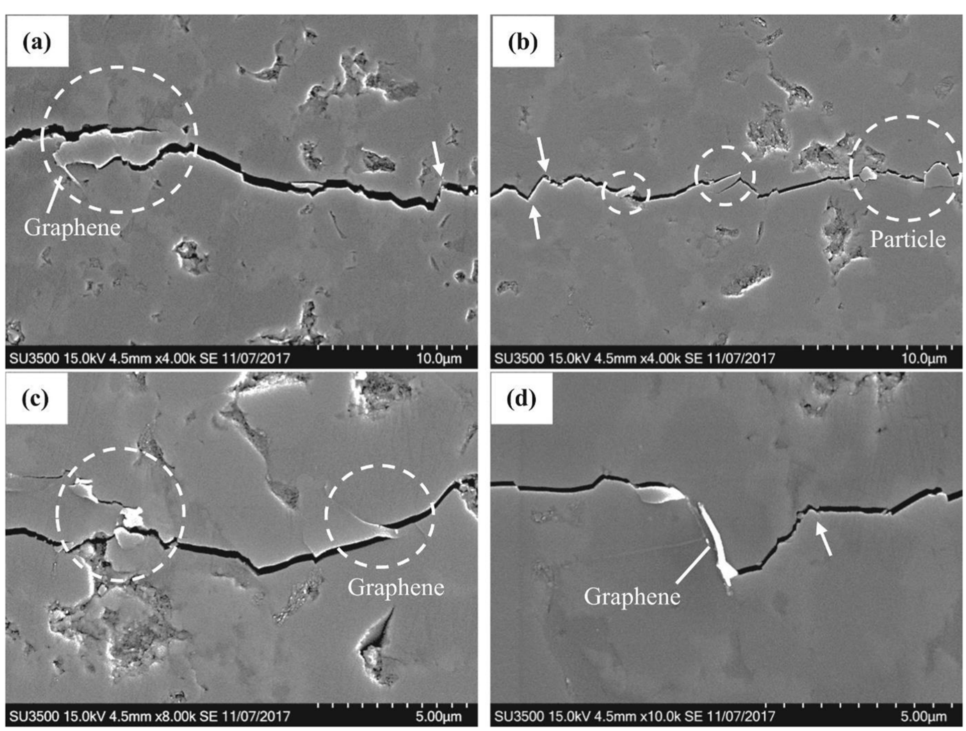

Figure 20: Various kinds of crack propagation phenomena: (a)–(d) graphene nanosheets toughened TiB_2/TiC composite [208].

growth and enhance homogeneous dispersion of Al_2O_3 nano-particulates in WC matrix than single addition of VC or Cr_3C_2. The authors have prepared five samples with varying contents of MLG from one sample of having none to another which has 0.2 wt% of MLG on both its surface and second layers. The graded ceramic has five symmetrical layers. The samples are shown in below Table 1. The sliding test was done between the samples and AISI 1045 steel. The friction coefficient dropped by 73.8% from 0.42 to 0.11 by the addition of MLG which shows the effect of lubricating additives on the tribological properties and it becomes a viable solution in retrospect to traditional lubrication. Graphene has a strong chemical bond between its atoms. But the bonds between the mono layers of graphene are much weaker, during the cutting operation, these mono layers are dispersed on the surface of the tool and the workpiece, creating a tribofilm and ultimately resulting in a reduction in the coefficient of friction [167]. It is reported that MLG containing composites of 0.1 wt% graphene showed an 82.65% reduction in wear rates compared to the monolithic ceramic. The surface topography of both of those samples was measured using a white light interferometer and a laser microscope. Both the depth and width of the wear track on the MLG-containing ceramic are smaller than that of the monolithic ceramic. Adhesion of Fe and O was present on the surface of the monolithic ceramic, which indicates both adhesion and oxidation during sliding, while on the surface of the MLG-containing ceramic, the surface was smooth and free of any ploughing damages or adhesion.

Table 1: Compositions of powder mixtures for five designed samples by weight [167]

Composites	WC	Al_2O_3	TiC	MLG	Cr_3C_2	VC
Ceramic ASL	95	3	2	0	0	0
Ceramic AIL	90	6	4	0	0	0
Ceramic ACL	84	9	6	0	0.6	0.4
Ceramic BSL	94.8	3	2	0.05	0	0
Ceramic BIL	89.8	6	4	0.05	0	0
Ceramic BCL	84	9	6	0	0.6	0.4
Ceramic CSL	94.6	3	2	0.1	0	0
Ceramic CIL	89.6	6	4	0.1	0	0
Ceramic CCL	84	9	6	0	0.6	0.4
Ceramic DSL	94.4	3	2	0.15	0	0
Ceramic DIL	89.4	6	4	0.15	0	0
Ceramic DCL	84	9	6	0	0.6	0.4
Ceramic ESL	94.2	3	2	0.2	0	0
Ceramic EIL	89.2	6	4	0.2	0	0
Ceramic ECL	84	9	6	0	0.6	0.4

SL: surface layer. IL: interlayer. CL: core layer.

Llorente *et al.* [169] have tested the wear and tribological behavior of FG graphene/SiC composites in dry sliding conditions using Si_3N_4 balls as counter bodies. They had five samples with varying volume percentages of graphene of 0 (Monolithic), 5, 10, and 20%. They have also made a GO/SiC composite using SPS in which graphene oxide is reduced to rGO at the sintering temperature. The ceramic powder used is 93 wt% of β − SiC added to it sintering additives of 5 wt% of Y_2O_3 and 2 wt% of Al_2O_3. The dry sliding tests were conducted using a tribometer with a linear reciprocating ball on plate setup. The ball is 10.3 mm in diameter and is made of Si_3N_4. The results of the sliding tests indicate that during the run-in period at the start of the test, the coefficient of friction decreased by 66% for the 20 wt% GGGNP-containing ceramic in comparison to the monolithic SiC. They reported that as the sliding distance continues, the steady-state coefficient of friction for the GNP-containing composites do not show a large improvement over the monolithic ceramic. The reason for the much lower coefficient of friction for the GNP-containing ceramic in the run-in period is that during the initial sliding, graphene layers are pulled from the material and act as wear debris. GNP ceramics exhibit higher wear resistance than bulk materials. This corresponds to the capability of graphene materials to be pulled out and exfoliated to for a wear-protective tribo-film. Graphene outperformed rGO, and the composite containing rGO reduced the wear rate by only 9%. Kim *et al.* [170] presented a research study on the compared graphene oxide, reduced graphene oxide, and exfoliated graphene sheets in an Al_2O_3 matrix and found that exfoliated graphene sheets outperformed graphene in relationship of mechanical and wear properties due to the reduced number of defects piece. The addition of CNTs to Al_2O_3 for self-lubrication was also investigated [171–174]. The mechanical properties of Al_2O_3 also benefit from the addition of small quantities of graphene [175].

6 Syntheses techniques

The number of processing steps necessary for producing ceramic cutting tool inserts with the requisite properties relies heavily on the synthesis methods used. The manufacturing of such tools is subject to numerous limitations and difficulties, especially when FGM with complex compositions are involved. Durability is one of the key criteria when developing cutting tools, and powder metallurgy is frequently employed to achieve this, especially for ceramic tools used in high-speed machining operations. The sintering process includes many phases, starting with the homogeneous combination of powders such as ceramics, solid lubricants, and reinforcements being compacted and formed into the appropriate shapes. These powder combinations are then heated in the furnace and subjected to pressure, where the sintered powders bond together *via* atomic transport, resulting in dense solids due to particle growth. The most essential of these phases is the sintering of the powder mixtures to produce the desired product properties. The main goal of sintering is always to obtain a fully dense product with a controlled microstructure, resulting in the best properties.

The *contact* and *noncontact* techniques are broad classifications of synthesis and sintering technologies used for ceramic cutting tools. Most traditional heating methods are based on three heat transmission modes: conduction, radiation, and convection. Because the heat energy is in direct touch with the specimen, these procedures are classified as direct contact methods. Other noncontact heating methods include radiofrequency, induction, and microwave heating because the specimens are heated by electromagnetic radiation [176]. Traditional high-pressure sintering (HPS) and SPS are the most often employed contact methods for ceramic-based tool inserts [177]. The traditional HPS process often necessitates an elevated working temperature slightly lower than the matrix's melting point, as well as a relatively extended holding time, which results in superfluous grain formation and poor mechanical properties [178]. SPS, an advanced technique, has enabled the sintering of powders and subsequent bonding in a very short time and low temperature by using electric energy with high-intensity plasma as a source of high temperature. Because of the lower sintering temperature and faster processing, the SPS leads to smaller grain growth, which results in suppressed powder decomposition and a controlled microstructure in the sintered insert [179].

MS is a relatively new noncontact pressure-less sintering technique that recently found a number of advantages over typical heating procedures. When compared to conventional hot and cold sintering processes, the MS technique is regarded as a rapid, efficient, and flexible sintering method that involves relatively lower energy consumption, short processing time, higher heating rate, and cheap production cost [180]. When compared to conventional sintering, the quick heating during MS is due to energy conversion rather than energy transfer, which results in volumetric heating and hence reduces processing time and densification temperature [181]. Table 2 shows a comparison of commonly used synthesis techniques using contact and noncontact methods [119]. The table compares the crystal sizes obtained by various sintering techniques. It should be noted that the evolution of a finer or coarser crystal size is dependent on the sintering parameters utilized in a particular sintering technique, such as sintering temperature, dwell/holding duration, pressure level, and so on. To achieve a controlled grain size with a homogenous and dense microstructure, a precise balance of temperature and sintering time is required. HPS and conventional noncontact heating at high pressure often result in coarse grains due to abnormally long sintering times and high temperatures, leading to worse properties. The main disadvantage of employing HPS is the compromise on sintered product homogeneity as a result of getting anisotropic properties, as well as the poor production rate as a result of the extended sintering time [182]. SPS, on the other hand, produces finer grain sizes when ceramic materials are

Table 2: Characteristics of commonly used synthesis techniques for cutting tools [119]

	Contact heating methods		**Non-contact heating methods**	
	HPS	**SPS**	**Conventional heating and sintering**	**MS**
Sintering duration	Long	Short	Long	Medium
Sintering temperature	High	Medium	High	High
Holding/dwell time	Long	Short	Long	Medium
Heating rate during sintering	Slow	Fast	Slow	Medium
Temperature gradient sintering	↓	+	↓	−
Grain boundary controlled sintering	↓	+	↓	Δ
Crystalline structure/grain size	Coarse	Fine	Coarse	Medium
Homogenous sintering	Δ	−	Δ	+
Production rate	Δ	+	Δ	−
Investment in equipment	Δ	+	Δ	−
Cost of running the equipment	Low	High	Low	Medium

Excellent (+), Good (−), Fair (Δ), Difficult (↓).

sintered at lower temperatures and shorter processing durations than other standard procedures such as HPS [183].

Many studies have been conducted on the effect of sintering aids on influencing the microstructure and grain size in addition to the processing parameters. The recent study [184] found that MS has better mechanical properties than traditional sintering procedures. This is mostly due to increased grain size and densification as a result of volumetric heating, as well as a lower sintering temperature and shorter sintering time.

Earlier research in the field of FGMs utilized tape casting, hot pressing, and cold isostatic pressing compaction followed by pressure-less sintering or a combination of the aforementioned techniques. Table 3 shows some of the selected literature utilizing these traditional techniques. More recent literature work relied heavily on SPS or MS, and the advantages of each will be explored below. A new frontier in the fabrication of FGMs is the use of AM techniques, such as laser-based processes. AM enhances the fabrication methods of graded materials by increasing control and an enhanced spatial resolution [13,185]. AM also adds the potential for porosity control [186], which could be beneficial in the design of cutting inserts or other FG parts. Some current research results are described in the following subsections to emphasize the applications of the most important techniques such as HPS, SPS, and MS processes for the development of ceramic composites in general and ceramic-based FGCTs tools in particular.

6.1 HPS

As discussed, HPS is a sintering technology that uses pressure to compact the powder during the sintering process. This pressure acts as an extra driving factor for densification, resulting in higher densities and better mechanical characteristics. Depending on the material being sintered, the pressure can be applied at a variety of temperatures. HPS generally necessitates greater temperatures than pressureless sintering. HPS has a number of advantages over pressureless sintering such as high densities, improved mechanical properties, reduced sintering time, and improved grain size control. However, HPS also has some disadvantages, including more expensive equipment, more complex process. Potential for damage the powder compact if the pressure is applied too quickly or unevenly.

Jianxin *et al.* [187] created an Al_2O_3/TiC cutting tool doped with CaF_2 as a solid lubricant using a hot-pressing sintering process. The raw powders were first ball-milled in alcohol for 100 h with cemented carbide balls, then dried, and compressed at a pressure of 100 MPa. They found that adding CaF_2 to the Al_2O_3/TiC matrix reduced fracture toughness, flexure strength, and hardness while improving tribological responsiveness. Wu *et al.* [188] used the hot pressing process with a vacuum at 1,550°C and 25 MPa pressure to produce Al_2O_3/(W,Ti)C cutting tools with CaF_2 and CaF_2@Ni as solid lubricants. The solid lubricants were added at a later stage of milling before sintering to prevent the Ni coating on the CaF_2 core from damage. When Al_2O_3/(W,Ti)C with CaF_2@Ni sintered samples are compared to Al_2O_3/(W,Ti)C with uncoated CaF_2 sintered samples, a more uniform and homogeneous microstructure is formed. This was related to enhanced densification as a result of liquid nickel at elevated temperatures, which resulted in grain growth control. Wu *et al.* [189] also used a hot sintering technique to produce Al_2O_3/(W,Ti)C composites with hBN and hBN@Ni as solid lubricants and reported enhanced mechanical properties as a result of Ni coating on the hBN for the reasons stated earlier. Chen *et al.* [165] used vacuum sintering to create Al_2O_3/TiC/CaF_2 and core–shell Al_2O_3/TiC/CaF_2@Al_2O_3 tools. The powders were wet dispersed, ball-milled, vacuum burned, sieved, and then filled in the required die before hot sintering. Densification during hot pressing was found to be better in the case of Al_2O_3/TiC/CaF_2@Al_2O_3 ceramic tools compared to uncoated CaF_2 ceramic tools. Because of its compatibility with the matrix material, the Al_2O_3 coating on CaF_2 increased its microstructure and mechanical properties.

6.2 SPS

SPS, also known as Field-assisted sintering technology (FAST), is a key technique that plays an excellent role in the fabrication of FGMs for high-performance applications, and SPS is based on the Joule heating principle by using a pulsed DC current, which passes through the graphite die and the sample for creating a uniform heating media along with uniaxial pressing by pistons [190]. One of the most important benefits of SPS is its low power consumption and high efficiency in comparison to the traditional hot isostatic pressing HIP method. Due to their very high heating rates >100°C·min^{-1} and their short sintering time, SPS does not require the addition of additives. Having a short sintering time is important to retain certain microstructural features that would otherwise differ in conventional methods such as having fine grain size and nano-scale microstructure [191]. Also, it may be useful to protect the microstructure of various lubricating additives such as graphene. SPS has been used extensively in recent times for FGMs [192–196].

Table 3: Some selected literature on ceramic composite fabricated by hot pressing or tape casting

Year	Ref.	Syntheses	Layers	Matrix	Sintering additives	Functional additives	Property tested	Sintering temp (°C)	Soaking time	Press pressure
2018	[101]	Hot pressing	5	TiC	NiO, MgO	Ni Mo Al_2O_3	F.S = 761 MPa, HV = 21.22 GPa, K1C = 9.07 MPa	1,700	10 m	32 MPa
2017	[198]	Hot pressing	1	Si_3N_4	Yb_2O_3, CeO_2	NA	K1C = 7.61–8.89	1,700–1,800	4 h	30 MPa
2014	[100]	Hot pressing	2	Al_2O_3, $ZrO_2(3Y)$	NA	SiC	HV = 20.6 GPa	1,650	30 m	25 MPa
2013	[155]	Hot pressing	5	Si_3N_4	8 vol% (Al_2O_3 + Y_2O_3)	TiC0.7N0.3	HV = 16.91 GPa, K1C = 9.54 GPa, F.S = 980 MPa	1,700	1 h	35 MPa
2013	[199]	Hot pressing	21	Al_2O_3, ZrO_2(3Y)	Y_2O_3, CuO	TiO_2 $BaSO_4$ CaF_2 Graphite	F.S = 348 MPa, K1C = 3.89, Hv = 12.7, work of fracture (J·m^{-2}) = 572	1,350	100 m	25 MPa
2013	[200]	Hot pressing	1	Al_2O_3, ZrO_2(3Y)	NA	3 vol% Co 40 nm TiC 0.4 μm TiC	F.S= 916 MPa, K1C = 8.3, hardness = 18 GPa	1,650	20 m	32 MPa
2013	[201]	Hot pressing	1	Si_3N_4	4 wt% Al_2O_3 6 wt % Y_2O_3	ZrO_2 3 wt% of exfoliated graphene	Porosity 20.1%, HV5 = 7.7 GPa	1,700	3 h	20 MPa
2007	[124]	Hot pressing	3	Ca-α-SiAlON/Ti_3SiC_2	NA	NA	—	1,600	60 m	20 MPa
2006	[202]	Tape casting	25	α and β SiAlON	Y_2O_3	NA	CIP sample HV2 = 17.5–14.5 GPa	1,800	1 h	15 + 7 MPa
2004	[127]	Hot pressing	2	α-SiAlON, β-SiAlON	Y, Ca, Sm	NA	Hardness = 19–15 GPa	1,700-1 h, 1,700-2 h, 1,800-1 h	1–2 h	300 MPa
2004	[113]	Cold isostatic pressing + hot pressing	2	α-SiAlON, β-SiAlON	Y_2O_3	NA	Hardness outer = 20 GPa, fracture toughness rim = 6.4 fracture toughness core = 5.8	1,780	2 h	30 MPa
2001	[203]	Hot pressing, hot isostatic pressing	1	Si_3N_4	Y_2O_3: Al_2O_3: SiO_2	TiB_2	Hot pressed HV = 17.4 GPa, KIc = 4.9, HIP KIc = 5.8 MPa	Hot pressing 1,500–1,700, hot isostatic pressing 1,550–1,700	NA	HP 30 MPa, HIP 160 MPa
2001	[204]	Hot pressing	20	Si_3N_4–Al_2O_3	Y_2O_3, Al_2O_3	NA	F.S = 581 MPa	1,700	2 h	50 MPa

The transition from small lab-scale tools for batch production to larger furnaces suitable for industrial production has been made possible by recent improvements. One significant factor is the lowering of the whole cycle duration, particularly the time-consuming phase for big samples of cooling to room temperature. Guillon *et al.* [197] reported the development of SeProFAST project (similar to "FAST" system) to effectively develop near-net-shaped products such as facetted cutting tool inserts with a cycle time less than 1 min.

SPS has been used extensively to fabricate FGMs in ceramic cutting tool inserts [205], to overcome challenges that relate to the high melting point and low diffusion coefficient of some ceramic-based inserts [206,207]. Yin *et al.* [208] fabricated TiB_2/TiC composite ceramics that contain 0.1% of graphene by using SPS at 1,800°C with a holding time of 5 min. TiB_2 has an intrinsic problem when it comes to sintering, which is its strong covalent bonding which requires high temperatures. The addition of graphene to this material increased the fracture toughening by 31.7% due to graphene bridging and crack deflection as shown in Figure 20 [208].

Bertolete *et al.* [152] have developed two types of FGM cutting inserts with six layers using an SPS at 1, 300°C and a holding time of 5 min. The composition of that inserts is presented in Table 4. They conducted machining process evaluations for the fabricated inserts on a traditional lathe by turning martensitic stainless steel (276.4 HV_{30}) at a cutting speed of 100 $m{\cdot}min^{-1}$, a feed rate of 0.205 $mm{\cdot}rev^{-1}$, and a depth of 2 mm. The results of the cutting forces are shown in Figure 21 for the two main FGM cutting tool inserts in comparison to cemented carbide cutting tool inserts. Along with the turning evaluation, a microstructure investigation was conducted to determine whether cracks have formed, and the results that confirm no cracks have developed which emphasizes the importance of modeling the various properties at the initial stages of the design before fabricating any insert.

Table 4: Al_2O_3 and cemented carbide volume fractions for the FG ceramics [152]

Layers	Volume fraction %	
	Al_2O_3-ZrO_3 or Al_2O_3-TiC	WC-Co
1	100	—
2	86	14
3	79	21
4	72	28
5	58	42
6	44	66

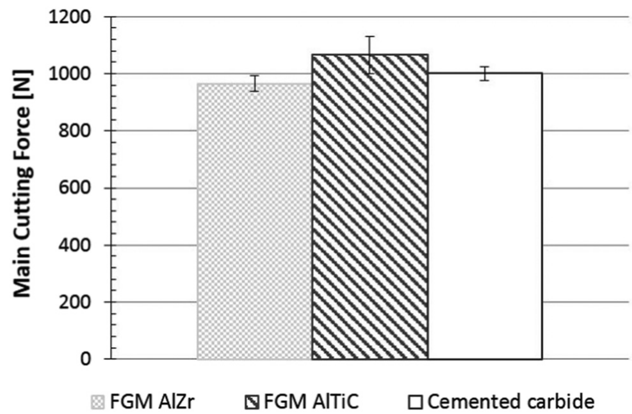

Figure 21: Cutting force results for turning martensitic stainless steel using FGM AlZr, FGM AlTiC, and conventional cemented carbide cutting tools [152].

SPS can become a disadvantage with powders that have low electrical and thermal conductivity and electric resistance of more than 1 Ω·m [209], but it can be overcome if the initial powders used included an electrically conductive element as shown in the work of Gutiérrez-González *et al.* [210], where they have managed to fabricate a composite of the following composition by 52 wt% of Al_2O_3, 26 wt% SiC_w, and 22 wt% TiC. The sintering was done at 1,780°C and a holding time of 2 min. Various tests were done including machining and a ball-on-disk wear test, and it showed a significant reduction in wear rate compared to a standard SANDVIK Coromant CC670. It is projected that this new material has a service life five times that of the standard insert. Y_2O_3 and Al_2O_3 are usually added to Si_3N_4 as sintering additives [211].

SPS is capable of producing functionally gradient Al_2O_3 ceramic in a single step, which offers a totally new era for the research and development in FGM cutting tools [212]. SPS can also be used to test and assess the diffusion pairings of different tool materials and workpieces, as demonstrated by Çelik *et al.* [83]. The authors have developed a novel technique to measure the diffusion between the Inconel 718 alloy and the manufactured specimens by carrying a diffusion couple test. From the prepared specimens in the gas sintering furnace, a cylindrical pellet was cut from two specimens sandwiching a specimen of Inconel 718 and put in a graphite mold in an SPS furnace to simulate the possible diffusion in the cutting temperature range.

6.3 MS

The issue with hot pressing is that heat is generated by external sources and then transmitted to the manufactured sample *via* heat conduction. The phenomenon of heat transmission occurs when heat is transported from the sample's surface to its core. The heat distribution is non-uniform and a gradient is created across the thickness of the sample. This leads to unwanted residual stresses and effects on material properties. MS furnaces generate electromagnetic energy, which is absorbed by the full volume of the sample and converted into heat. This removes any undesirable thermal strains. Another advantage is that lower sintering temperatures and shorter processes are required [213].

There has recently been progress in MS of FG ceramics, including cutting tools, by using electromagnetic radiation to raise the temperature and densify the ceramic powders [45,214,215]. There are many advantages to MS compared to traditional methods which include:

- Short sintering time.
- Lower energy consumption.
- High heating rates.
- High-density materials can be obtained.
- Flexible geometry compared to SPS.

The energy in MS is electromagnetic with a frequency ranging from 300 MHz to 300 GHz, and the material is heated up when it absorbs the electromagnetic energy volumetrically. When compared to conventional heating methods, this technology has the advantage of improved heat diffusion, lower energy consumption, and shorter production periods, especially when compared to hot pressing [181]. Tang *et al.* [166] have prepared a FG and self-lubricating insert composed of WC, TiC, Ni_3Al, and CaF_2 using MS. Due to insufficient density, this combination of materials *via* a typical sintering procedure resulted in low overall hardness. MS was used to tackle this type of issue since it minimizes the activation energy necessary to achieve densification.

Cheng *et al.* [213] have developed A_2O_3/TiC ceramic cutting tool by MS and compared its cutting performance to that of a hot-pressed tool of the same composition. The material used in the cutting operation is 40Cr hardened alloy steel and T10A hardened tool steel. The sample prepared was using a 2.45 GHz furnace at 1,700°C for 10 min. After the turning process of 40Cr alloys steel the microwave-sintered ceramic cutting tool showed a higher tool life for various cutting speeds (173, 260, 350 m·min^{-1}) in comparison to that made by hot pressing, and this was measured by the total cutting length of each tool, which gives an accurate measure of the tool life. Figure 22 shows the wear damage on the flank of the sintered tool, which shows both adhesion and abrasion wear. As can be observed in Figure 22(a) and (b), the abrasive wear is characterized by the grooving line.

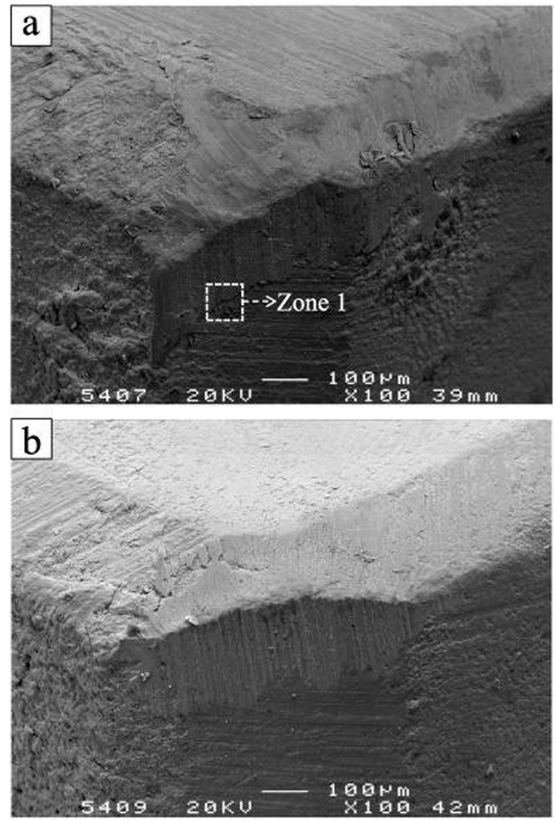

Figure 22: SEM micrographs of the microwave sintered ceramic insert after turning of hardened steel 40Cr at the cutting speed of (a) 260 m·min^{-1} and (b) 350 m·min^{-1} [213].

Menezes and Kiminami [216] were able to fabricate Al_2O_3 composites with varying volume fractions of ZrO_2 using MS in 35 min and obtained a uniform microstructure without any pores and cracks and reached 99% of the theoretical density. This was achieved as a result of the short sintering cycle they were able to suppress unwanted grain growth.

7 Numerical modeling: process and performance simulation

Understanding the machining process of ceramic types of cutting tools on different materials such as composites and alloys requires numerical modeling and simulation for performance analysis of FG ceramics cutting tool inserts. Therefore, the implementations of simulation study are essential in the design of FG ceramics cutting tool inserts to predict the two most important criteria. The tool life, morphology of machined surface, and machinability performance of cutting tools are the key factors, and hence, carefully tailored properties are essential to improve these factors. The simulation must take into consideration the manufactured tool (composition, number of layers, geometry, *etc.*) along with the cutting process parameters. Cutting processes are complex, and all variables, such as cutting speed, cutting conditions, feed rate, and depth of cut, are interdependent. Each cutting process must be optimized for a specific workpiece material, which has a direct impact on tool wear and machining topography. This makes the use of FEM simulations for the design and development of FG ceramic cutting tool inserts essential.

Fattahi *et al.* [190] simulated an SPS process to sinter TiB_2 sample to obtain the current density and temperature profile of the sample with various holding times and sintering temperatures. FEM can also be used to determine the thermal residual stresses during the design phase as shown in the work of Zhu *et al.* [87]. By modeling the composition, thickness, and number of layers of inserts that are comprised of TiB_2/TiN/WC, they found that with an increase in the number of layers, the mechanical properties are enhanced, and thermal residual stresses are reduced. Von Mises stresses were also investigated by FEM simulations during the design stage by Wu *et al.* [217] for the fabrication of Al_2O_3/TiC/CaF_2 multicomponent gradient self-lubricating ceramic.

Wang and Liu [218] conducted 2D FEM simulations in Abaqus/Explicit due to its capability to avoid convergence, which may be caused by the contact or material complexity. They used the Johnson-Cook (JC) model to simulate material degradation and chip formation mechanisms. The purpose of conducting FEM simulation is to investigate the JC fracture constants on the chip formation while cutting Ti_6Al_4 compared to those to experimental values. The authors found both the experimental and numerical analyses in close agreement. The most interesting results that can be obtained from FEM simulations are as follows:

- If cutting speeds increase, the chip serrated degree increases until it fragments as units as shown in Figure 23. This highlights the accuracy of the FEM study compared to actual chips from the cutting process.
- If the cutting speed increases, the cutting force decreases until the chips transform from serrated to units at ultra-high cutting speeds. This led to a rapid increase in both the fluctuant frequency and the fluctuant amplitude of the cutting force, which was associated with the chip formation zone that transitioned from ductile to brittle.
- When the JC fracture constants decrease, the shear localized sensitivity is positive and *vice versa*.

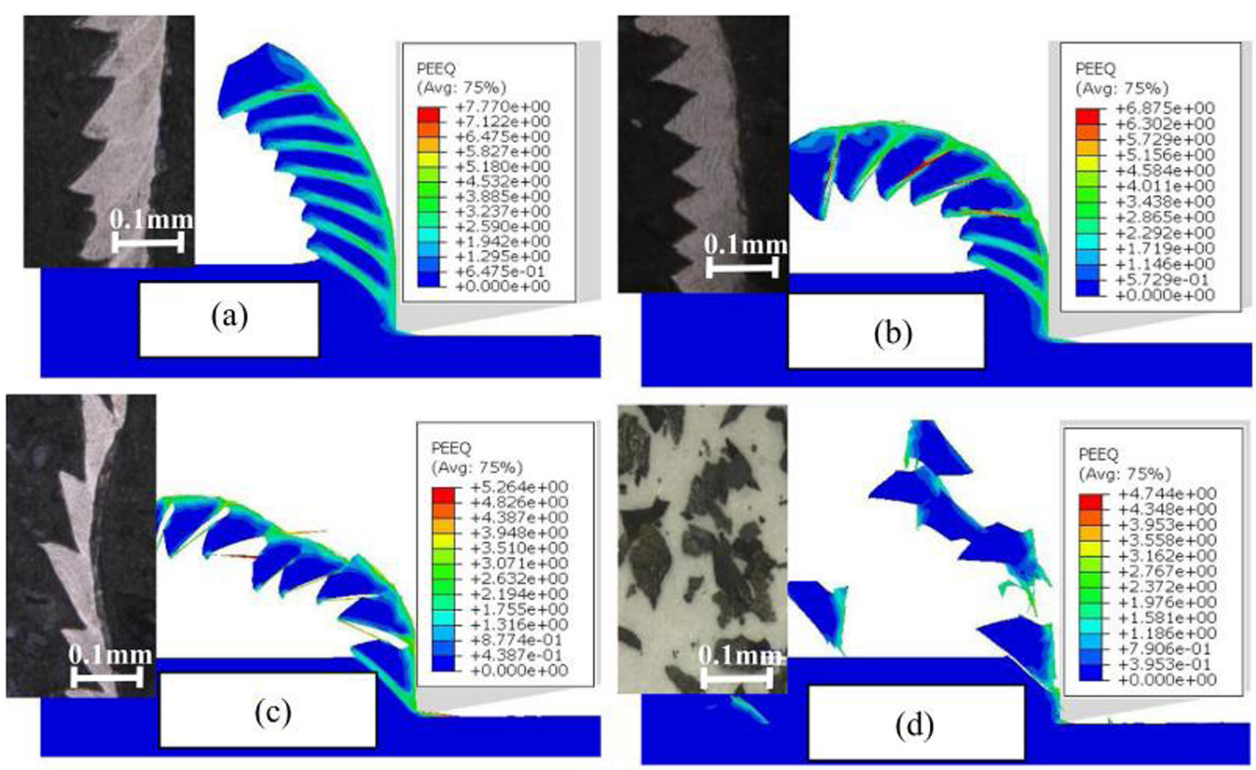

Figure 23: Variation of chip morphologies with different cutting speeds [218]. (a) 50 $m \cdot min^{-1}$ (b) 500 $m \cdot min^{-1}$ (c) 1,500 $m \cdot min^{-1}$ (d) 2,500 $m \cdot min^{-1}$.

AdvantEdge® software is widely used as dedicated software provided by Third Wave Systems for the simulation of machining. It has a built-in library containing 140 materials, including widely used Inserts. The software works to optimize the cutting process to counteract certain tool damages such as abrasive wear by reducing pressure and temperature or chipping by reducing principal stresses *etc*. AdvantEdge® also provides chips analysis, which is important for the integrity cutting apparatus and the mechanical properties of the workpiece. Because the software is designed for industrial use, utilizing it for simulation is a simple process, especially if the cutting method and materials are generic. The software does not contain an option to functionally grade cutting tool inserts, but there is an option to add seven layers of coating to the insert, which can be used theoretically as FGCT inserts. Coolants can also be simulated by inserting the properties of the coolant and its contact area whether it is fully immersed or excluding the tip area. Tecplot is a powerful model to accurately measure the cutting temperatures and forces on both the cutting tool inserts and the workpiece.

FEM Simulations in AdvantEdge® can be simulated as 2D or 3D models. The 2D simulation models of the cutting process are excellent for displaying the machining result and are relatively quick to look at how cutting angles (rake, relief, and edge) affect the machining outcomes, chip formation, and temperatures without going deep into the 3D models. The 3D models are excellent to determine stresses in the cutting tool inserts along with temperatures and chip shapes and loads. Tool designs can also be imported from Alicona STL files. Alicona has very interesting machines and applications, for example, their COBOT system is used to measure tool and workpiece life and wear mechanism as a real-time measurement during manufacturing. They also have 3D scanning machines to analyze the tools postcutting for an accurate measure of tool wear.

Feng *et al.* [219] have used AdvantEdge® to simulate the cutting performance on three of their *in-situ* formed ceramic cutting tool inserts with micro-texturing on the rake face. They used graphite grains in these micro-textures to provide self-lubricating films. The base material is a ceramic that contains the following constituents Al_2O_3, TiC, MgO, and Mo. The cutting temperature and stress field predicted from the simulations are shown in Figures 24 and 25.

Following the FEM simulation, it is critical to validate its accuracy, particularly cutting temperatures, by conducting a turning machining process performance

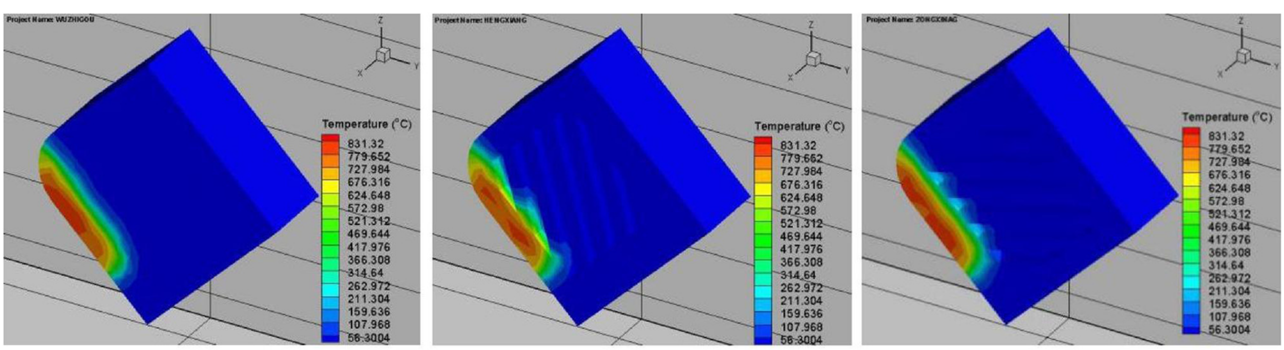

Figure 24: Temperature profile of using different directions of micro texturing on the rake face [219].

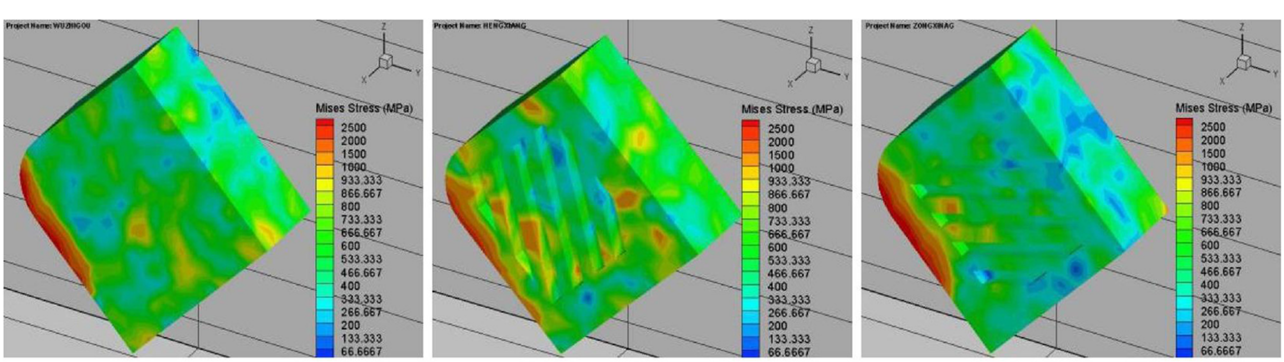

Figure 25: Von Misses stress distribution of the various inserts [219].

evaluation. This can be accomplished by monitoring the temperature of the cutting process using thermography. Another method is to evaluate the insert's microstructure and compare it to conventional and commercially available cutting tool inserts. AdvantEdge software can also be used to simulate chip profiles and thickness, which must be understood ahead of time so that these chips do not curl around workpieces or fixtures [220]. Chip morphology is also important to determine the mechanical and thermophysical properties of the workpiece being machined. Ji *et al.* [220] performed the study on the chip morphology of the cut 17-4 PH stainless steel. They performed the machining process using through the graded cermet cutting tools. The morphology is shown in Figure 26 with different cutting speeds. As the cutting speed increases, the cutting temperature rises, reducing the strength of the workpiece and making chip breaking more difficult owing to plasticity.

Xu *et al.* [63] performed the FEM modeling to design FG ceramic cutting tools composed of Al_2O_3/TiC/CaF_2 layers (the so-called ATC) with CaF_2 as a self-lubricating layer. They studied the residual stresses with different compositional distribution exponent (n) values considering symmetrically distributed gradient ceramic tools. The optimum design results were then used to fabricate a gradient self-lubricating ceramic tool material with target mechanical properties using the hot-pressing method. The contour plots of the FG structures are shown in Figure 27(a–d), which demonstrates that the distribution of radial stresses is symmetrical. Furthermore, regardless of the value of the distribution exponent n, the maximum tensile stress happens in the middle layer and the maximum compressive stress exists in the surface layers. Moreover, as shown in Figure 27(e), when the component distribution exponent n varies between 0.6 and 1.2, the maximum radial tensile stress reduces noticeably and the maximum radial

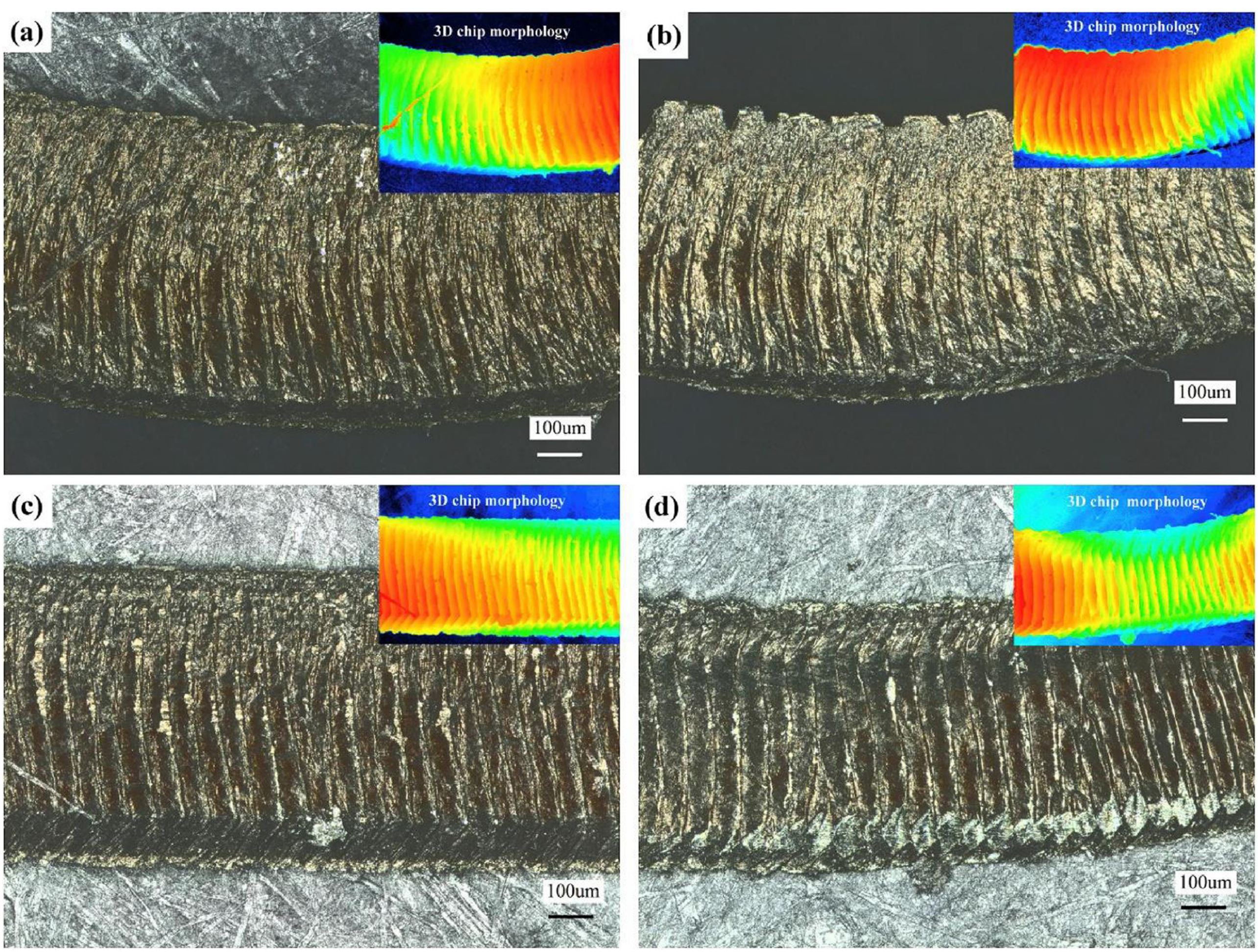

Figure 26: Morphology at different speeds: (a) 150 m·min^{-1}, (b) 200 m·min^{-1}, (c) 250 m·min^{-1}, and (d) 300 m·min^{-1} [220].

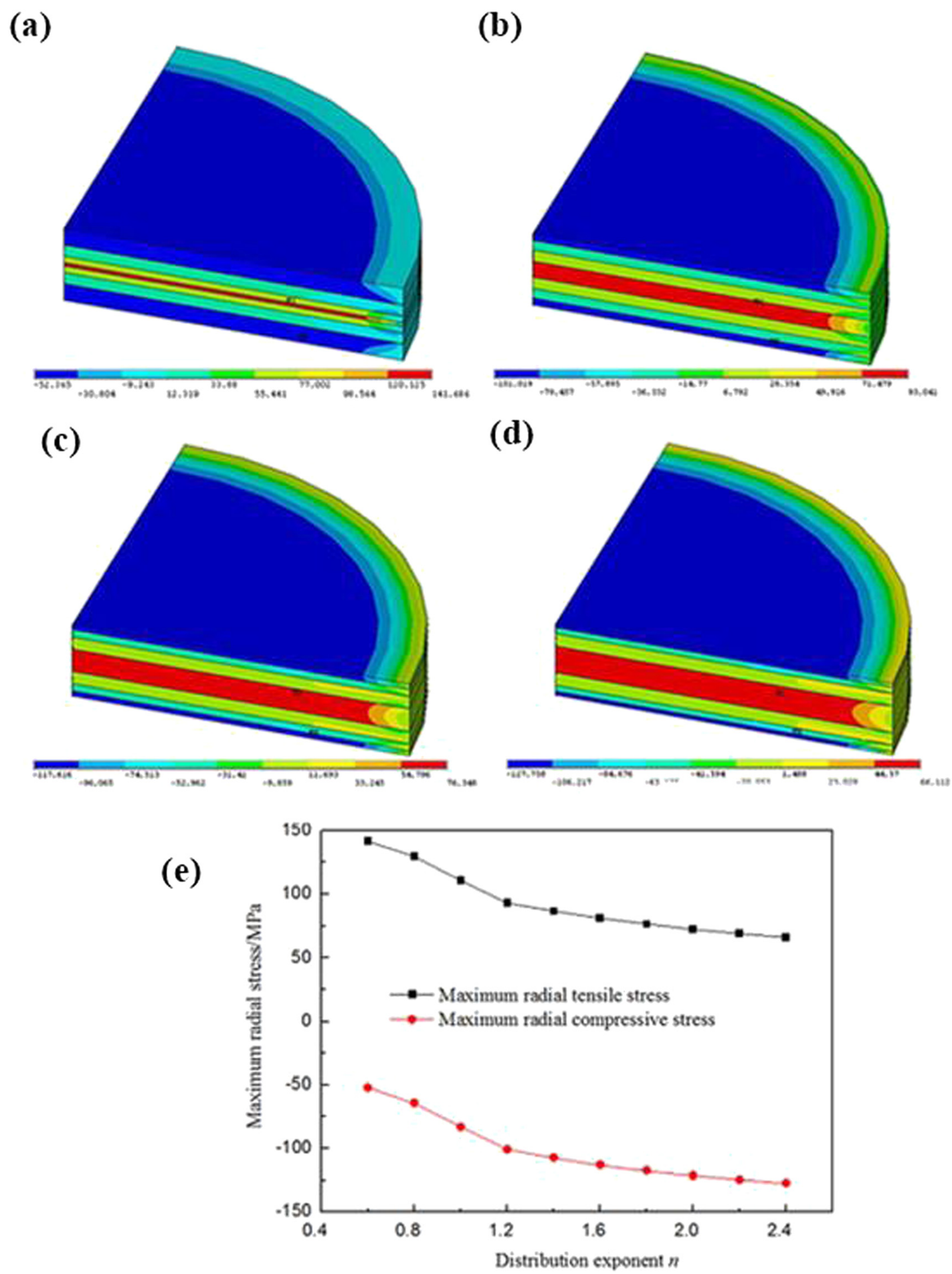

Figure 27: Images of radial stress for ATC self-lubricating ceramic tool: (a) n = 0.6, (b) n = 1.2, (c) n = 1.8, (d) n = 2.4, and (e) the maximum radial tensile and compressive stresses versus distribution exponent n [63].

compress (absolute value) rises noticeably. However, when *n* varies between 1.2 and 2.4, both stresses change gradually. They demonstrated that the residual stresses calculated using FEM and indentation crack measurements with real samples were in close agreement.

8 Research gaps and future directions

Because of the complexity of cutting operations on difficult-to-machine alloys such as Inconel 718, comparing various cutting tools as found in the literature is a difficult task due to large variations in workpiece materials and cutting setups, and because tool wear is governed by the tribological system, which is a system response [63]. The use of FG ceramic cutting tool inserts is a potential solution to improve the tool life and workpiece machined surface. Research in this field lacks a systematic machining setup to directly compare various cutting tools and workpiece materials. SiAlON is a promising material for machining hard-to-cut alloys, but there is limited research on how FG SiAlON-based materials influence tool wear and machined surface. The optimum lubricating additives such as MLG and CaF_2 have not been thoroughly investigated. It was shown in the literature that reducing the cutting forces results in a prolonged tool life, which is done at high-speed machining, where the workpiece material is softened but at temperatures below the softening of the tools. Lubricating additives and their performance when added in FG tools at elevated temperatures have not been properly investigated.

The most current FGCTs have been found to be either Al_2O_3 or Si_3N_4-based, with no direct comparison identified in the literature, owing to the lack of established cutting tests and procedures. Using FGCT inserts for cutting operations is still a new field, and there is no one cutting tool insert configuration that can be considered a standard for super-alloy cutting. A FG ceramics cutting tool insert based on SiAlON is a viable candidate. More research is needed on functionally grading cutting tools, utilizing them with additives for self-lubrication and dry-cutting operations, and increasing fracture toughness and tool wear resistance.

The computational design approach is most likely the most essential tool that can lead to the development of FG materials with tailored properties through systematic property management. Experimenting with property–microstructure relationships can aid in developing the constitutive behavior of the resulting composite graded structures and identifying macroscopic response. Excessive labor and manufacturing expenses result from the hit-and-trial experimental approach to FG composite synthesis. Computational modeling and simulation can be used to study the composition and structure of a material before it is developed. There has been a very limited amount of research available in the literature, which focuses on the utilization of computational modeling to design the FG cutting inserts. Recent work by the author and his coworkers [61] describes a systematic computational material design technique with an emphasis on ceramic cutting tools. To predict the optimum structural and thermal properties for the desired properties of cutting tool materials, they develop codes based on the mean-field homogenization approach and effective medium approximation. Figure 28 shows their general design and development method.

A similar approach based on the mean-field homogenization model was also used in another study by Akhtar *et al.* [90] to improve the mechanical and thermal properties of Al_2O_3 by the inclusion of nickel with varying compositions 5, 10, 15, and 20%. This composite was sintered by an SPS at 1,400°C. The authors have recently designed and developed FG Co/hBN and TiCN/h-BN Yb_2O_3-SiAlON

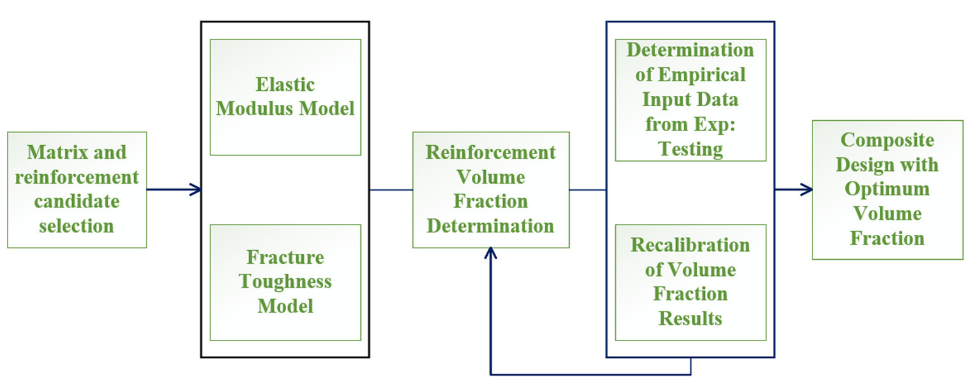

Figure 28: Steps in the design of FGM inserts.

composites as insert materials for high-temperature cutting operations [221]. The FG SiAlON composite has inhomogeneities at two scales, *i.e.*, within the individual layer (mesoscale) and bulk layered structure (macroscale). As a result, it was essential to use a two-scale modeling approach to optimize the FG SiAlON composite's useful properties. To estimate the useful properties of the FG SiAlON composite, the study suggested combining the predictions from the mean-field and computational homogenization theories. The useful properties of the individual layers in the FG structure are estimated using the mean field homogenization theories using chosen inclusion material, particle sizes, volume fractions, porosity, interfacial properties, *etc*. The effective characteristics of the bulk laminated FG structure are then predicted using computational homogenization theories. The key composite parameters needed to accomplish the desired structural and thermal properties for the FG composite are optimized using computational simulations developed using homogenization theories. Based on the results of the computational simulations, FG SiAlON-based hybrid ceramic cutting tool inserts were synthesized by SPS as a validation followed by testing and characterization. The approach is summarized in Figure 29. The properties predictions of the FG composites were found in close agreement with the experimental results. Apart from tailoring the thermal and mechanical properties from core to the surface of the insert, a prolonged interfacial crack growth and high strain energy density formed in the topmost layers due to the development of compressive residual stresses has significantly increased the interfacial fracture toughness of the FG TiCN/hBN/SiAlON composite. As a result, the FG TiCN/hBN/SiAlON composite outperformed all prepared composites in terms of structural and thermal performance for the intended application.

Furthermore, in the future, research should be conducted on various other approaches such as microscale and mesoscale modeling for FGMs to analyze and measure the performance and changing behavior of various material properties, predictive phase diagram modeling, microstructure models, and the different combinations of other materials. Because various industries are quickly growing toward AM technology, it can also be studied and implemented for the development process of ceramic FGMs for

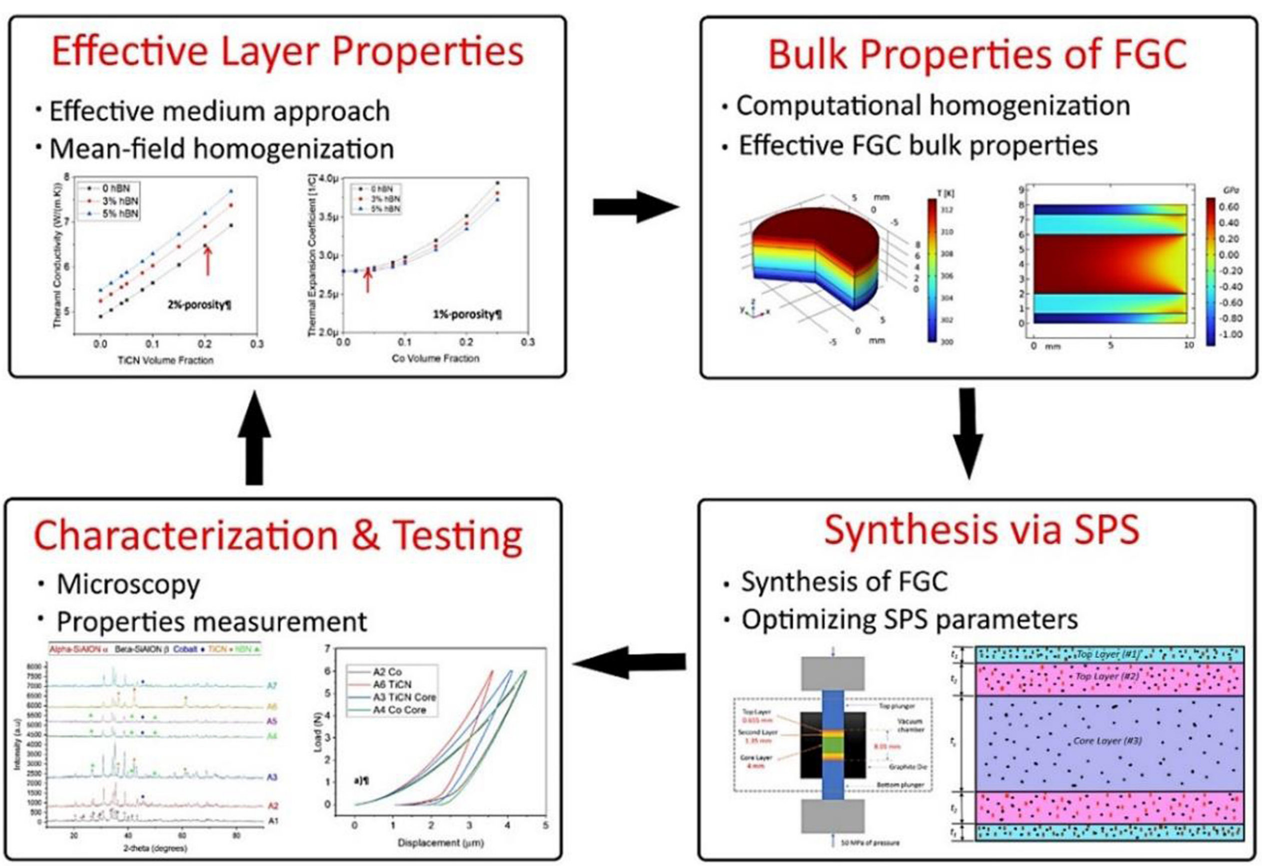

Figure 29: An integrated approach: A multiscale computational approach, synthesis of FG composites, characterization, and validation framework developed for SiAlON-based FG composites [221].

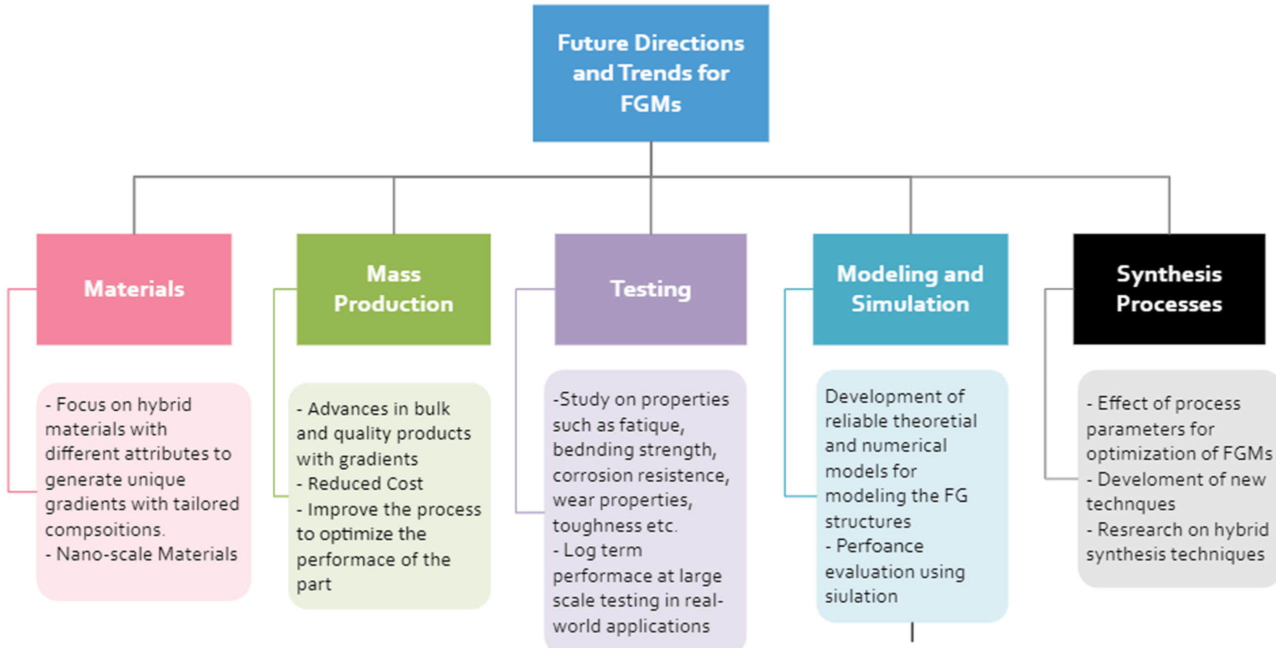

Figure 30: Future directions and trends for FGMs.

various purposes. However, there is a need to work on appropriate AM process methods and their parameter optimization for optimum performance of developed parts. Figure 30 depicts the various future directions and trends for FGMs, such as various types of materials, mass production techniques, testing, simulation methodology, and synthesis techniques.

9 Summary and outlook

A thorough review of the current state and future trends in ceramic-based FGCTs has been conducted. Significant research interest and published work have been uncovered, especially in the previous 10 years. These materials have the potential to form the basis of a novel technology that could improve the performance of cutting tools. They have already made significant contributions to the subject, and there is yet room for additional research and improvement. FGCTs are ideal for cutting difficult-to-machine materials such as superalloys and composites. Nevertheless, the design of these tools is a complex process that needs considering a variety of requirements, including material properties, machining application, and cost. Moreover, FGMT fabrication is a challenging process that requires the use of modern manufacturing techniques such as powder metallurgy and additive manufacturing. There is still a need for the development of novel production methods capable of manufacturing FGMTs with high precision and quality.

In contrast to bulk and homogeneous cutting tool inserts, functional grading approach adds layers to the design. The design includes variables such as the number of layers, thickness ratio, the volume fraction of secondary phases, nano- or micro-sized particles, and solid lubricants. The development of FGCTs is impeded by the involvement of too many variables and relying on experimental trial and error. A very limited work is found on the systematic computational material design, process modeling, simulation, and numerical optimization, which is essential to develop innovative FGCTs with target properties with minimum cost. Several researchers have worked hard to develop several models for predicting the properties of FGMs using different techniques such as analytical, numerical, and theoretical. According to the papers reviewed in this study, it appears feasible for designers to develop novel FGCTs for various machining configurations. Based on considerable experimental data, more comprehensive and systematic computational models may be developed that describe the effect of intrinsic matrix and secondary phase properties and their combinations in the FG structure, and synthesis techniques. This may give rise to tailored structural, thermal, and tribological properties of such tools for specific applications.

The self-lubricating phase of FGCTs can aid in reducing friction between the tool and the workpiece, which can result in a variety of benefits, including improved wear resistance, enhanced machinability, reduced cutting forces, and improved chip control. In general, no single lubricant type can deliver the required low friction coefficient under a wide range of working conditions. Alkaline-earth fluorides (especially CaF_2), lamellar solids with layered structures, and hBN are the most researched high-temperature solid lubricants for ceramic cutting tools. In general, these materials displayed better tribological performance over a wide temperature range. However, various constraints such as sintering difficulty, susceptibility to humidity and high temperatures, and decomposition make it difficult to use these solid lubricants in high-temperature cutting applications.

The current critical review demonstrated various processing techniques for FGMs, which are found in advanced composite materials developed in the last decade. Nevertheless, there have been few studies on the real-time implementation of such existing or proposed models for specific manufacturing applications. Such methods necessitate a mass production strategy to lower manufacturing costs for manufactured components. Hot sintering has been identified as the primary synthesis technique for ceramic-based FGCTs. However, this traditional sintering approach necessitates a high working temperature and a lengthy holding period, resulting in unnecessary grain growth and poor mechanical properties. Despite its numerous advantages, the SPS method is currently underutilized in the cutting tool manufacturing and research community. Some researchers are also investigating MS technology, which could be an effective way of minimizing the problems associated with complex-shaped cutting tools. There is still a need for the development of novel production methods, such as AM, that can make high-quality, accurate FGMTs.

For optimized design and enhanced performance of FGTs, numerical modeling is a powerful tool. It can be utilized to predict the cutting forces, temperatures, and tool wear, allowing for better design and development. A breakthrough in the industry is expected to occur if predictive simulation and modeling of the tool properties and the machining process are widely developed and adapted to this approach. Through the integration of FEM models and various fabrication techniques, the machining industry can now develop variety of cutting tool inserts for specific metal cutting operations and machinability demands. However, the cost, time, and effort used in the research and development of the cutting tool inserts is still a challenge.

Acknowledgments: The authors would like to acknowledge the support of the Interdisciplinary Research Center for Intelligent Manufacturing and Robotics at King Fahd University of Petroleum and Minerals (KFUPM), Dhahran, for funding this work through Project # INMR2102.

Funding information: The support of the Interdisciplinary Research Center for Intelligent Manufacturing and Robotics at King Fahd University of Petroleum and Minerals (KFUPM), Dhahran, is acknowledged for funding for funding this work through Project # INMR2102.

Author contributions: All authors have accepted responsibility for the entire content of this manuscript and approved its submission.

Conflict of interest: The authors state no conflict of interest.

References

[1] Parihar, R. S., R. K. Sahu, and S. G. Setti. Adhesive wear performance of self-lubricating functionally graded cemented tungsten carbide prepared by spark plasma sintering. *International Journal of Refractory Metals and Hard Materials*, Vol. 104, 2022, id. 105788.

[2] Tang, S., P. Li, D. Liu, P. Li, and Q. Niu. Cutting performance of a functionally graded cemented carbide tool prepared by microwave heating and nitriding sintering. *High Temperature Materials and Processes*, Vol. 38, 2019, pp. 582–589.

[3] Surya, M. S. and G. Prasanthi. Effect of silicon carbide weight percentage and number of layers on microstructural and mechanical properties of Al7075/SiC functionally graded material. *Silicon*, Vol. 14, 2022, pp. 1339–1348.

[4] Xu, W., Z. Fu, and Q. Xi. Thermal conductivity identification in functionally graded materials via a machine learning strategy based on singular boundary method. *Mathematics*, Vol. 10, 2022, id. 458.

[5] Ambigai, R. and S. Prabhu. Analyzing the mechanical properties and characterization of aluminium (ADC-14) based functionally graded materials (FGM). *Silicon*, Vol. 14, 2022, pp. 2839–2850.

[6] Mohammadpour, M., P. Abachi, and K. Pourazarang. Effect of cobalt replacement by nickel on functionally graded cemented carbonitrides. *International Journal of Refractory Metals and Hard Materials*, Vol. 30, 2012, pp. 42–47.

[7] Chen, L. and T. Goto. *Functionally graded materials*, Handbook of Advanced Ceramics, Elsevier, UK, 2017, pp. 445–464.

[8] Saleh, B., J. Jiang, R. Fathi, T. Al-hababi, Q. Xu, L. Wang, et al. 30 Years of functionally graded materials: An overview of manufacturing methods. *Applications and Future Challenges, Composites Part B: Engineering*, Vol. 201, 2020, p. 108376

[9] Naebe, M. and K. Shirvanimoghaddam. Functionally graded materials: A review of fabrication and properties. *Applied Materials Today*, Vol. 5, 2016, pp. 223–245.

[10] Sajjad, A., W. Z. W. Bakar, S. Basri, and S. N. S. Jamaludin. Functionally graded materials: An overview of dental applications. *World Journal of Dentistry*, Vol. 9, 2018, pp. 137–144.

[11] El-Galy, I. M., B. I. Saleh, and M. H. Ahmed. Functionally graded materials classifications and development trends from industrial point of view. *SN Applied Sciences*, Vol. 1, 2019, id. 1378.

[12] Li, Z., W. Chen, C. Wang, C. Xiang, W. Lan, C. Wang, et al. Finite element analysis of functionally graded materials for tibial prosthesis. *Chinese Journal of Tissue Engineering Research*, Vol. 26, 2022, pp. 3543–3549.
[13] Reichardt, A., A. A. Shapiro, R. Otis, R. P. Dillon, J. P. Borgonia, B. W. McEnerney, et al. Advances in additive manufacturing of metal-based functionally graded materials. *International Materials Reviews*, Vol. 66, 2021, pp. 1–29.
[14] Ostolaza, M., J. I. Arrizubieta, A. Lamikiz, S. Plaza, and N. Ortega. Latest developments to manufacture metal matrix composites and functionally graded materials through AM: A state-of-the-art review. *Materials*, Vol. 16, 2023, id. 1746.
[15] Nejad, M. Z., N. Alamzadeh, and A. Hadi. Thermoelastoplastic analysis of FGM rotating thick cylindrical pressure vessels in linear elastic-fully plastic condition. *Composites Part B: Engineering*, Vol. 154, 2018, pp. 410–422.
[16] Laghari, R. A., J. Li, and M. Mia. Effects of turning parameters and parametric optimization of the cutting forces in machining SiCp/Al 45 wt% composite. *Metals (Basel)*, Vol. 10, 2020, id. 840.
[17] Laghari, R. A., J. Li, A. A. Laghari, and S. Wang. A review on application of soft computing techniques in machining of particle reinforcement metal matrix composites. *Archives of Computational Methods in Engineering*, Vol. 27, 2020, pp. 1363–1377.
[18] Li, J. and R. A. Laghari. A review on machining and optimization of particle-reinforced metal matrix composites, The. *International Journal of Advanced Manufacturing Technology*, Vol. 100, 2019, pp. 2929–2943.
[19] Laghari, R. A., J. Li, and Y. Wu. Study of machining process of SiCp/Al particle reinforced metal matrix composite using finite element analysis and experimental verification. *Materials*, Vol. 13, 2020, id. 5524.
[20] Wei, Z., S. Liu, D. Liu, J. Wu, H. Xia, B. Wang, et al. Fabrication and properties of symmetrical W/Si3N4/W functionally graded materials by spark plasma sintering. *Journal of Alloys and Compounds*, Vol. 896, 2022, id. 163077.
[21] Sethuramalingam, P. and R. Ambigai. The performance analysis of functionally graded material (FGM) based single point cutting tool. *International Journal on Interactive Design and Manufacturing (IJIDeM)*, Vol. 15, 2021, pp. 259–270.
[22] Singh Parihar, R., R. Kumar Sahu, and S. Gangi Setti. , Novel design and composition optimization of self-lubricating functionally graded cemented tungsten carbide cutting tool material for dry machining. *Advances in Manufacturing*, Vol. 9, 2021, pp. 34–46.
[23] Jun, Z., A. Xing, D. Jianxin, and W. Jinghai. Thermal shock behaviors of functionally graded ceramic tool materials. *Journal of the European Ceramic Society*, Vol. 24, 2004, pp. 847–854.
[24] Vaziri, M. R., S. M. Nowruzpour Mehrian, M. H. Naei, and J. Y. Sheikh Ahmad. Modification of shock resistance for cutting tools using functionally graded concept in multilayer coating. *Journal of Thermal Science and Engineering Applications*, Vol. 7, 2015, p. 011014(1-8).
[25] Xu, C. Development of multicomponent graded self-lubricating ceramic cutting tool materials. *Journal of Mechanical Engineering*, Vol. 50, 2014, pp. 94–101.
[26] Wu, G. Y., C. H. Xu, Y. L. Zhang, and M. D. Yi. Development of Al_2O_3/TiC/CaF_2 graded self-lubricating ceramic cutting tool materials. *Materials Science Forum*, Vol. 723, 2012, pp. 258–263.
[27] Xu, C. H., G. Y. Wu, G. C. Xiao, and B. Fang. Al_2O_3/(W,Ti)C/CaF_2 multi-component graded self-lubricating ceramic cutting tool material. *International Journal of Refractory Metals and Hard Materials*, Vol. 45, 2014, pp. 125–129.
[28] Yan, J., Y. Murakami, and J. P. Davim. In: *Tool design, tool wear and tool life*, Springer, London, UK, 2009, pp. 117–149.
[29] J. P. Davim, editor. Machining: Fundamentals and recent advances, Springer, London, 2008.
[30] Davim, J. P. *Modern machining technology*, Woodhead Publishing Limited, Cambridge, UK, 2011.
[31] Astakhov, V. P. and J. P. Davim. Tools (Geometry and Material) and Tool Wear. In: *Machining*, Springer, London, n.d, pp. 29–57.
[32] Astakhov, V. P. Tribology of Cutting Tools, In: Tribology in Manufacturing Technology, Springer Berlin Heidelberg, 2012, pp. 1–66.
[33] Laghari, R. A. and J. Li. Modeling and optimization of cutting forces and effect of turning parameters on SiCp/Al 45% vs SiCp/Al 50% metal matrix composites: a comparative study. *SN Appl Sci*, Vol. 3, 2021, id. 706.
[34] Ali Laghari, R., J. Li, A. A. Laghari, M. Mia, S. Wang, W. Aibo, et al. Carbide tool life prediction and modeling in SiCp/Al turning process via artificial neural network approach. *IOP Conf Ser Mater Sci Eng*, 2019, Vol. 600, No. 1, id. 012022.
[35] Laghari, R. A., S. Mekid, S. S. Akhtar, A. A. Laghari, and M. Jamil. Investigating the tribological aspects of tool wear mechanism and tool life in sustainable lubri-cooling face milling process of particle reinforced SiCp/Al metal matrix composites. In: *Advanced manufacturing*, American Society of Mechanical Engineers, Columbus, Ohio, USA, Vol. 2B, 2022, pp. 1–8.
[36] Abdelrazek, A. H., I. A. Choudhury, Y. Nukman, and S. N. Kazi. Metal cutting lubricants and cutting tools: a review on the performance improvement and sustainability assessment. *The International Journal of Advanced Manufacturing Technology*, Vol. 106, 2020, pp. 4221–4245.
[37] Wang, X., C. Li, Y. Zhang, H. M. Ali, S. Sharma, R. Li, et al. Tribology of enhanced turning using biolubricants: A comparative assessment. *Tribology International*, Vol. 174, 2022, id. 107766.
[38] Duan, Z., C. Li, Y. Zhang, M. Yang, T. Gao, X. Liu, et al. Mechanical behavior and semiempirical force model of aerospace aluminum alloy milling using nano biological lubricant. *Frontiers of Mechanical Engineering*, Vol. 18, 2023, id. 4.
[39] Laghari, R. A., M. Jamil, A. A. Laghari, A. M. Khan, S. S. Akhtar, and S. Mekid. A critical review on tool wear mechanism and surface integrity aspects of SiCp/Al MMCs during turning: prospects and challenges. *The International Journal of Advanced Manufacturing Technology*, Vol. 126, 2023, pp. 2825–2862.
[40] Ali Laghari, R. and S. Mekid. Comprehensive approach toward IIoT based condition monitoring of machining processes. *Measurement*, Vol. 217, 2023, id. 113004.
[41] Kandavalli, S. R., A. M. Khan, A. Iqbal, M. Jamil, S. Abbas, R. A. Laghari, et al. Application of sophisticated sensors to advance the monitoring of machining processes: analysis and holistic review. *The International Journal of Advanced Manufacturing Technology*, Vol. 125, No. 3-4, 2023, pp. 989–1014.
[42] Liang, J., J. Sun, W. Wei, and R. Laghari. Dynamic constitutive analysis of aluminum alloy materials commonly used in railway vehicles big data and its application in LS-DYNA. *ICST Transactions on Scalable Information Systems*, Vol. 9, No. 34, 2018, id. 171169.
[43] Cho, J. R. and H. J. Park. High strength FGM cutting tools: finite element analysis on thermoelastic characteristics. *Journal of Materials Processing Technology*, Vol. 130131, 2002, pp. 351–356.
[44] Davim, J. P., editor. *Machining of hard materials*, Springer, London, London, 2011.

[45] Grigoriev, S. N., S. V. Fedorov, and K. Hamdy. Materials, properties, manufacturing methods and cutting performance of innovative ceramic cutting tools - A review. *Manufacturing Review (Les Ulis)*, Vol. 6, 2019., pp. 1–27
[46] Laghari, R. A., M. K. Gupta, and J. Li. Evolutionary algorithm for the prediction and optimization of SiCp/Al metal matrix composite machining. *Journal of Production Systems and Manufacturing Science*, Vol. 2, 2020, pp. 59–69.
[47] Laghari, R. A., J. Li, Z. Xie, and S. Wang. Modeling and optimization of tool wear and surface roughness in turning of Al/SiCp using response surface methodology. *3D Research*, Vol. 9, 2018, id. 46.
[48] Jamil, M., N. He, W. Zhao, A. M. Khan, and R. A. Laghari. Tribology and machinability performance of hybrid Al_2O_3 -MWCNTs nanofluids-assisted MQL for milling Ti-6Al-4 V. *The International Journal of Advanced Manufacturing Technology*, Vol. 119, 2022, pp. 2127–2144.
[49] Xue, Q., X. Ai, J. Zhao, Y. Liu, and Y. Zhou. Analysis of microstructure and mechanical properties of graded nano-composite Si_3N_4-based ceramic cutting tool material. In: *Proceedings of 2011 International Conference on Electronic & Mechanical Engineering and Information Technology*, IEEE, 2011, pp. 3539–3542.
[50] Sun, J., J. Zhao, M. Chen, X. Ni, Z. Li, and F. Gong. Determination of microstructure and mechanical properties of VC/Cr3C2 reinforced functionally graded WC-TiC-Al_2O_3 micro-nano composite tool materials via two-step sintering. *Journal of Alloys and Compounds*, Vol. 709, 2017, pp. 197–205.
[51] Wu, G., C. Xu, G. Xiao, and M. Yi. Recent progress in self-lubricating ceramiccomposites. In: *Self-lubricating composites*, Springer Berlin Heidelberg, Berlin, Heidelberg, 2018, pp. 133–154.
[52] Feng, Y., J. Zhang, L. Wang, W. Zhang, and D. Yuanpei. Study on secondary cutting phenomenon of micro-textured self-lubricating ceramic cutting tools with different morphology parameters formed via in situ forming of Al_2O_3-TiC. *The International Journal of Advanced Manufacturing Technology*, Vol. 104, 2019, pp. 3821–3833.
[53] Yi, M., J. Wang, G. Xiao, Z. Chen, J. Zhang, H. Chen, et al. Effect of gradient design on the mechanical property and friction performance of nano self-lubricating ceramic cutting tool material. *Ceramics International*, Vol. 48, 2022, pp. 7045–7055.
[54] Chauvin, M. Metal Cutting Tools Market Size 2022-2028 (US $ Billion), 2022.
[55] Bhaumik, S. K., C. Divakar, and A. K. Singh. Machining Ti 6Al 4V alloy with a wBN-cBN composite tool. *Materials & Design*, Vol. 16, 1995, pp. 221–226.
[56] Kanta Das, D., P. C. Mishra, S. Singh, and R. K. Thakur. Tool wear in turning ceramic reinforced aluminum matrix composites—A review. *Journal of Composite Materials*, Vol. 49, 2015, pp. 2949–2961.
[57] Kamalizadeh, S., S. A. Niknam, A. Asgari, and M. Balazinski. Tool wear characterization in high-speed milling of titanium metal matrix composites. *The International Journal of Advanced Manufacturing Technology*, Vol. 100, 2019, pp. 2901–2913.
[58] Xue, Q., X. Ai, J. Zhao, Y. Liu, and Y. Zhou. Analysis of microstructure and mechanical properties of graded nano-composite Si 3 N 4-based ceramic cutting tool material. In: *Proceedings of 2011 International Conference on Electronic & Mechanical Engineering and Information Technology*, IEEE, 2011, pp. 3539–3542.
[59] Li, G., W. Lü, S. Liu, C. Li, Y. Zhou, and Q. Wang. Multilayer-growth of TiAlN/WS self-lubricating composite coatings with high adhesion and their cutting performance on titanium alloy. *Composites Part B: Engineering*, Vol. 211, 2021, id. 108620.
[60] Wickramasinghe, K. C., H. Sasahara, E. A. Rahim, and G. I. P. Perera. Recent advances on high performance machining of aerospace materials and composites using vegetable oil-based metal working fluids. *Journal of Cleaner Production*, Vol. 310, 2021, id. 127459.
[61] Akhtar, S. S., T. Waqar, A. S. Hakeem, A. F. M. Arif, and K. S. Al-Athel. Design and development of hybrid Al_2O_3 based composites with toughening and self-lubricating second-phase inclusions. *Materials*, Vol. 12, 2019, id. 2378.
[62] Muthuraja, A. and S. Senthilvelan. Abrasive wear performance of tungsten carbide based self-lubricant cutting tool material. *International Journal of Refractory Metals and Hard Materials*, Vol. 51, 2015, pp. 91–101
[63] Xu, C., G. Xiao, Y. Zhang, and B. Fang. Finite element design and fabrication of Al_2O_3/TiC/CaF_2 gradient self-lubricating ceramic tool material. *Ceramics International*, Vol. 40, 2014, pp. 10971–10983.
[64] Uemura, S. The activities of FGM on new application. *Materials Science Forum*, Vol. 423–425, 2003, pp. 1–10.
[65] Zhu, D., X. Zhang, and H. Ding. Tool wear characteristics in machining of nickel-based superalloys. *The International Journal of Machine Tools and Manufacture*, Vol. 64, 2013, pp. 60–77
[66] Pervaiz, S., A. Rashid, I. Deiab, and M. Nicolescu. Influence of tool materials on machinability of titanium- and nickel-based alloys: a review. *Materials and Manufacturing Processes*, Vol. 29, 2014, pp. 219–252.
[67] Liang, X., Z. Liu, and B. Wang. State-of-the-art of surface integrity induced by tool wear effects in machining process of titanium and nickel alloys: A review. *Measurement*, Vol. 132, 2019, pp. 150–181.
[68] Mouritz, A. *Introduction to aerospace materials*, American Institute of Aeronautics and Astronautics, Inc., Washington, DC, 2012.
[69] Ezugwu, E. O. Key improvements in the machining of difficult-to-cut aerospace superalloys. *The International Journal of Machine Tools and Manufacture*, Vol. 45, 2005, pp. 1353–1367.
[70] Okafor, A. C. Cooling and machining strategies for high speed milling of titanium and nickel super alloys. In: *High Speed Machining*, Elsevier, United Kingdom, 2020, pp. 127–161.
[71] Akhtar, W., J. Sun, P. Sun, W. Chen, and Z. Saleem. Tool wear mechanisms in the machining of Nickel based super-alloys: A review. *Frontiers of Mechanical Engineering*, Vol. 9, 2014, pp. 106–119.
[72] Vanmeensel, K., G. Anné, D. Jiang, J. Vleugels, and O. van der Biest. Processing of a graded ceramic cutting tool in the Al_2O_3-ZrO_2-Ti(C,N) system by electrophoretic deposition. *Materials Science Forum*, 2005, Vol. 492, pp. 705–710.
[73] Zhao, J., Y. Li, and X. Ai. Transient thermal stress analysis of a plate with double-sided FGM coatings. *Key Engineering Materials*, Trans Tech Publications Ltd, Switzerland, 2008, pp. 1807–1810.
[74] Waqar, T., S. S. Akhtar, A. F. M. Arif, and A. S. Hakeem. Design and development of ceramic-based composites with tailored properties for cutting tool inserts. *Ceramics International*, Vol. 44, 2018, pp. 22421–22431
[75] Kumar, A. S., A. R. Durai, and T. Sornakumar. Wear behaviour of alumina based ceramic cutting tools on machining steels. *Tribology International*, Vol. 39, 2006, pp. 191–197.
[76] Ding, X., W. Y. H. Liew, and X. D. Liu. Evaluation of machining performance of MMC with PCBN and PCD tools. *Wear*, Vol. 259, 2005, pp. 1225–1234.
[77] Bushlya, V., D. Johansson, F. Lenrick, J.-E. Ståhl, and F. Schultheiss. Wear mechanisms of uncoated and coated cemented carbide tools in machining lead-free silicon brass. *Wear*, Vol. 376–377, 2017, pp. 143–151.

[78] Rech, J. Influence of cutting tool coatings on the tribological phenomena at the tool-chip interface in orthogonal dry turning. *Surface and Coatings Technology*, Vol. 200, 2006, pp. 5132–5139.

[79] Akhyar Ibrahim, G., C. H. Che Haron, J. Abdul Ghani, A. Y. M. Said, and M. Z. Abu. Yazid, performance of PVD-coated carbide tools when turning inconel 718 in dry machining. *Advances in Mechanical Engineering*, Vol. 3, 2011, id. 790975.

[80] Shokrani, A., I. Al-Samarrai, and S. T. Newman. Hybrid cryogenic MQL for improving tool life in machining of Ti-6Al-4V titanium alloy. *Journal of Manufacturing Processes*, Vol. 43, 2019, pp. 229–243.

[81] Ezugwu, E. O., J. Bonney, and Y. Yamane. An overview of the machinability of aeroengine alloys. *Journal of Materials Processing Technology*, Vol. 134, 2003, pp. 233–253

[82] López de Lacalle, L. N., G. Urbicain Pelayo, A. Fernández-Valdivielso, A. Alvarez, and H. González. Wear-dependent specific coefficients in a mechanistic model for turning of nickel-based superalloy with ceramic tools. *Open Engineering*, Vol. 7, 2017, pp. 175–184.

[83] Çelik, A., M. Sert Alağaç, S. Turan, A. Kara, and F. Kara. Wear behavior of solid SiAlON milling tools during high speed milling of Inconel 718. *Wear*, Vol. 378, 2017, pp. 58–67.

[84] Jomaa, W., V. Songmene, P. Bocher, and A. Gakwaya. FEA-based comparative investigation on high speed machining of aluminum alloys AA6061-T6 and AA7075-T651. *Solid State Phenomena*, Vol. 261, 2017, pp. 347–353.

[85] Zhao, B., H. Liu, C. Huang, J. Wang, B. Wang, and Y. Hou. Cutting performance and crack self-healing mechanism of a novel ceramic cutting tool in dry and high-speed machining of Inconel 718. *The International Journal of Advanced Manufacturing Technology*, Vol. 102, 2019, pp. 3431–3438.

[86] Zhang, H., J. Dang, W. Ming, X. Xu, M. Chen, and Q. An. Cutting responses of additive manufactured Ti6Al4V with solid ceramic tool under dry high-speed milling processes. *Ceramics International*, Vol. 46, 2020, pp. 14536–14547.

[87] Zhu, J., H. Zhou, B. Qin, and Z. Zhao. Design, fabrication and properties of TiB_2/TiN/WC gradient ceramic tool materials. *Ceramics International*, Vol. 46, 2020., pp. 6497–6506

[88] El-Wardany, T. I., E. Mohammed, and M. A. Elbestawi. Cutting temperature of ceramic tools in high speed machining of difficult-to-cut materials. *The International Journal of Machine Tools and Manufacture*, Vol. 36, 1996, pp. 611–634.

[89] Jianxin, D., C. Tongkun, and L. Lili. Self-lubricating behaviors of Al_2O_3/TiB_2 ceramic tools in dry high-speed machining of hardened steel. *Journal of the European Ceramic Society*, Vol. 25, 2005, pp. 1073–1079.

[90] Akhtar, S. S., M. U. Siddiqui, R. Kabeer, A. Hakeem, L. Kareem, and A. F. Arif. A computational and experimental study on the effective properties of Al_2O_3-Ni composites. *International Journal of Applied Ceramic Technology*, Vol. 14, 2017, pp. 1–13

[91] Munir, Z. A., U. Anselmi-Tamburini, and M. Ohyanagi. The effect of electric field and pressure on the synthesis and consolidation of materials: A review of the spark plasma sintering method. *Journal of Materials Science*, Vol. 41, 2006, pp. 763–777

[92] Belmonte, M., M. I. Nieto, M. I. Osendi, and P. Miranzo. Influence of the SiC grain size on the wear behaviour of Al_2O_3/SiC composites. *Journal of the European Ceramic Society*, Vol. 26, 2006, pp. 1273–1279

[93] Teng, X., H. Liu, and C. Huang. Effect of Al_2O_3 particle size on the mechanical properties of alumina-based ceramics. *Materials Science and Engineering A*, Vol. 452, 2007, pp. 545–551.

[94] Wang, L., J. L. Shi, J. H. Gao, and D. S. Yan. Influence of tungsten carbide particles on resistance of alumina matrix ceramics to thermal shock. *Journal of the European Ceramic Society*, Vol. 21, 2001, pp. 1213–1217

[95] Jianxin, D. and A. Xing. Wear resistance of Al_2O_3/TiB_2 ceramic cutting tools in sliding wear tests and in machining processes. *Journal of Materials Processing Technology*, Vol. 72, 1997, pp. 249–255

[96] Lipetzky, P., S. R. Nutt, and P. F. Becher. Creep Behavior of an Al_2O_3-Sic Composite. *MRS Proceedings*, Vol. 120, 1988, pp. 271–277

[97] Tjong, S. C., Z. Y. Ma, and R. K. Y. Li. The dynamic mechanical response of Al_2O_3 and TiB_2 particulate reinforced aluminum matrix composites produced by in-situ reaction. *Materials Letters*, Vol. 38, 1999, pp. 39–44

[98] Kim, Y.-W. and J.-G. Lee. Pressureless sintering of alumina-titanium carbide composites. *Journal of the American Ceramic Society*, Vol. 72, 1989, pp. 1333–1337

[99] Xu, C. and R. I. Todd. Functionally graded ceramics by a new in situ processing route: Residual stress and wear resistance. *Journal of the European Ceramic Society*, Vol. 35, 2015, pp. 2693–2698

[100] Dancer, C. E., N. A. Yahya, T. Berndt, R. I. Todd, and G. De Portu. Effect of residual compressive surface stress on severe wear of alumina–silicon carbide two-layered composites. *Tribology International*, Vol. 74, 2014, pp. 87–92.

[101] Gong, F., J. Zhao, Z. Li, J. Sun, X. Ni, and G. Hou. Design, fabrication and mechanical properties of multidimensional graded ceramic tool materials. *Ceramics International*, Vol. 44, 2018, pp. 2941–2951.

[102] Dong, Q., Q. Tang, and W. Li. Al_2O_3-TiC-ZrO_2 nanocomposites fabricated by combustion synthesis followed by hot pressing. *Materials Science and Engineering A*, Vol. 475, 2008, pp. 68–75

[103] Qi, Y., Y.-S. Zhang, and L.-T. Hu. High-temperature self-lubricated properties of Al_2O_3/Mo laminated composites. *Wear*, Vol. 280–281, 2012, pp. 1–4.

[104] Xing, A., Z. Jun, H. Chuanzhen, and Z. Jianhua. Development of an advanced ceramic tool material - Functionally gradient cutting ceramics. *Materials Science and Engineering A*, Vol. 248, 1998, pp. 125–131

[105] Bitterlich, B., S. Bitsch, and K. Friederich. SiAlON based ceramic cutting tools. *Journal of the European Ceramic Society*, Vol. 28, 2008, pp. 989–994

[106] Zheng, G., J. Zhao, Z. Gao, and Q. Cao. Cutting performance and wear mechanisms of Sialon–Si_3N_4 graded nano-composite ceramic cutting tools. *The International Journal of Advanced Manufacturing Technology*, Vol. 58, 2012, pp. 19–28.

[107] Kovalčíková, A., J. Balko, C. Balázsi, P. Hvizdoš, and J. Dusza. Influence of hBN content on mechanical and tribological properties of Si_3N_4/BN ceramic composites. *Journal of the European Ceramic Society*, Vol. 34, 2014, pp. 3319–3328

[108] Carrapichano, J. M., J. R. Gomes, and R. F. Silva. Tribological behaviour of Si_3N_4-BN ceramic materials for dry sliding applications. *Wear*, Vol. 253, 2002, pp. 1070–1076

[109] Tian, X., J. Zhao, X. Wang, H. Yang, and Z. Wang. Performance of Si_3N_4/(W, Ti)C graded ceramic tool in high-speed turning iron-based superalloys. *Ceramics International*, Vol. 44, 2018, pp. 15579–15587

[110] Tian, X. H., J. Zhao, F. Gong, W. Z. Qin, and Q. Z. Xu. *Development of Si3N4/(W,Ti)C/Co graded nano-composite ceramic tool and its performance in turning GH2132 Alloy*. International Manufacturing Science and Engineering Conference (MSEC), American Society of Mechanical Engineers, 2015, p. 6

[111] Tian, X., J. Zhao, X. Wang, F. Gong, W. Qin, and H. Pan. Fabrication and mechanical properties of Si_3N_4/(W, Ti)C/Co graded nano-composite ceramic tool materials. *Ceramics International*, Vol. 41, 2015, pp. 3381–3389

[112] Mori, N. and A. Ikegaya. Evaluation of tiebar-cut punch made by co composition graded cemented carbide. *J Jpn Soc Powder Powder Metall*, Vol. 50, 2003, pp. 411–417.

[113] Bulić, F. I., G. Korb, P. Šajgalík, and Z. Lenčéš. Gradient Structures in SiAlON´s for improved cutting performance. *Key Engineering Materials*, Vol. 264–268, 2004, pp. 901–904.

[114] Zheng, G., J. Zhao, A. Li, X. Cui, and Y. Zhou. Failure mechanisms of graded ceramic tool in ultra high speed dry milling of Inconel 718. *International Journal of Precision Engineering and Manufacturing*, Vol. 14, 2013, pp. 943–949

[115] Zheng, G. and J. Zhao. Performance of Sialon/Si3N4 graded ceramic tools at high speed machining. *High Speed Machining*, Elsevier, United Kingdom, 2020, pp. 27–62.

[116] Lengauer, W. and K. Dreyer. Functionally graded hardmetals. *Journal of Alloys and Compounds*, Vol. 338, 2002, pp. 194–212.

[117] Jain, A. and V. Bajpai. *Introduction to high-speed machining (HSM)*, Elsevier Inc, United Kingdom, 2020.

[118] Brandt, G., B. Johannesson, and R. Warren. Fracture behaviour of selected mixed-ceramic tool materials up to 1200°C. *Materials Science and Engineering*, Vol. 105, 1988, pp. 193–200.

[119] Akhtar, S. S. A critical review on self-lubricating ceramic-composite cutting tools. *Ceramics International*, Vol. 47, 2021, pp. 20745–20767

[120] Reis, P., J. P. Davim, X. Xu, and J. M. F. Ferreira. A note on tribological behaviour of α-sialon/steel couples under dry conditions. *Materials & Design*, Vol. 28, 2007, pp. 1343–1347.

[121] Zhang, Z., Y. Liu, and H. Liu. Mechanical properties and microstructure of spark plasma sintered Al_2O_3-SiCw-Si3N4 composite ceramic tool materials. *Ceramics International*, Vol. 48, 2022, pp. 5527–5534.

[122] Lee, C. S., S.-G. Kim, S.-H. Ahn, L. C. DeJonghe, and G. Thomas. Three dimensional analysis of thermal stress and prediction of failure of polytypoidally joined Si3N4-Al_2O_3 Functionally Graded Material (FGM). *Materials Transactions*, Vol. 48, 2007, pp. 2489–2493.

[123] Šajgalík, P. α-β phase transformation of silicon nitride — computer simulation. *Journal of Materials Science*, Vol. 26, 1991, pp. 6083–6090.

[124] Lin, T., W. Cao, J. Li, and C. Ge. Fabrication of layered Ti3SiC2 α-SiAlON material, *Key Engineering Materials*, Vol. 336, 2007, pp. 2572–2574.

[125] Mandal, H. and N. Ç. Acikbas. SiAlON based functionally graded materials. In: *Ceramic-matrix composites: microstructure, properties and applications*, Woodhead Publishing, Cambridge, UK, 2006, pp. 154–177.

[126] Calis Acikbas, N., H. Yurdakul, H. Mandal, F. Kara, S. Turan, A. Kara, et al. Effect of sintering conditions and heat treatment on the properties, microstructure and machining performance of α-β-SiAlON ceramics. *Journal of the European Ceramic Society*, Vol. 32, 2012, pp. 1321–1327

[127] Çaliş, N., A. Kara, F. Kara, and H. Mandal. Development of laminar type functionally graded SiAlON ceramics. *Key Engineering Materials*, Vol. 264, 2004, pp. 1095–1098

[128] Sarkar, S., R. Halder, M. Biswas, and S. Bandyopadhyay. Densification, microstructure and tribomechanical properties of SPS processed β-SiAlON bonded WC composites. *International Journal of Refractory Metals and Hard Materials*, Vol. 92, 2020, pp. 1–10

[129] Abo-Naf, S. M., U. Dulias, J. Schneider, K. H. Z. Gahr, S. Holzer, and M. J. Hoffmann. Mechanical and tribological properties of Nd- and Yb-SiAlON composites sintered by hot isostatic pressing. *Journal of Materials Processing Technology*, Vol. 183, 2007, pp. 264–272

[130] Sugihara, T., R. Kobayashi, and T. Enomoto. Direct observations of tribological behavior in cutting with textured cutting tools. *The International Journal of Machine Tools and Manufacture*, Vol. 168, 2021, id. 103726.

[131] Zawada-Michałowska, M., P. Pieśko, and J. Józwik. Tribological aspects of cutting tool wear during the turning of stainless steels. *Materials*, Vol. 13, 2019, id. 123.

[132] Gajrani, K. K., R. Pavan Kumar Reddy, and M. Ravi Sankar. Tribo-mechanical and surface morphological comparison of untextured, mechanical micro-textured (MμT), and coated-MμT cutting tools during machining. *Proceedings of the Institution of Mechanical Engineers, Part J: Journal of Engineering Tribology*, Vol. 233, 2019, pp. 95–111.

[133] Moradnazhad, M. and H. O. Unver. Energy efficiency of machining operations: A review. *Proceedings of the Institution of Mechanical Engineers, Part B: Journal of Engineering Manufacture*, Vol. 231, 2017, pp. 1871–1889.

[134] Pervaiz, S., S. Kannan, I. Deiab, and H. Kishawy. Role of energy consumption, cutting tool and workpiece materials towards environmentally conscious machining: A comprehensive review. *Proceedings of the Institution of Mechanical Engineers, Part B: Journal of Engineering Manufacture*, Vol. 234, 2020, pp. 335–354.

[135] Davim, J. P., editor. *Metal cutting technologies*, De Gruyter, Germany, 2016.

[136] Oliaei, S. N. B., Y. Karpat, J. P. Davim, and A. Perveen. Micro tool design and fabrication: A review. *Journal of Manufacturing Processes*, Vol. 36, 2018, pp. 496–519.

[137] Pramanik, A., M. N. Islam, A. Basak, and G. Littlefair. Machining and tool wear mechanisms during machining titanium alloys. *Advanced Materials Research*, Vol. 651, 2013, pp. 338–343.

[138] Olsson, M., V. Bushlya, F. Lenrick, and J.-E. Ståhl. Evaluation of tool wear mechanisms and tool performance in machining single-phase tungsten. *International Journal of Refractory Metals and Hard Materials*, Vol. 94, 2021, id. 105379.

[139] Wang, J., G. Zhang, N. Chen, M. Zhou, and Y. Chen. A review of tool wear mechanism and suppression method in diamond turning of ferrous materials. *The International Journal of Advanced Manufacturing Technology*, Vol. 113, 2021, pp. 3027–3055.

[140] Kumari, S., M. Shah, Y. Modi, D. Bandhu, K. Zadafiya, K. Abhishek, et al. Effect of various lubricating strategies on machining of titanium alloys: A state-of-the-art review. *Coatings*, Vol. 12, 2022, id. 1178.

[141] Mohd Khalil, A. N., A. I. Azmi, M. N. Murad, and M. A. Mahboob Ali. Influence of hybrid cooling-lubricating strategy in the turning of ASTM F2063 austenitic nickel-titanium alloy. *Tribology in Industry*, Vol. 43, 2021, pp. 83–95.

[142] Besisa, D. H. A. and E. M. M. Ewais. Advances in functionally graded ceramics – processing, sintering properties and applications. In: *Advances in functionally graded materials and structures*, InTech, London, United Kingdom, 2016.

[143] Jamaludin, S. N., F. Mustapha, D. M. Nuruzzaman, and S. N. Basri. A review on the fabrication techniques of functionally graded ceramic-metallic materials in advanced composites. *Scientific Research and Essays*, Vol. 8, No. 21, 2013, pp. 828–840.

[144] Hoier, P., K. B. Surreddi, and U. Klement. Tool wear by dissolution during machining of alloy 718 and Waspaloy: a comparative study

using diffusion couples. *The International Journal of Advanced Manufacturing Technology*, Vol. 106, 2020, pp. 1431–1440.

[145] Cantero, J. L., J. Díaz-Álvarez, M. H. Miguélez, and N. C. Marín. Analysis of tool wear patterns in finishing turning of Inconel 718. *Wear*, Vol. 297, 2013, pp. 885–894.

[146] Zhuang, K., D. Zhu, X. Zhang, and H. Ding. Notch wear prediction model in turning of Inconel 718 with ceramic tools considering the influence of work hardened layer. *Wear*, Vol. 313, 2014, pp. 63–74.

[147] Yıldırım, Ç.V., M. Sarıkaya, T. Kıvak, and Ş. Şirin. The effect of addition of hBN nanoparticles to nanofluid-MQL on tool wear patterns, tool life, roughness and temperature in turning of Ni-based Inconel 625. *Tribology International*, Vol. 134, 2019, pp. 443–456.

[148] Ezugwu, E. O., Z. M. Wang, and A. R. Machado. The machinability of nickel-based alloys: a review. *Journal of Materials Processing Technology*, Vol. 86, 1999, pp. 1–16.

[149] Bushlya, V., F. Lenrick, A. Bjerke, H. Aboulfadl, M. Thuvander, J.-E. Ståhl, et al. Tool wear mechanisms of PcBN in machining Inconel 718: Analysis across multiple length scale. *CIRP Annals*, Vol. 70, 2021, pp. 73–78.

[150] Zeilmann, R. P., F. Fontanive, and R. M. Soares. Wear mechanisms during dry and wet turning of Inconel 718 with ceramic tools. *The International Journal of Advanced Manufacturing Technology*, Vol. 92, 2017, pp. 2705–2714.

[151] Tokita, M. Recent progress of Spark Plasma Sintering (SPS) Method and industrial use of Funcionally Graded Materials (FGMs), *Proceedings of the 13th International Symposium on Multiscale, Multifunctional and Functionally Graded Materials*, São Paulo: Editora Edgard Blücher: 2014, pp. 90–93.

[152] Bertolete, M., P. A. Barbosa, W. de Rossi, C. Fredericci, and I. F. Machado. Mechanical characterisation and machining evaluation of ceramic cutting tools functionally graded with six layers. *Ceramics International*, Vol. 46, 2020, pp. 15137–15145.

[153] Tsuda, K. Development of functionally graded hard material. *Funtai Oyobi Fummatsu Yakin/Journal of the Japan Society of Powder and Powder Metallurgy*, Vol. 67, 2020, pp. 545–552.

[154] Ming, W., X. Huang, M. Ji, J. Xu, F. Zou, and M. Chen. Analysis of cutting responses of Sialon ceramic tools in high-speed milling of FGH96 superalloys. *Ceramics International*, Vol. 47, 2021, pp. 149–156.

[155] Zheng, G., J. Zhao, Y. Zhou, A. Li, X. Cui, and X. Tian. Performance of graded nano-composite ceramic tools in ultra-high-speed milling of Inconel 718. *The International Journal of Advanced Manufacturing Technology*, Vol. 67, 2013, pp. 2799–2810.

[156] Song, X. Y. and J. Zhao. Failure mechanisms of carbide tool in high speed milling of inconel 718. *Advanced Materials Research*, Vol. 97–101, 2010, pp. 1920–1924.

[157] Kitagawa, T., A. Kubo, and K. Maekawa. Temperature and wear of cutting tools in high-speed machining of Inconel 718 and Ti-6Al-6V-2Sn. *Wear*, Vol. 202, 1997, pp. 142–148.

[158] Jianxin, D., L. Lili, L. Jianhua, Z. Jinlong, and Y. Xuefeng. Failure mechanisms of TiB_2 particle and SiC whisker reinforced Al_2O_3 ceramic cutting tools when machining nickel-based alloys. *The International Journal of Machine Tools and Manufacture*, Vol. 45, 2005, pp. 1393–1401.

[159] Vleugels, J. and O. Van Der Biest. Chemical wear mechanisms of innovative ceramic cutting tools in the machining of steel. *Wear*, Vol. 225–229, 1999, pp. 285–294.

[160] Slipchenko, K. V., D. A. Stratiichuk, V. Z. Turkevich, N. M. Belyavina, V. M. Bushlya, and J.-E. Ståhl. Sintering of cBN based materials with a TaC binder for cutting tool application. *Journal of Superhard Materials*, Vol. 42, 2020, pp. 51–57.

[161] Zhang, Y., Y. Su, Y. Fang, Y. Qi, and L. Hu. High-performance self-lubricating ceramic composites with laminated-graded structure. In: *Advances in functionally graded materials and structures*, InTech, London, United Kingdom, 2016.

[162] Evans, A. G. and T. R. Wilshaw. Quasi-static solid particle damage in brittle solids-I. Observations analysis and implications. *Acta Metallurgica*, Vol. 24, 1976, pp. 939–956.

[163] Kong, L., Q. Bi, M. Niu, S. Zhu, J. Yang, and W. Liu. High-temperature tribological behavior of ZrO 2-MoS 2-CaF 2 self-lubricating composites. *Journal of the European Ceramic Society*, Vol. 33, 2013, pp. 51–59.

[164] Rho, B. H. and K. W. Kim. Tribological behaviour and wear mechanism of MoS2-Cr coatings sliding against various counterbody. *Tribology International*, Vol. 36, 2003, pp. 11–23.

[165] Chen, Z., L. Ji, N. Guo, and R. Guo. Mechanical properties and microstructure of Al_2O_3/TiC based self-lubricating ceramic tool with CaF_2@Al (HO)3. *International Journal of Refractory Metals and Hard Materials*, Vol. 75, 2018, pp. 50–55.

[166] Tang, S., R. Wang, P. Liu, Q. Niu, G. Yang, W. Liu, et al. Preparation of WC-TiC-Ni3Al-CaF_2 functionally graded self-lubricating tool material by microwave sintering and its cutting performance. *High Temperature Materials and Processes*, Vol. 39, 2020, pp. 45–53.

[167] Sun, J., J. Zhao, M. Chen, Y. Zhou, X. Ni, Z. Li, et al. Multilayer graphene reinforced functionally graded tungsten carbide nanocomposites. *Materials & Design*, Vol. 134, 2017, pp. 171–180.

[168] Fan, Y., M. Estili, G. Igarashi, W. Jiang, and A. Kawasaki. The effect of homogeneously dispersed few-layer graphene on microstructure and mechanical properties of Al_2O_3 nanocomposites. *Journal of the European Ceramic Society*, Vol. 34, 2014, pp. 443–451.

[169] Llorente, J., B. Román-Manso, P. Miranzo, and M. Belmonte. Tribological performance under dry sliding conditions of graphene/silicon carbide composites. *Journal of the European Ceramic Society*, Vol. 36, 2016, pp. 429–435.

[170] Kim, H. J., S. M. Lee, Y. S. Oh, Y. H. Yang, Y. S. Lim, D. H. Yoon, et al. Unoxidized graphene/alumina nanocomposite: Fracture-and wear-resistance effects of graphene on alumina matrix. *Scientific Reports*, Vol. 4, 2014, pp. 1–10.

[171] Yamamoto, G., M. Omori, K. Yokomizo, T. Hashida, and K. Adachi. Structural characterization and frictional properties of carbon nanotube/alumina composites prepared by precursor method. *Materials Science and Engineering: B. Solid State Materials Advanced Technology*, Vol. 148, 2008, pp. 265–269.

[172] Puchy, V., P. Hvizdos, J. Dusza, F. Kovac, F. Inam, and M. J. Reece. Wear resistance of Al_2O_3-CNT ceramic nanocomposites at room and high temperatures. *Ceramics International*, Vol. 39, 2013, pp. 5821–5826.

[173] Cui, E., J. Zhao, X. Wang, and S. Song. Cutting performance, failure mechanisms and tribological properties of GNPs reinforced Al_2O_3/Ti(C,N) ceramic tool in high speed turning of Inconel 718. *Ceramics International*, Vol. 46, 2020, pp. 18859–18867.

[174] Kim, W., H. S. Oh, and I. J. Shon. The effect of graphene reinforcement on the mechanical properties of Al_2O_3 ceramics rapidly sintered by high-frequency induction heating. *International Journal of Refractory Metals and Hard Materials*, Vol. 48, 2015, pp. 376–381.

[175] Ahmad, I., M. Islam, H. S. Abdo, T. Subhani, K. A. Khalil, A. A. Almajid, et al. Toughening mechanisms and mechanical properties of graphene nanosheet-reinforced alumina. *Materials & Design*, Vol. 88, 2015, pp. 1234–1243.

[176] Agrawal, D. Microwave sintering of ceramics, composites and metal powders. In: *Sintering of advanced materials*, Woodhead Publishing, Cambridge, UK, 2010.

[177] Porwal, H., S. Grasso, and M. J. Reece. Review of graphene-ceramic matrix composites. *Advances in Applied Ceramics*, Vol. 112, No. 8, 2013, pp. 443–454.

[178] Matizamhuka, W. R. Spark plasma sintering (SPS) - An advanced sintering technique for structural nanocomposite materials. *Journal of the Southern African Institute of Mining and Metallurgy*, Vol. 116, No. 12, 2016, pp. 1171–1180.

[179] Santanach, J. G., A. Weibel, C. Estourns, Q. Yang, C. Laurent, and A. Peigney. Spark plasma sintering of alumina: Study of parameters, formal sintering analysis and hypotheses on the mechanism(s) involved in densification and grain growth. *Acta Materialia*, Vol. 59, 2011, pp. 1400–1408.

[180] Borrell, A., M. D. Salvador, M. Miranda, F. L. Penaranda-Foix, and J. M. Catala-Civera. Microwave technique: a powerful tool for sintering ceramic materials. *Current Nanoscience*, Vol. 10, 2014, pp. 32–35.

[181] Oghbaei, M. and O. Mirzaee. Microwave versus conventional sintering: A review of fundamentals, advantages and applications. *Journal of Alloys and Compounds*, Vol. 494, 2010, pp. 1234–1243.

[182] Yin, Z., S. Yan, J. Ye, Z. Zhu, and J. Yuan. Cutting performance of microwave-sintered sub-crystal Al_2O_3/SiC ceramic tool in dry cutting of hardened steel. *Ceramics International*, Vol. 45, No. 13, 2019, pp. 16113–16120.

[183] Ghasali, E. and M. Shahedi Asl. Microstructural development during spark plasma sintering of ZrB2–SiC–Ti composite. *Ceramics International*, Vol. 44, No. 15, 2018, pp. 18078–18083.

[184] Manshor, H., E. C. Abdullah, A. Z. A. Azhar, Y. W. Sing, and Z. A. Ahmad. Microwave sintering of zirconia-toughened alumina (ZTA)-TiO2-Cr2O3 ceramic composite: The effects on microstructure and properties. *Journal of Alloys and Compounds*, Vol. 722, 2017, pp. 458–466.

[185] Zhang, C., F. Chen, Z. Huang, M. Jia, G. Chen, Y. Ye, et al. Additive manufacturing of functionally graded materials: A review. *Materials Science and Engineering A*, Vol. 764, 2019, id. 138209.

[186] Ozbolat, I. T. and A. K. M. B. Khoda. Design of a new parametric path plan for additive manufacturing of hollow porous structures with functionally graded materials. *Journal of Computing and Information Science in Engineering*, Vol. 14, 2014, p. 041005.

[187] Jianxin, D., C. Tongkun, Y. Xuefeng, and L. Jianhua. Self-lubrication of sintered ceramic tools with CaF_2 additions in dry cutting. *The International Journal of Machine Tools and Manufacture*, Vol. 46, 2006, pp. 957–963.

[188] Wu, G., C. Xu, G. Xiao, M. Yi, Z. Chen, and L. Xu. Self-lubricating ceramic cutting tool material with the addition of nickel coated CaF_2 solid lubricant powders. *International Journal of Refractory Metals and Hard Materials*, Vol. 56, 2016, pp. 51–58.

[189] Wu, G., C. Xu, G. Xiao, M. Yi, Z. Chen, and H. Chen. An advanced self-lubricating ceramic composite with the addition of core-shell structured h-BN@Ni powders. *International Journal of Refractory Metals and Hard Materials*, Vol. 72, 2018, pp. 276–285.

[190] Fattahi, M., M. Najafi Ershadi, M. Vajdi, F. Sadegh Moghanlou, A. Sabahi Namini, and M. Shahedi Asl. On the simulation of spark plasma sintered TiB_2 ultra high temperature ceramics: A numerical approach. *Ceramics International*, Vol. 46, 2020, pp. 14787–14795.

[191] Maros, M. B., A. K. Németh, Z. Károly, E. Bódis, Z. Maros, O. Tapasztó, et al. Tribological characterisation of silicon nitride/multilayer graphene nanocomposites produced by HIP and SPS technology. *Tribology International*, Vol. 93, 2015, pp. 269–281.

[192] Feng, H., Q. Meng, Y. Zhou, and D. Jia, Spark plasma sintering of functionally graded material in the Ti-TiB 2-B system, *Materials Science and Engineering: A*, Vol. 397, 2005, pp. 92–97.

[193] Hong, C.-Q., X.-H. Zhang, W.-J. Li, J.-C. Han, and S.-H. Meng. A novel functionally graded material in the ZrB 2-SiC and ZrO 2 system by spark plasma sintering. *Materials Science and Engineering A*, Vol. 498, 2008, pp. 437–441.

[194] Mishina, H., Y. Inumaru, and K. Kaitoku. Fabrication of ZrO 2 /AISI316L functionally graded materials for joint prostheses. *Materials Science and Engineering A*, Vol. 475, 2008, pp. 141–147.

[195] Qiao, Z., J. Räthel, L.-M. Berger, and M. Herrmann, Investigation of binderless WC-TiC-Cr3 C2 hard materials prepared by spark plasma sintering (SPS), *International Journal of Refractory Metals and Hard Materials*, Vol. 38, 2013, pp. 7–14.

[196] Watanabe, Y., Y. Iwasa, H. Sato, A. Teramoto, K. Abe, and E. Miura-Fujiwara. Microstructures and mechanical properties of titanium/biodegradable-polymer FGM for bone tissue fabricated by spark plasma sintering method. *Journal of Materials Processing Technology*, Vol. 211, 2011, pp. 1919–1926.

[197] Guillon, O., J. Gonzalez-Julian, B. Dargatz, T. Kessel, G. Schierning, J. Räthel, et al. Field-assisted sintering technology/spark plasma sintering: mechanisms, materials, and technology developments. *Advanced Engineering Materials*, Vol. 16, 2014, pp. 830–849.

[198] Han, W., Y. Li, G. Chen, and Q. Yang. Effect of sintering additive composition on microstructure and mechanical properties of silicon nitride. *Materials Science and Engineering A*, Vol. 700, 2017, pp. 19–24.

[199] Qi, Y. E., Y. S. Zhang, Y. Fang, and L. T. Hu. Design and preparation of high-performance alumina functional graded self-lubricated ceramic composites. *Composites Part B: Engineering*, Vol. 47, 2013, pp. 145–149.

[200] Yin, Z., C. Huang, B. Zou, H. Liu, H. Zhu, and J. Wang. Study of the mechanical properties, strengthening and toughening mechanisms of Al_2O_3/TiC micro-nano-composite ceramic tool material. *Materials Science and Engineering A*, Vol. 577, 2013, pp. 9–15.

[201] Hvizdoš, P., J. Dusza, and C. Balázsi. Tribological properties of Si3N4-graphene nanocomposites. *Journal of the European Ceramic Society*, Vol. 33, 2013, pp. 2359–2364.

[202] Acikbas, N. C., E. Suvaci, and H. Mandal. Fabrication of functionally graded SiAlON ceramics by tape casting. *Journal of the American Ceramic Society*, Vol. 89, 2006, pp. 3255–3257.

[203] Jones, A. H., R. S. Dobedoe, and M. H. Lewis. Mechanical properties and tribology of Si3N4-TiB_2 ceramic composites produced by hot pressing and hot isostatic pressing. *Journal of the European Ceramic Society*, Vol. 21, 2001, pp. 969–980.

[204] Lee, C. S., L. C. De Jonghe, and G. Thomas. Mechanical properties of polytypoidally joined Si3N4-Al_2O_3. *Acta Materialia*, Vol. 49, 2001, pp. 3767–3773.

[205] Tokita, M., G. Fantozzi, C. Estournes, A. L. Ortiz, and K. Morita, Ceramics progress of Spark Plasma Sintering (SPS) method, systems, *Ceramics Applications and Industrialization*, Vol. 4, No. 2, 2021, pp. 160–198.

[206] Salamon, D., Z. Shen, and P. Šajgalík. Rapid formation of α-sialon during spark plasma sintering: Its origin and implications. *Journal of the European Ceramic Society*, Vol. 27, 2007, pp. 2541–2547.
[207] Liu, L., F. Ye, Y. Zhou, Z. Zhang, and Q. Hou. Fast bonding α-SiAlON ceramics by spark plasma sintering. *Journal of the European Ceramic Society*, Vol. 30, 2010, pp. 2683–2689.
[208] Yin, Z., J. Yuan, W. Xu, K. Liu, and S. Yan. Graphene nanosheets toughened TiB_2-based ceramic tool material by spark plasma sintering. *Ceramics International*, Vol. 44, 2018, pp. 8977–8982.
[209] Díaz, L. A., M. A. Montes-Morán, P. Y. Peretyagin, Y. G. Vladimirov, A. Okunkova, J. S. Moya, et al. Zirconia-alumina-nanodiamond composites with gemological properties. *Journal of Nanoparticle Research*, Vol. 16, 2014, pp. 1–9.
[210] Gutiérrez-González, C. F., S. Pozhidaev, S. Rivera, P. Peretyagin, W. Solís, L. A. Díaz, et al. Longer-lasting Al_2O_3-SiCw-TiC cutting tools obtained by spark plasma sintering. *International Journal of Applied Ceramic Technology*, Vol. 14, 2017, pp. 367–373.
[211] Liu, C. C. and J. L. Huang. Effect of the electrical discharge machining on strength and reliability of TiN/Si3N4 composites. *Ceramics International*, Vol. 29, 2003, pp. 679–687.
[212] Bódis, E. and Z. Károly. Fabrication of graded alumina by spark plasma sintering. *The International Journal of Advanced Manufacturing Technology*, Vol. 117, 2021, pp. 2835–2843.
[213] Cheng, Y., H. Hu, S. Sun, and Z. Yin. Experimental study on the cutting performance of microwave sintered Al_2O_3/TiC ceramic tool in the machining of hardened steel. *International Journal of Refractory Metals and Hard Materials*, Vol. 55, 2016, pp. 39–46.
[214] Bykov, Y. V., S. V. Egorov, A. G. Eremeev, I. V. Plotnikov, K. I. Rybakov, V. E. Semenov, et al. Fabrication of metal-ceramic functionally graded materials by microwave sintering. *Inorganic Materials: Applied Research*, Vol. 3, 2012, pp. 261–269.
[215] Wang, D., D. Zhou, S. Zhang, Y. Vardaxoglou, W. G. Whittow, D. Cadman, et al. Cold-sintered temperature stable Na 0.5 Bi 0.5 MoO 4 –Li 2 MoO 4 microwave composite ceramics. *ACS Sustainable Chemistry & Engineering*, Vol. 6, 2018, pp. 2438–2444.
[216] Menezes, R. R. and R. H. G. A. Kiminami. Microwave sintering of alumina-zirconia nanocomposites. *Journal of Materials Processing Technology*, Vol. 203, 2008, pp. 513–517.
[217] Wu, G., C. Xu, G. Xiao, M. Yi, and Z. Chen. Structure design of Al_2O_3/TiC/CaF_2 multicomponent gradient self-lubricating ceramic composite and its tribological behaviors. *Ceramics International*, Vol. 44, 2018, pp. 5550–5563.
[218] Wang, B. and Z. Liu. Investigations on the chip formation mechanism and shear localization sensitivity of high-speed machining Ti6Al4V. *International Journal of Advanced Manufacturing Technology*, Vol. 75, 2014, pp. 1065–1076.
[219] Feng, Y., J. Zhang, L. Wang, W. Zhang, Y. Tian, and X. Kong. Fabrication techniques and cutting performance of micro-textured self-lubricating ceramic cutting tools by in-situ forming of Al_2O_3-TiC. *International Journal of Refractory Metals and Hard Materials*, Vol. 68, 2017, pp. 121–129.
[220] Ji, W., B. Zou, S. Zhang, H. Xing, H. Yun, and Y. Wang. Design and fabrication of gradient cermet composite cutting tool, and its cutting performance. *Journal of Alloys and Compounds*, Vol. 732, 2018, pp. 25–31.
[221] Abubakar, A. A., S. S. Akhtar, A. D. Alotaibi, K. S. Al-Athel, A. S. Hakeem, and A. Y. Adesina. Development and analysis of functionally-graded SiAlON composites with computationally designed properties for cutting inserts. *Journal of Materials Research and Technology*, Vol. 23, 2023, pp. 5861–5879.